PRACA DOKTORSKA

Title: Improvement of microbial assays in water-in-oil droplets

PhD thesis by

M.Sc. Artur Ruszczak

Prepared under supervision of

Prof. Piotr Garstecki

Associate Prof. Ott Scheler, PhD

And auxiliary supervision of

Ladislav Derzsi, PhD

Within the International PhD Studies at the

Institute of Physical Chemistry

Polish Academy of Sciences

Kasprzaka 44/52

01-224 Warsaw

IChF

Warsaw, April 2023

Table of contents

Abstract

Over the past 20 years, many microbial assays have been demonstrated in droplet-microfluidic format. Tools made possible with microfluidic techniques opened up new possibilities in the rapid detection of infections, determination of antimicrobial resistance, single-cell bacterial population characterization, increasing the taxonomic richness by avoiding species competition or studying bacterial responses in complex consortia.

The fundamental premise of droplet microfluidics is that each droplet can be treated as an independent and isolated bio-reactor. The ease of generation of many microreactors in a short time allowed for efficient operations on many separate reactions simultaneously. This feature is especially useful when studying bacterial populations, as numerous reactors provide excellent statistics and allow the analysis on a single bacterial cell level.

One strict technical requirement for microreactors is that the droplet interfaces must present a barrier to transporting chemical ingredients between droplets. It is essential that the dyes used to detect the growth of microbes cannot migrate between droplets to allow reliable assessment of bacterial growth in a single droplet. Similarly, tested antimicrobial agents whose effect on the growth of bacteria must be remained inside the droplets with a constant concentration not to interrupt the experiment results.

Nevertheless, recent studies report molecular transport between droplets raising highly relevant questions about the compatibility of droplet-based systems for biological applications. This work presents a problem of the molecular transfer in monodispersed emulsions on the example of tracking the leakage of fluorescent metabolic dyes and non-fluorescent antibiotics.

Metabolic markers are commonly used to rapidly visualize viable bacteria in droplets. One of the most popular fluorescent compounds – resorufin, has a significant limitation related to its fast leakage from droplets, interrupting the experiment's accurate read-out. Dodecylresorufin (C12R) is a promising alternative as a marker of droplet-encapsulated bacteria as it exhibits less leakage between the droplets. The fluorescent signal from C12R is more stable over time, and the signal-to-noise ratio is higher. The C12R assay accuracy is improved because the true positive and true negative rates are higher than in the case of standard resorufin. As a result of their higher precision,

C12R droplet-based assays present exciting new opportunities for high-throughput screening and study in microbiology.

Molecular transport between droplets is relatively easy to track with the help of model fluorophores. However, determination of the leakage of antimicrobial agents is hard to perform, primarily due to their weak fluorescence. The second part of this work attempt to find the chemical factors that accelerate the escape of antimicrobials from droplets. The physicochemical model proposed in this study predicts antibiotic retention in droplets according to their partition coefficient and fractional polar surface area. The model was verified by monitoring growth inhibition by antibiotic-loaded neighboring droplets. As a result of this study, a better understanding of how tiny compounds are retained in water-in-oil emulsions will help design droplet-based antibiotic assays in the future.

Streszczenie

W ciągu ostatnich 20 lat, wiele eksperymentów mikrobiologicznych zostało przeprowadzonych z zastosowaniem mikroprzepływów kropelkowych. Narzędzia, które stały się możliwe dzięki technikom mikroprzepływowym, otworzyły nowe sposoby szybkiego wykrywania infekcji, określania oporności na środki przeciwdrobnoustrojowe, charakteryzowania populacji bakterii na poziomie pojedynczych komórek, zwiększania bogactwa taksonomicznego poprzez unikanie konkurencji między gatunkami lub badania oddziaływań bakterii w złożonych konsorcjach.

Podstawowym założeniem mikroprzepływów kropelkowych jest to, że każdą kroplę można traktować jako niezależny i izolowany bioreaktor. Łatwość generowania wielu mikroreaktorów w krótkim czasie pozwoliła na efektywne prowadzenie wielu niezależnych reakcji jednocześnie. Ta cecha jest szczególnie przydatna podczas badania populacji bakterii, ponieważ liczne reaktory zapewniają doskonałe statystyki i pozwalają na analizę pojedynczych komórek bakteryjnych.

Jednym ze ścisłych wymagań technicznych mikroreaktorów kropelkowych jest to, by ich powierzchnia stanowiła barierę dla transportu składników chemicznych między kropelkami. Wiarygodna ocena wzrostu kolonii bakteryjnych w pojedynczej kropli, ma miejsce wtedy, gdy barwniki stosowane do wykrywania wzrostu drobnoustrojów nie mogą migrować między kroplami. Podobnie jest z badaniem środków o działaniu przeciwdrobnoustrojowym, które wpływają na wzrost bakterii. Takie substancje muszą pozostać wewnątrz kropelek w stałym stężeniu, aby nie zakłócać wyników eksperymentu.

Niemniej jednak ostatnie badania naukowe donoszą o transporcie molekularnym między kropelkami, co rodzi bardzo istotne pytania dotyczące zgodności systemów opartych na kropelkach w zastosowaniach biologicznych. W niniejszej pracy przedstawiono problem transferu molekularnego w monodyspersyjnych emulsjach na przykładzie śledzenia wycieku fluorescencyjnych barwników metabolicznych i niefluorecencyjnych antybiotyków.

Markery metaboliczne, to substancje powszechnie stosowane do szybkiej wizualizacji żywych bakterii w kropelkach. Jeden z najbardziej popularnych fluoroforów – resorufina posiada ograniczenia związane z jej szybkim wyciekiem z kropelek, co w konsekwencji zakłóca dokładny odczyt eksperymentu. Dodecylorezorufina (C12R) jest obiecującą alternatywą jako marker

metaboliczny, ponieważ wykazuje mniejszy wyciek między kropelkami. Sygnał fluorescencyjny C12R jest bardziej stabilny w czasie, a stosunek sygnału do szumu jest wyższy. Eksperymenty z zastosowaniem C12R wykazują większą dokładność, a odsetek wyników prawdziwie dodatnich i prawdziwie ujemnych jest wyższy niż w przypadku resorufiny. Dzięki większej precyzji testy kropelkowe C12R stwarzają nowe perspektywy do wysokowydajnych badań przesiewowych i badań mikrobiologicznych.

Transport molekularny między kropelkami można łatwo śledzić za pomocą modelowych fluoroforów. Niemniej jednak określenie wycieku substancji przeciwdrobnoustrojowych jest trudne do wykonania, przede wszystkim ze względu na ich słabą fluorescencję. W drugiej części pracy podjęto próbę znalezienia czynników chemicznych, które przyspieszają ucieczkę antybiotyków z kropelek. Model fizykochemiczny zaproponowany w tym badaniu przewiduje retencję antybiotyku w kropelkach na podstawie ich współczynnika podziału (XlogP) i ułamkowego polarnego pola powierzchni (fractional polar surface area). Model zweryfikowano przez monitorowanie hamowania wzrostu przez sąsiadujące kropelki z antybiotykiem. W wyniku tych badań lepsze zrozumienie, w jaki sposób drobne związki są zatrzymywane w emulsjach typu woda w oleju, pomoże w przyszłości zaprojektować kropelkowe testy antybiotykowe.

List of publications

Publications described in this work

1. **Ruszczak A**, Jankowski P, Vasantham SK, Scheler O, Garstecki P: Physicochemical Properties Predict Retention of Antibiotics in Water-in-Oil Droplets. Analytical Chemistry 2023.

2. Scheler O, Kaminski TS, **Ruszczak A**, Garstecki P: Dodecylresorufin (C12R) Outperforms Resorufin in Microdroplet Bacterial Assays. ACS Appl Mater Interfaces 2016, 8:11318-11325.

Other publications

3. **Ruszczak A**, Bartkova S, Zapotoczna M, Scheler O, Garstecki P: Droplet-based methods for tackling antimicrobial resistance. Current Opinion in Biotechnology 2022, 76:102755.

4. Rangam NV, Sudagar AJ, **Ruszczak A**, Borowicz P, Tóth J, Kövér L, Michałowska D, Roszko MŁ, Noworyta KR, Lesiak B: Valorizing the Unexplored Filtration Waste of Brewing Industry for Green Silver Nanocomposite Synthesis. Nanomaterials 2022, 12:442.

5. Sudagar AJ, Rangam NV, **Ruszczak A**, Borowicz P, Tóth J, Kövér L, Michałowska D, Roszko MŁ, Noworyta KR, Lesiak B: Valorization of Brewery Wastes for the Synthesis of Silver Nanocomposites Containing Orthophosphate. Nanomaterials 2021, 11:2659.

6. Kao Y-T, Kaminski TS, Postek W, Guzowski J, Makuch K, **Ruszczak A**, von Stetten F, Zengerle R, Garstecki P: Gravity-driven microfluidic assay for digital enumeration of bacteria and for antibiotic susceptibility testing. Lab on a Chip 2020, 20:54-63.

7. Scheler O, Makuch K, Debski PR, Horka M, **Ruszczak A**, Pacocha N, Sozanski K, Smolander OP, Postek W, Garstecki P: Droplet-based digital antibiotic susceptibility screen reveals single-cell clonal heteroresistance in an isogenic bacterial population. Sci Rep 2020, 10:3282.

8. Opalski AS, **Ruszczak A**, Promovych Y, Horka M, Derzsi L, Garstecki P: Combinatorial Antimicrobial Susceptibility Testing Enabled by Non-Contact Printing. Micromachines 2020, 11:142.

9. Horka M, Sun S, **Ruszczak A**, Garstecki P, Mayr T: Lifetime of Phosphorescence from Nanoparticles Yields Accurate Measurement of Concentration of Oxygen in Microdroplets, Allowing One To Monitor the Metabolism of Bacteria. Anal Chem 2016, 88:12006-12012.

10. Churski K, **Ruszczak A**, Jakiela S, Garstecki P: Droplet Microfluidic Technique for the Study of Fermentation. Micromachines 2015, 6:1514-1525.

Abbreviations

AMK – amikacin

BSA- bovine serum albumine

C12R- dodecyloresarufin

CAZ - ceftazidime

CFU- colony forming unit

CHL- chloramphenicol

CIP- ciprofloxacin

CMC- critical micelle concentation

CTX- cefotaxime

ddPCR- droplet digital PCR

ddLAMP –droplet digital loop-mediated isothermal amplification

DOX- doxycycline

EGFP- enhanced GFP

FOF- fosfomycin

GEN- gentamycin

GFP- green fluorescent protein

IPM- imipenem

J- Youden index

KAN- kanamycin

LVX- levofloxacin

MEM- meropenem

MIC- minimal inhibitory concentration

NCDK- NET Chemistry Development Kit

NIT- nitrofurantoin

NOR- norfloxacin

PC- polycarbonate

PCR- polymerase chain reaction

PDMS- polydimethylsiloxane

PEG- polyethylene glycol

PFPE- perfluoropolyether

PSA- polar surface area

ROC- receiver operating characteristic

SNR- signal to noice ratio

SPT- spectinomycin

TET- tetracycline

TOB- tobramycin

TVA- trovafloxacin

XlogP- partition coefficient

1. Introduction and literature review

Chapter 1 describes the origins and fundamental premise of droplet-based microfluidics and reviews applications of droplet microbioractiors in microbiology, with the greatest focus on studies on antimicrobial resistance. The second part introduces the basic requirements for surfactant biocompatibility and the latest developments in creating new surfactants for droplet-based techniques.

The final part of the introduction raises the problem of the molecular transfer between droplets in complex emulsions.

1.1. Origins and definition of microfluidics

The fundamental premise of microfluidics is to condense nearly all biological and chemical reactions into a tiny scale (between 10^{-9} and 10^{-18} liters) [1]. There are many benefits of scaling down experimental conditions. First, it considerably lowers reagent consumption, which is apparent when using expensive chemicals (i.e. antibodies). Downscaling can speed up many relevant processes, like detecting infections [2,3]. All of the above led to the recent development of numerous miniature, automated devices known as "*lab-on-a-chip*", which allowed to move experiments from the laboratory bench to a microfluidic chip.

Although microfluidics originates in basic sciences like physics and chemistry, the advancement of new engineering methods significantly impacts its evolution. Therefore, the beginning of microfluidics cannot be attributed to a single discovery. The idea of miniature total chemical analysis systems (µTAS), first introduced by Manz et al. in 1990, served as the impetus for the development of microfluidics [4]. Nevertheless, the evolvement of chemical analytical techniques like chromatography and capillary electrophoresis in the late 1970s inspired the concept [1].

Another mile stone in microfluidics was the invention of soft lithography, a technique for fabricating elastomer-based chips [5,6]. Undoubtedly, one of the revolutionary breakthroughs in microfluidics was the first drop-producing geometry initially reported two decades ago. The publication's authors demonstrated the generation of tiny aqueous droplets and indicated the possibility of using them as nano-liter reactors in the future [7].

Nowadays, microfluidic systems are the next step in revolutionizing many aspects of microbiology, eliminating laboratory pipettes and manual work and opening new perspectives in research [8-10]. Since a droplet's volume is constrained, metabolic waste products and other significant molecules produced by the cell can accumulate more quickly than they would if the organism were living in the bulk culture. This trait offers new possibilities for the early identification of cells and secreted microbial substances, enabling the development of new tools for the rapid diagnosis of sepsis or the fast detection of antimicrobial resistance.

Moreover, the capacity to analyze vast numbers of individual droplets—possibly millions—is one of the most significant benefits of droplet microfluidics. This feature is handy in studies of phenotypic and genetic variations at the level of individual cells in microbial populations. The spatial separation of microbes facilitates learning about the microbial population's nature at a single-cell level. This feature can be easily implemented for robust enumeration of the bacterial population, searching for rare mutants or tracking single-cell responses in the presence of antimicrobials.

1.2 Droplet microfluidics

There are two main types of microfluidics based on the number of fluid phases used. One-phase microfluidics uses continuous streams of miscible liquids. When liquids flow in miniaturized channels with (dimensions from tens to hundreds of microns), the Reynolds number decreases; thus, the flow becomes highly organized. This well-organized behavior of liquid streams is called laminar flow. Droplet-based microfluidics is a subdivision that uses two or more immiscible fluids to generate droplets. Dispersing aqueous droplets in the oil phase leads to the production of the emulsion, consisting of a massive number of monodispersed droplets with strictly defined volumes. Aqueous droplets can serve as unique and isolated environments for microbial growth, thus allowing for high-throughput experimentations on thousands or millions of parallel incubation compartments.

Methods for droplets generation
Droplets can be generated in many ways depending on channel geometries. Typical channel modes for droplet formations are i) flow-focusing [11,12], ii) T-junction [7,13], iii) co-flowing [14], and iv) step emulsification [15] (**Fig. 1**). In most droplet generators, two immiscible phases meet, and viscous shear forces break off tiny aqueous droplets and disperse them in the continuous oil phase.

Recently, droplets can be generated with high efficiency reaching frequencies up to hundreds of kHz [16-18]. Step emulsification is a simple method for rapid droplet generation where the dispersed phase liquid exits through a wide and shallow rectangular nozzle to a large reservoir filled with another immiscible liquid. The sudden confinement relief causes the tip of the to-be-dispersed phase to change its shape to spherical, which leads to the formation of a "neck" at the nozzle,

which ultimately pinches off. Rapid production of high-volume emulsions with highly uniform droplets can be obtained by parallelizing many nozzles [18,19].

A. Flow focusing

B. T- junction

C. Co-flow

D. Step emulsification
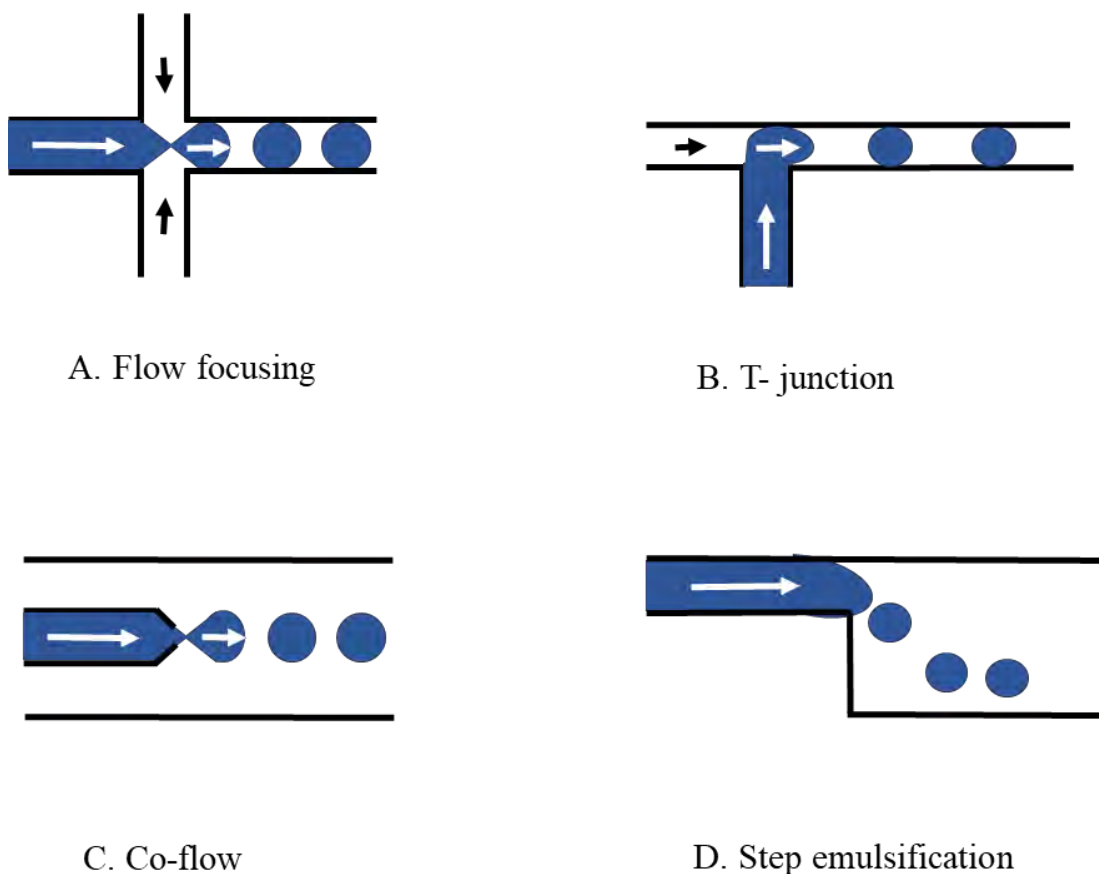
Fig. 1 *Types of geometries for generation of droplets. A. Flow-focusing generation of droplets, B. T-junction generator, C. Co-flow, D. Droplet generation on a step.*

New improvements in production techniques are being developed day by day. Particular attention is paid to the development of new methods that facilitate the easy and fast generation of large volumes of emulsions without the need for additional tools such as syringe pumps [19,20]. Polydisperse emulsions may be simply and quickly created by employing inexpensive tabletop equipment like a vortex or a stirrer (**Fig. 2**). It has been shown that polydisperse emulsions allow for the growth and precise quantification of bacterial cells [21]. Detection of genetic material in polydispersed emulsions obtained by digital droplet polymerase chain reaction (ddPCR) stays in high agreement with commercial ddPCR systems like BioRad [22]. This approach can be particularly

convenient for users who do not deal with microfluidics and do not have access to microfluidic infrastructure.

Another novel improvement in microfluidics is to minimize the need to use all tools required for precise droplet generation. Most diagnostic laboratories do not have expensive equipment for producing and operating microfluidic chips, i.e. soft-lithography setups or accurate pumps. Hatori et al. demonstrated a unique microfluidics-free technique for ddPCR and single-cell cultivation of microorganisms[23]. In their study, microfluidics has been limited to the step of the generation of uniform hydrogel bead templates. Templates may be delivered to laboratories where they can be stored for a long time in the fridge. In the first step of the experiment, hydrogel templates are incubated with test samples. During incubation, most reagents diffuse into the gel beads. In the next step, sample-loaded gel templates are vortexed with the oil to produce monodispersed emulsion without requiring additional devices. The big advantage of this approach (apart from being an equipment-free technique) is a significant decrease in the generation time of high-volume samples. The generation of two milliliters of a monodispersed emulsion by vortexing last 30 sec, while the same volume requires 12 h in the standard microfluidic method [23].

A. Microfluidics **B.** Vortexed **C.** Detection from polydispersed emulsion
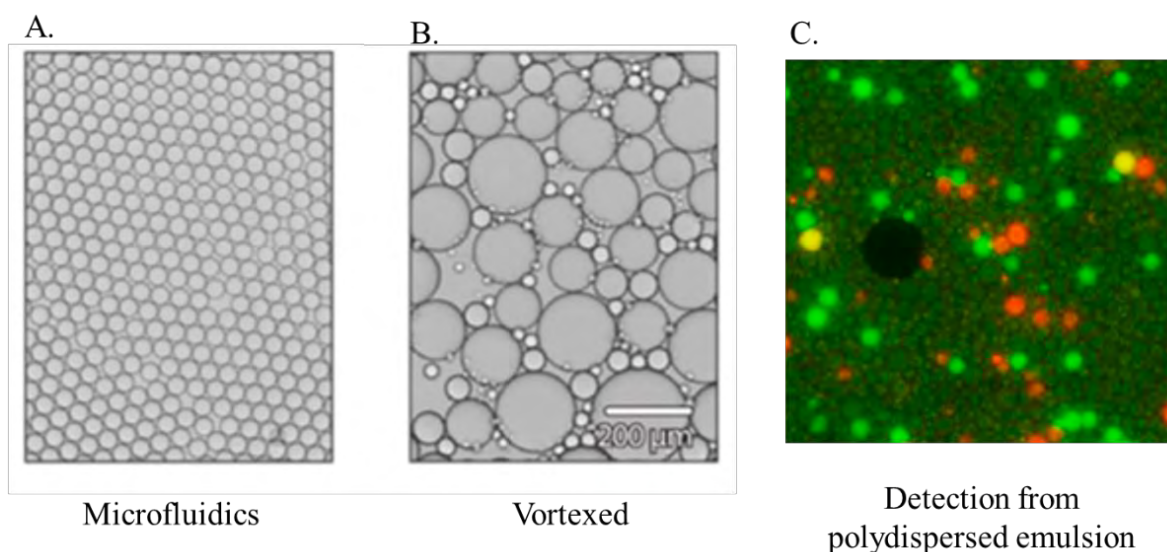
Fig. 2 *Microscopic photographs of emulsions created by A. microfluidic method, B. emulsification by vortexing. C. ddPCR performed in the polydispersed emulsion. Adapted from Hatori et al., Anal Chem, 90: 9813-9820, (2018) and Byrnes et al., Anal Chem, 90: 9374-9380, (2018)*

1.3 Droplet microfluidics for microbiology

### 1.3.1 Droplet as an optimal bioreactor

In 2008, Boedicker et al. made one of the first, most significant attempts to employ droplets as distinct habitats for microbial growth [24]. Since then, droplet methods have gained a lot of popularity in the field of microbiology. Droplet bioreactors satisfy several criteria that make them suitable as a habitat for growing microorganisms.

Gas permeability in droplets

Bioreactors need to be gas permeable as the presence of respiratory gases is a necessary factor for aerobic bacteria. Studies have shown that liquid droplets dispersed in fluorinated oils enable microorganisms to access oxygen continuously (19, 20). Fluorinated oils are characterized by excellent solubility for respiratory gases like oxygen or carbon dioxide [25]. Moreover, droplet reactors are oxygenated efficiently because of the faster diffusion on a small scale [26].

On the other hand, anaerobic bacteria need an anoxic environment to reproduce. Droplet techniques may also satisfy these criteria by employing low-permeability mineral oils and incubating the emulsion without oxygen [27,28].

Boitard et al. compared growth rates of bacteria growing in droplets, bulk cultures in a glass flask, and a multiwell plate. Surprisingly, the better biomass production was obtained in the droplet bioreactors than in the microplate (**Fig. 3**). The authors explain this with the excellent oxygen availability in droplets. Tiny water droplets have a bigger surface-to-volume ratio compared to traditional reactors. At the same time, mixing in a multiwell plate is inefficient, which can significantly affect the growth rate of microorganisms [26].
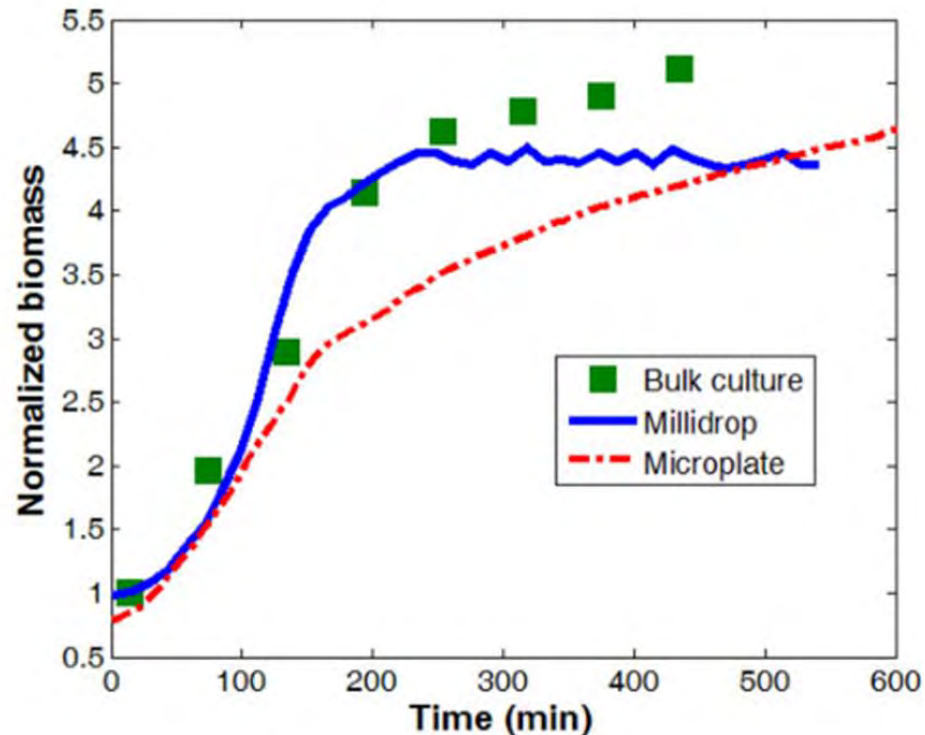
Fig. 3 *Bacterial growth in three different incubation conditions. Green squares represent bacterial growth in a flask (bulk). The Red line demonstrates the growth of bacteria in micro-wells; the decrease in the growth results from the poor mixing and oxygenation of small-volume wells. The bacterial growth rate in 200 nl droplet is presented as the blue line. Adapted from Boitard et al., Eng. Life Sci., 00, 1-9 (2015).*

Multi-component composition of the droplet

The complex droplet content can be controlled by dosing the appropriate volume of the reactants or by combining pairs of droplets with different chemical compositions. It significantly facilitates high-throughput studies on the response of microorganisms to various (multidimensional) conditions. This advantage is crucial in searching for new, active combinations of drugs against bacteria resistant to most available antibiotics [29-31].

One of the exciting microfluidic platforms for the generation of 'droplets on demand' was demonstrated by Churski et al. in 2012. The authors of the work used electromagnetic valves to dose a precise volume of mixtures of antibiotics during the formation of droplets [32]. The improvement to this method has been lately demonstrated by Kulesa et al. by random pairing and

merging droplets with different compositions and concentrations of antibiotics. This drug combination discovery platform streamlined the research on the synergistic activity between more than 4.000 investigational and approved drugs [30]. High-throughput generation of droplets with different chemical content can also be an attractive technique for selecting optimal conditions in biotechnological production [33]. Using traditional laboratory methods for recreating conditions of the above experimental set-ups is cumbersome and work-intensive, accounting for the limitations of studies on synergistic interactions between antimicrobial agents.

Fast mixing

In one-phase microfluidics, the laminar flow of fluids is highly organized, mixing of reagents is limited to diffusion; therefore, it is quite slow. Droplets offer accelerated methods of mixing by flow through curved channels. Droplets are stretched and folded in serpentine channels, which enables their chemical content to be mixed quickly (**Fig. 4**). Fast and effective mixing of droplets can be beneficial when studying the kinetics of, e.g. enzymatic reactions for testing the susceptibility of microorganisms to antibiotic mixtures or optimizing the reaction conditions [34].
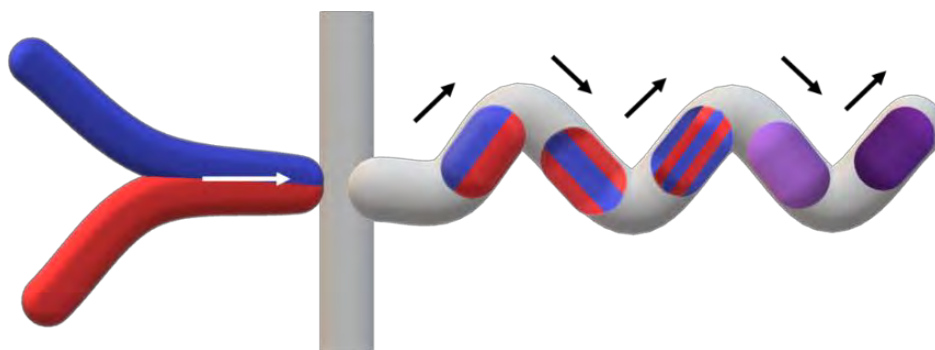
Fig. 4 Mixing of the droplet in a curved channel. The droplet flowing in the serpentine channel is stretched and folded, significantly accelerating the mixing of the reactants.

Convenient methods for the detection and quantification of bacteria

Detecting positive droplets (with microorganisms actively growing inside) may be made simple by directly monitoring dividing cells [35], measuring their metabolic activity [36,37] or detecting genetic material [38,39] (**Fig.5**).

One of the most popular methods for the rapid detection of bacteria in droplets is tracking their metabolic activity [20,24,32,40]. Most of the molecular markers are fluorophores sensitive to the

metabolic activity of cells. Resazurin is an example of one of the most common compounds for tracking bacterial metabolism. Resazurin possesses a weak fluorescence, but viable cells can quickly convert it into a highly fluorescent form- resorufin [41-44]. The reduction can occur on the intracellular level as a result of enzyme activity or on the extracellular level due to a chemical reaction in the medium [45]. There are few modified versions of the resorufin available on the market. The molecule can be complexed with a fluorescence- quenching component, and the dye's release is possible through specific bacterial enzymes' activity. This method has been applicated in droplet digital platforms for bacterial enumeration and in the analysis of enzyme kinetics [46-49]. The Amplex® Red is another widely used resorufin-based product. It undergoes a two-step conversion to resorufin. In the first step, specific microbial oxidase enzymes generate hydrogen peroxide. Next, the addition of the enzyme peroxidase lead to the transformation of the substrate to fluorescent resorufin. Amplex® Red reagent has been successfully used in high-throughput screening of microorganisms for metabolic production or consumption of certain substrates and in droplet experiments to evaluate enzyme activity [36,37,50,51].

Nevertheless, resazurin has a few significant limitations, restricting its compatibility with droplet-based methods. First, resazurin is reduced to fluorescent resorufin after oxidation. Thus, this metabolic dye is active in aerobic bacteria cultures only. Secondly, as many studies demonstrated, resorufin is prone to leak from the droplets, significantly disturbing the detection and long-term incubation in droplets [52,53].

Other alternative methods of reading the metabolic activity of bacteria include monitoring their oxygen consumption or tracking the change in pH of the droplets [35,54-57]. Utilizing the enzymatic activity of microorganisms is another strategy. Bacterial enzymes transform a substrate into its fluorescent form, which can serve as a signal for detection [58,59].

Direct detection of viable bacterial cells in droplets is also achievable. The test microbes can be genetically engineered to produce fluorescent proteins such as the popular green fluorescent protein (GFP) [60-63]. Nevertheless, genetic modifications interfere with cells, for example, through the metabolic burden associated with producing additional proteins or by adding resistance genes on plasmids coding fluorescent proteins. Thus, genetic modifications are not

suitable for clinical isolates. Therefore, developing label-free approaches for detecting unlabeled microbes in nanoliter droplets is crucial. Pacocha et al. demonstrated a label-free system for detecting bacteria in droplets based on the intensity of scattered or native fluorescence light. The method is suitable for detecting unlabeled Gram-negative and Gram-positive species with a high screening frequency of 1200 droplets/s [35].
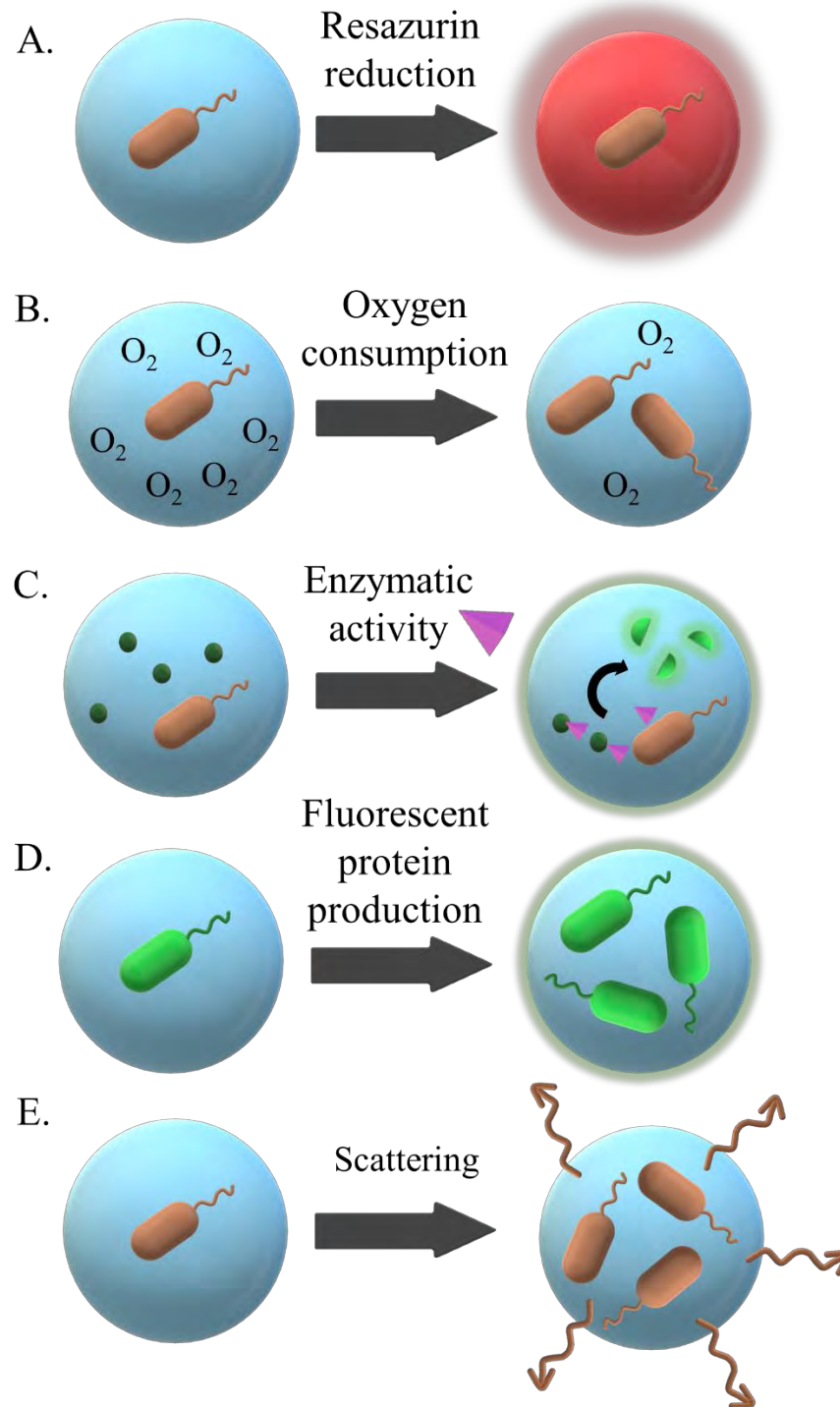
Fig. 5 *Different methods for the detection of bacteria in droplets. A. Conversion of resazurin to fluorescent resorufin by metabolic activity, B. Monitoring of oxygen consumption, C. Tracking of enzymatic activity, D. Increase of fluorescent signals in GFP-producing bacteria, E. Signals from native fluorescence.*

1.3.2 Application of droplet microfluidics in microbiology with an outlook for clinical diagnostics methods

Microfluidic droplet systems have recently been found to be highly appealing analytic techniques in antimicrobial susceptibility testing (AST) and antimicrobial resistance (AMR) mechanisms. Researchers employed microfluidics to comprehend better the global health crisis caused by the fast spread of resistant infections and a shortage of new antibiotics [64,65]. Microfluidics can serve as a suitable platform for the rapid detection of diseases [39], characterization of bacterial populations at the single-cell levels [61], increasing taxonomic richness of clinical samples [27], or responses of bacteria in complex consortia [63].

Fast detection of pathogens

The faster identification of microorganisms is the undeniable benefit of employing microfluidics in diagnostics. Bacteria encapsulated in droplets multiply in a limited space and accumulate indicative metabolites, reducing the time required for detecting a viable population. Droplet methods can significantly decrease the time for detecting resistant cells by removing pre-incubation steps [66-68].

Zhang et al. showed a rapid phenotype-based detection tool called SCALe-AST (Single-Cell Assembly Line AST) that can evaluate antibiotic resistance directly from urine samples based on the readout of bacterial viability in 90 min [40]

Applying droplet-based genetic methods for detection (ddPCR –droplet digital polymerase chain reaction or ddLAMP –droplet digital loop-mediated isothermal amplification) significantly enhances AMR diagnostic speed. One-step ddPCR for pathogen identification (16S rRNA) and resistance gene detection directly from clinical blood samples shortened the timeframe to eight hours for multistep assays and one hour for a single-step experiment [2,39]. ddLAMP enables pathogen identification combined with AST directly from urine samples and offers decreased detection time of 30 mins [66,69]. A LAMP-based point-of-care technique employing smartphone contact angle measurement can identify bacterial cells in a low time- 5 minutes [70].

Single-cell analysis of populations

Droplet microfluidics can be applied successfully in single-cell studies on microbial populations. Specific criteria must be met to encapsulate only one cell in small droplet bioreactors. Bacterial

inoculums have to be well diluted. Encapsulation of highly dilute suspensions leads to the creation of libraries of droplets where most compartments remain unsealed (empty). According to Poisson's distribution, encapsulation to generate below 10% bacteria-containing droplets ensures that most droplets contain just one cell [71]. This approach, called droplet compartmentalization, is beneficial in searching for distinctive phenotypes in microbial populations. Single-cell screening has proven successful in i) biotechnology, in searching for strains with overconsumption or overproduction of substrates (56), specific enzyme production [72,73]; ii) clinical microbiology, for the detection and analysis of resistant subpopulations [61,74].

Large populations traditionally can be analyzed at a single-cell level by spatial separation in micro-wells or flow cytometry. Nevertheless, micro-well cultivation is laborious and suffers from poor mixing and high evaporation rates. Flow cytometry is hard to perform for bacteria due to their small size. Although flow cytometry is ideally suited to characterize features like size distribution or the immediate expression of internal proteins. However, it cannot provide information on strain productivity (excreted products are lost in solutions)[26]. Droplet-based methods eliminate most of the problems that affect classical bulk experiments.

One potentially helpful strategy in the battle against antimicrobial resistance (AMR) is searching for rare (less abundant) resistant bacterial subpopulations that may give rise to chronic infections. Resistant mutants are typically rare- less than 1 per 10^3 CFU; thus, some bacterial populations may be undetected by classical diagnostic methods and misclassified as sensitive [75-77]. The microfluidic droplet approach was used by Lyu et al. to screen diverse populations at a single-cell resolution quantitatively. They found that bacterial compartmentalization provides a more sensitive method for identifying less abundant resistant subpopulations (ca. 10^{-6})[74].

On the other hand, high-density inoculum could also contribute to the incorrect rise in detectable MIC values, known as the "inoculum effect". This effect is characteristic of antibiotics that may be neutralized by proteolytic enzymes released by resistant bacteria to the extracellular environment (e.g., β-lactams). Hence MIC found at the single-cell level reflects a concentration preventing the establishment of new populations from a single bacterial cell regardless of inoculum density. Separating eliminates the influence of cooperation with other cells from the population [61].

Traditional culture methods in microbiology are inadequate to maintain the growth of all species in the polymicrobial consortia. Fast-growing microorganisms usually supersede rare or fastidious species, which reduces taxonomic richness[27,78]. Competitive species need spatial segregation (one microbe per droplet) to prevent inhibitory interactions (**Fig.6**). Watterson et al. found that bacterial separation in distinct droplets enhances stool taxonomic richness fourfold compared to agar plates. The classical method missed the identification of 21 resistant strains detected by droplet single-cell microfluidic technology [27]. The use of this technique may facilitate research on the structure of the human microbiome in the future[79-81].

Analysis of bacterial consortia

Spatial separation does not enable direct cell-to-cell interactions and does not determine the forces shaping community behaviors. As it is frequently demonstrated in the literature, different bacteria species can cooperate, which can lead to the reduction of their susceptibility. In such cases, the proportion of each strain will significantly influence the shape of the polymicrobial population [82-85]. Droplet-based microfluidics streamlines inter-species studies by preparing different microbial consortia by stochastic encapsulating random sub-communities into separate compartments (**Fig.6**)[63,86]. Microfluidic platform designed by Hsu et al. couple droplet microfluidics and computational image analysis to rapidly determine the absolute abundance of each bacterial member within the polymicrobial consortia. As one of the applications, they demonstrated that the exposition of various antibiotics could significantly modulate interactions between three bacterial species and lead to antimicrobial tolerance [63].
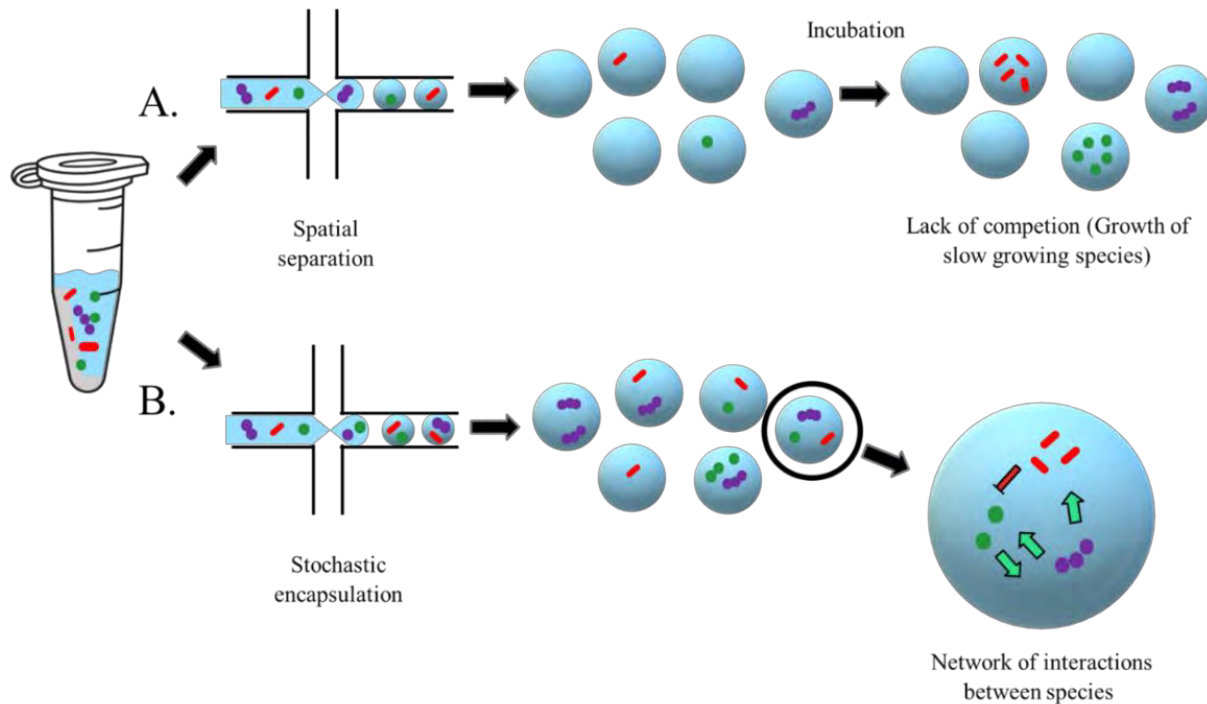
Fig.6 *Different approaches in the cultivation of polymicrobial consortia. A. Spatial separation decreases competition between species [27,79], B. Stochastic encapsulation leads to the generation of consortia with different species compositions [63,86].*

1.4 Biocompatible oils for droplet microfluidics

Culturing bacteria in droplets imposes specific requirements on the oils used as the continuous phase that supports droplets. Primarily, the oil should remain neutral to the materials for chip manufacturing. Moreover, cultivating cells in water-in-oil droplets requires a lack of oil toxicity and the transport of respiratory gases into the droplet. The final, fundamental requirement is to keep reagents insoluble in oil and prevent inter-droplet molecular transport. Fluorinated compounds that conveniently satisfy these requirements are represented by commercially available engineered fluids like Novec 7500 or FC40 (**Fig.7**) [87].

Fluorinated oils contain carbon-hydrogen (C-H) bonds that are replaced with carbon-fluorine (C-F) bonds (one of the strongest bonds in chemistry). Perfluorocarbons are strongly nonpolar with decreased solubility of organic molecules, even though C-F bonds are strongly polarized due to fluorine electronegativity. This is because the dipole moments in perfluorocarbon molecules cancel

each other [88]. Moreover, weak intermolecular forces in fluorinated compounds result in high interstitial spaces between molecules. Hence, respiratory gases (such as oxygen or carbon dioxide) have exclusively high solubility in fluorinated oils [25,55,88-91].

A.

FC40

B.
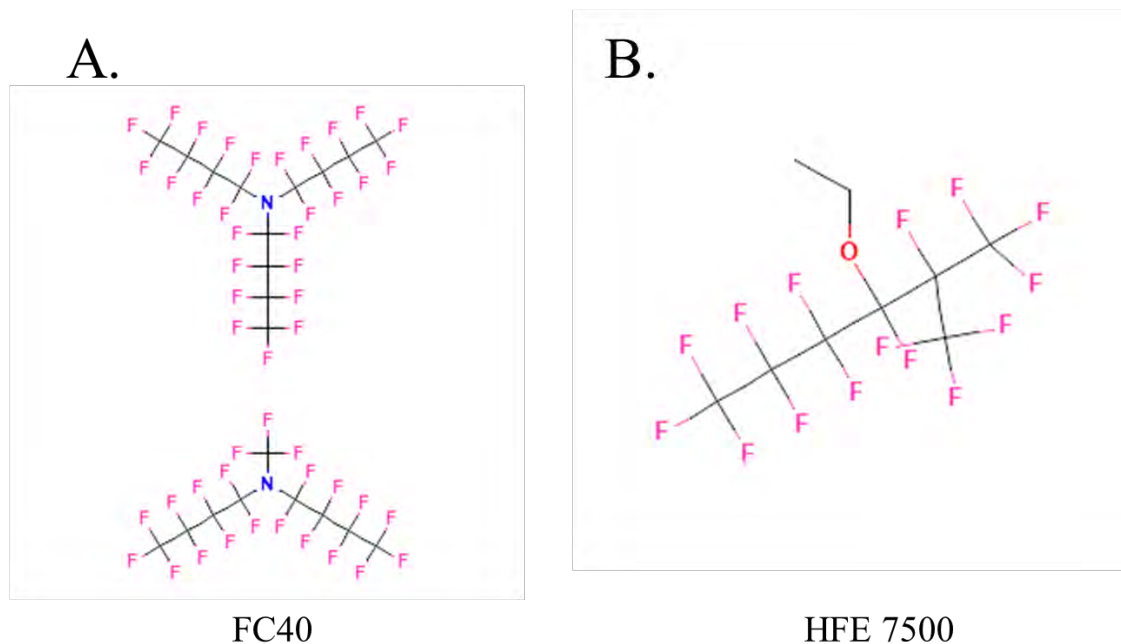
HFE 7500

Fig. 7 *Chemical structure of the two most popular representatives of fluorinated oils. A. Two-component product Fluorinert FC-40. B. HFE 7500. Adapted from PubChem.*

Another essential property of fluorinated oils concerns their compatibility with materials for chip fabrication. Polydimethylsiloxane (PDMS) is the most common polymer for chip manufacturing, primarily due to its compatibility with soft lithography, low cost, and good permeability. Fluorinated compounds do not cause swelling of PDMS and thus do not change channel geometry [6,91].

Finally, most fluorinated oils have a high boiling point. Some biological applications, like PCR, require high temperatures (over 90°C), meaning the continuous phase can not evaporate under these conditions [88,92,93].

1.5 Surfactants

1.5.1 Definition of surfactants

All emulsions are metastable systems subject to ageing, like coalescence, flocculation, aggregation, creaming, sedimentation and Ostwald ripening. Thus, additional stabilizers of two-phase emulsions are essential. Name surfactants came from *surface active agents,* representing amphiphilic molecules with high adsorbing properties on the surface interfaces. A typical surfactant molecule consists of a hydrophilic head that adsorbs to the water surface of a droplet and a hydrophobic one (diblock) or two bonds (triblock) with an affinity for the oil phase (**Fig. 8A**).

In biological applications of droplet microfluidics, surfactants are typically soluble in the oil phase. Below specific concentrations (and temperature), surfactant molecules remain uniformly dispersed in the solution and quickly adsorb at the surface of the aqueous droplets. Above a certain saturation point, called critical micelle concertation (CMC), molecules of surfactants form aggregates and micelles (**Fig.8B**)[94].
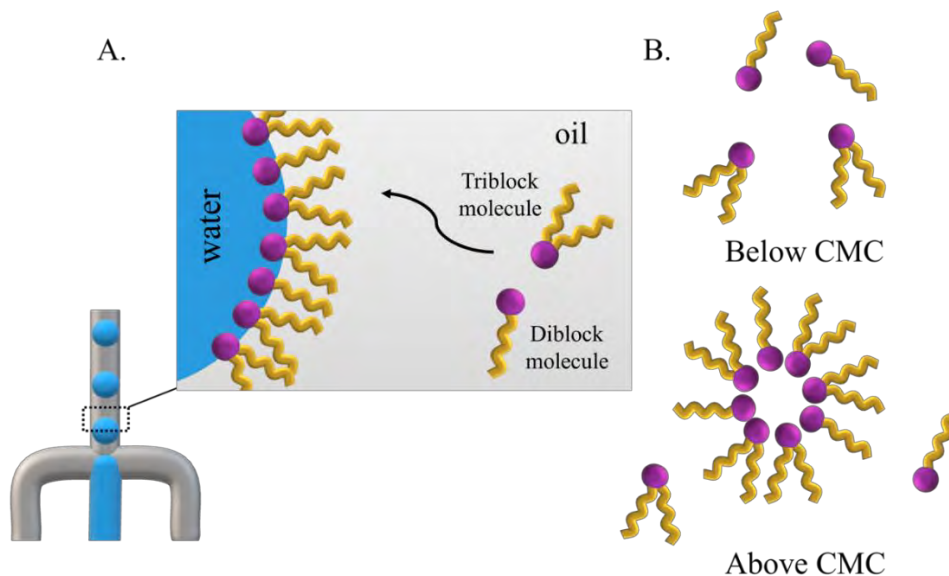
*Fig. 8* *During the generation of droplets, surfactant molecules diffuse to the droplet's surface and stabilize it against coalescence. Typically, surfactants used in microfluidics contain di- or tri- block molecules (or their mixtures). B. Below critical micelle concentration (CMC), surfactants remain uniformly dissolved in the oil; above CMC, surfactants create complexes of molecules called micelles.*

1.5.2 Biocompatibility of surfactants

Finding a suitable surfactant for droplet microfluidics for biological applications can be challenging. Similarly to continuous fluids, surfactants should meet several essential requirements. First, they should dissolve in fluorinated oils (the most popular oils in biological applications), ensure good stability for as long as possible, and not respond to adverse conditions. The physiological environment of biological reactions characterizes high salinity, which may affect the activity of some surfactants. Moreover, the metabolic activity of the growing microorganisms can lead to gas production and pH change, limiting the use of some pH-sensitive surfactants in droplet stabilization. Some reactions, such as PCR, require extremely high temperatures, which drastically affect the stability of the emulsion, becoming a significant challenge for droplet microfluidics. Finally, the cultivation of cells sometimes requires long-term incubation. Thus, surfactants must prevent emulsion coalescence over a long period [56,90,95,96].

Another crucial factor in selecting a suitable surfactant for biological applications is the lack of its toxicity. Some surfactants, as surface-active compounds, significantly affect the physiology and viability of microbial and mammalian cells and have found use as antimicrobial agents. Most possible mechanisms include destabilizing cell membranes, binding to proteins or influencing enzymatic activity [97-100]. Moreover, ionic head groups of surfactants can interact with oppositely charged biomolecules like nucleic acids or proteins (**Fig. 9**). It can lead to the adsorption of those molecules to the droplet's surface and interrupt experiments [101]. Therefore most of the biocompatible surfactants available today are nonionic.
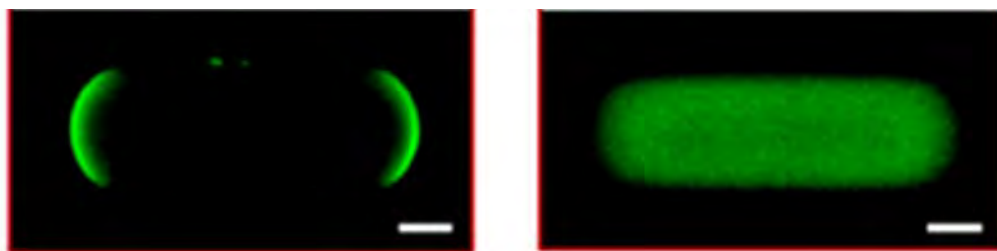
Fig. 9 *The adsorption of fluorescent fibrinogen to the polar head group of surfactant. The left picture represents an example of protein interaction with a surfactant molecule (1H,1H,2H,2H-perfluoro-1-octanol) (accumulation of the fluorescent dye on the surface), and the right image*

shows the reduction of protein adsorption phenomenon by modifying the polar head of the surfactant. The fibrinogen labelled with the fluorescent protein is present in the entire drop volume. Adapted from Spencer Roach et al., Anal Chem, 1; 77(3): 785-796, (2005).

The generation of droplets in microfluidic chips is a fast process (up to mega Hz frequency) [102,103]. Hence, surfactant molecules must be quickly transported and adsorbed to the droplet surface. The surfactant's diffusion time will significantly depend on its molecular weight. Due to this fact, the molecular size of the surfactant needs to be relatively small. Short fluorotelomer tails diffuse fast to the surface, but small surfactant molecules fail in the long-term stability of the emulsion[104-106]. Therefore, it is crucial to choose the ideal molecular weight for the surfactant molecule, which will diffuse rapidly to the surface and ensure the long-term stabilization of the droplets.

### 1.5.3 Reported biocompatible surfactants

All the previously mentioned requirements for appropriate surfactant properties and biocompatibility make finding a suitable surfactant challenging. Perfluoropolyether (PFPE)- base surfactants with different hydrophilic head bonds are the most commonly used in droplets for biological research [104]. Nevertheless, PFPE carboxylic head groups are highly ionic. As mentioned before, ionic heads bind to proteins, are harmful to cells, and thus cannot meet biocompatibility requirements [97,107]. Therefore nonionic PFPE-bond surfactants cannot contain unreacted carboxylic groups as it affects the biocompatibility of the surfactant.

The reaction of a carboxylic group with the amine group of polyethylene glycol (PEG) enabled the creation of one of the first nonionic tri-block fluorosurfactant [97,104]. Many studies have confirmed that PEG-PFPE$_2$ copolymer is biocompatible and highly efficient in long-term incubation of yeast, mammalian or bacterial cells (**Fig. 10**) [20,97,104]. Most recently, PEG-headed fluorosurfactants are one of the most popular, commercially available stabilizers in droplet microfluidics.

However, some properties of PEG-heads limit their appeal in biological applications. First of all, PEG solubility drastically decreases with increasing temperature. PEG-PFPE$_2$ fail to protect droplet stability in reactions performed in elevated temperatures, like PCR [95,108-110]. Furthermore, the

PEG-heads decrease solubility in droplets with high salt concentrations, creating a problem for most biological reactions characterized by high salinity [95,96,109].

Finally, the chemical transport between PEG-PFPE$_2$ stabilized droplets is the biggest concern. Fluorophores like fluorescein or rhodamine can escape and lead to the inter-contamination of droplets [52,96]. All the above forced the microfluidic community to search for new methods for exchanging PEG bonds with other heads. Modifying hydrophilic heads can eliminate previously described problems, the source of which is PEG.
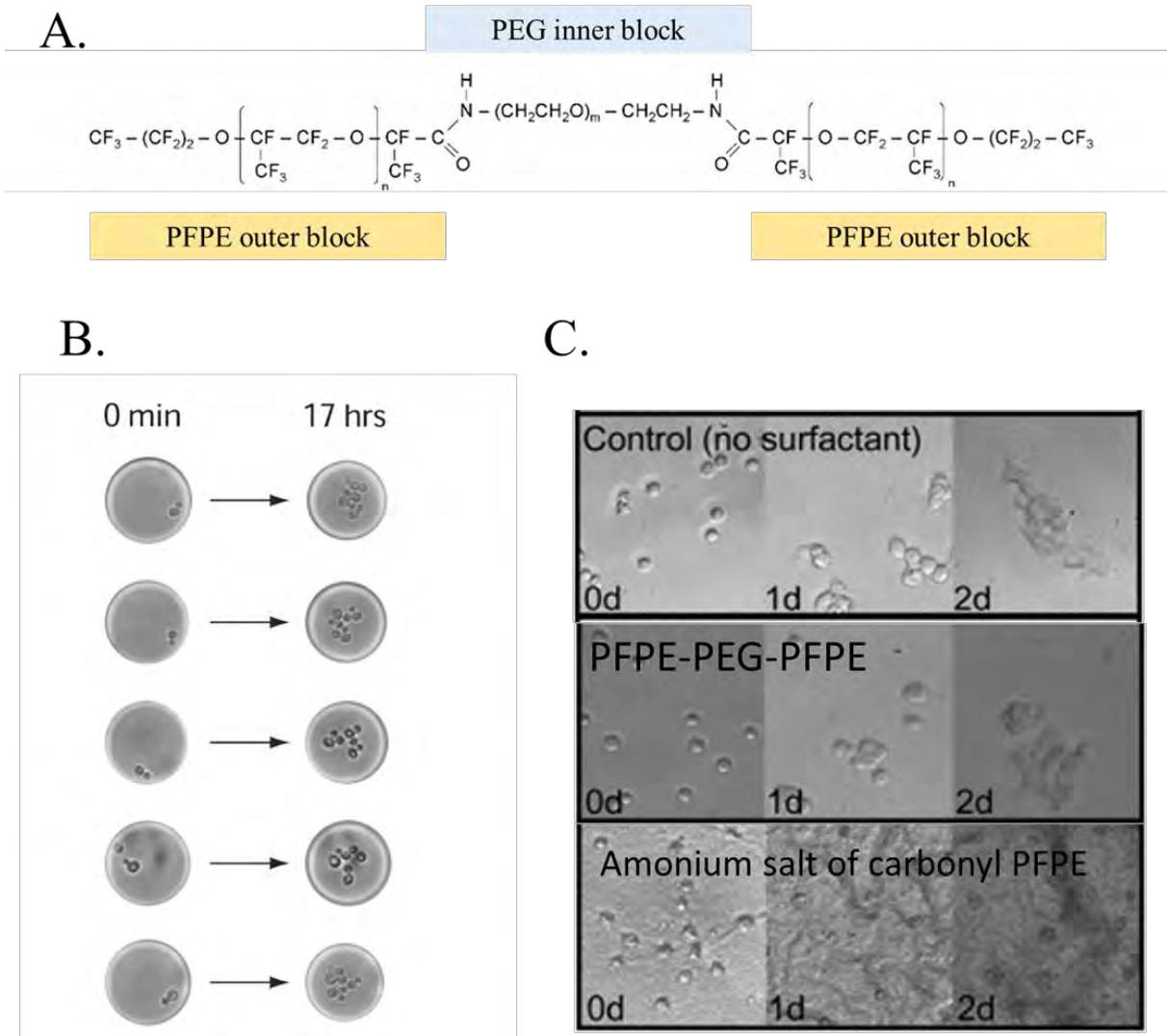
Fig. 10 Biocompatibility of PEG-PFPE$_2$ surfactant. A. The structure of the PEG-PFPE$_2$ triblock molecule of surfactant. B. Yeast cells before and after 17 h of incubation in droplets stabilized with PEG-PFPE$_2$ surfactant. C. HEK293T (mammalian) cells incubated 48h with and without (control) 0.5% w/w PEG-PFPE$_2$ surfactant in FC40. Cells that remain viable do not show any toxic influence of the PEG-PFPE$_2$ surfactant. At the same time, the ammonium salt of carbonyl PFPE exhibit a harmful effect on tested cells and thus does not meet the biocompatibility criteria. Adapted from: A and B- Holtze et al., Lab Chip, 8, 1632-1639, (2008); C- Clausell-Tormos et al., Chemistry and Biology, 15, 427 (2008)
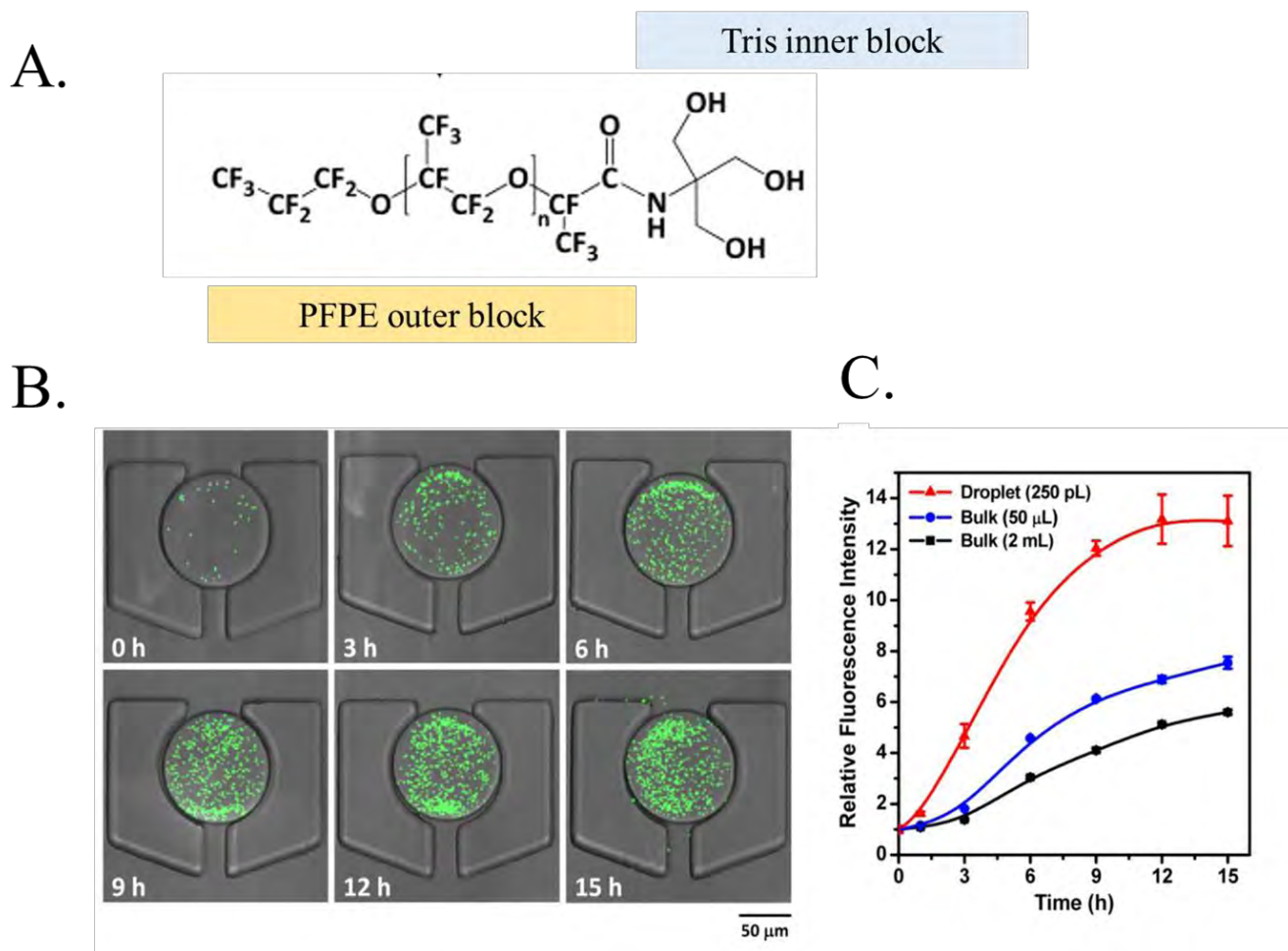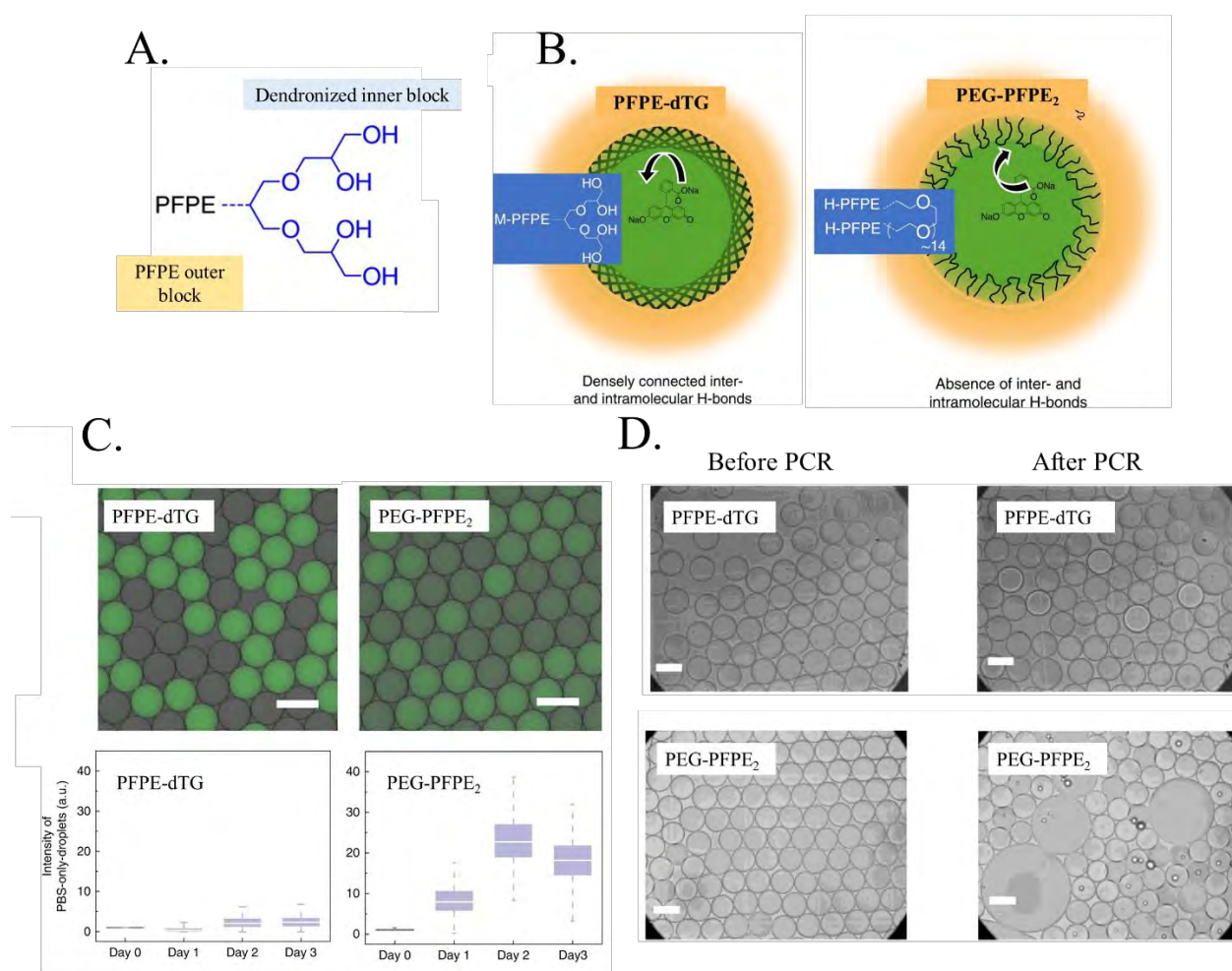
Fig. 11 *Biocompatibility of PFPE-Tris surfactants. A. The structure of the molecule of PFPE-Tris surfactant. B. E. coli expressing green fluorescent protein (GFP) growing in droplet stabilized with PFPE-Tris surfactant during 15h of incubation. C. Proliferation rate of E. coli in droplet microbioreactor is higher than 50 ul and 2 mL bulk cultures. Adapted from Chiu et al., ACS Nano, 8 (4), 3913-3920, (2014).*

One of the alternatives is exchanging PEG head groups with (hydroxymethyl)methyl groups (Tris). Such surfactant does not influence the enzymatic activity of cells and enables long-term cultivation of bacteria in droplets without coalescence (**Fig. 11**) (19). However, leakage of fluorescein salt from droplets stabilized with PFPE-Tris fluorosurfactant has already been reported [110].

Chowdhury et al. demonstrated new, very promising PFPE-bond surfactants with dendronized and linear triglycerol-based headgroups. Those newly synthesized fluorosurfactants provide better thermal stability of emulsions and minimize the inter-droplet transfer of fluorophores [110,111].
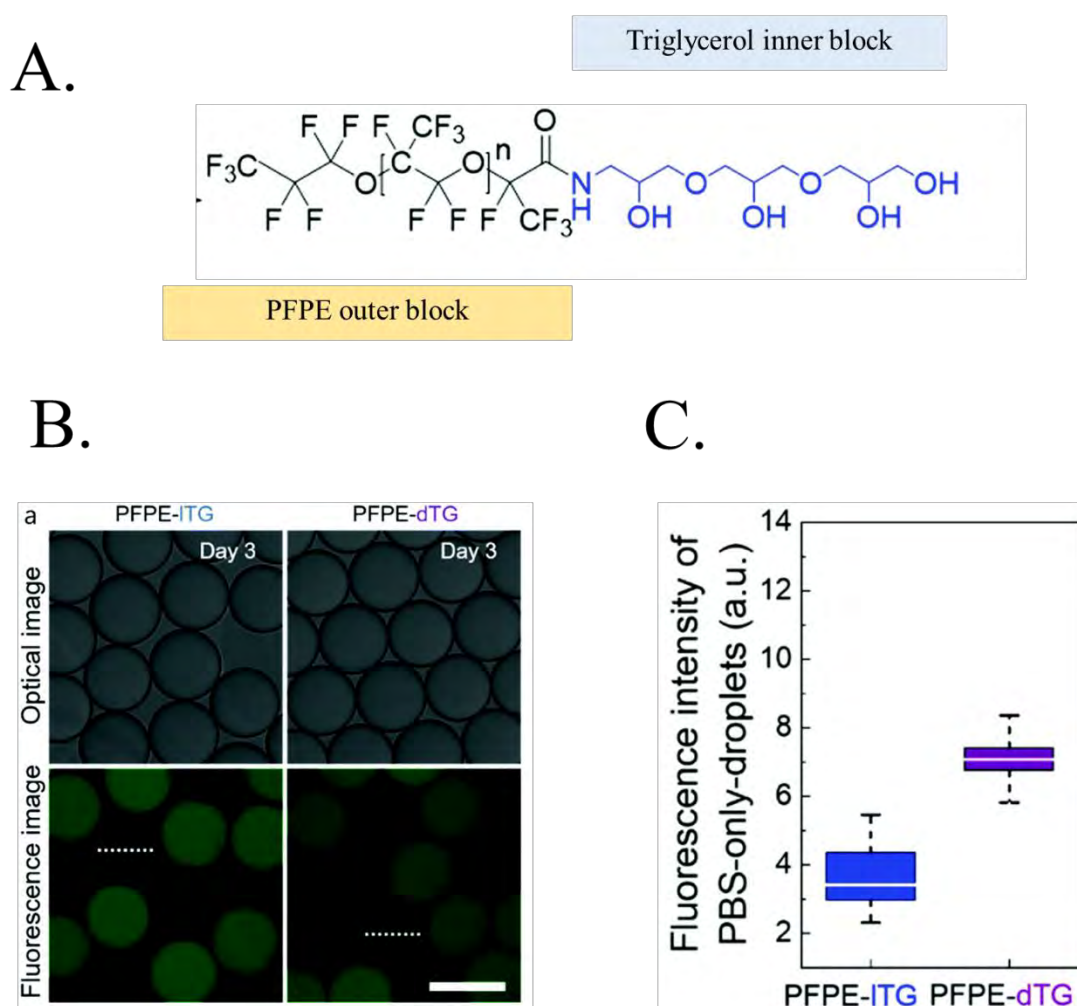
The dendronized fluorosurfactants (PFPE-dTG) consist of four polar hydroxy-groups. Inter- and intramolecular hydrogen bonding between those groups form a dense droplet surface network (**Fig. 12**). This network significantly increases droplet stability in elevated temperatures. Droplets remain stable after PCR, giving these surfactants a significant chance for widespread use in genetic research with microfluidics. Furthermore, dendronized fluorosurfactants significantly limit the transfer of fluorescein between droplets. However, PFPE-dTG does not eliminate the transfer of the doxycycline – a representative of the antimicrobials- indicating a possible problem with using this surfactant in antimicrobial susceptibility testing[110].

Fig.12 *Biocompatibility of dendronized fluorosurfactants. A. Scheme of the chemical structure of dendronized surfactant. B. A dense hydrogen bond network model in dendronized fluorosurfactant (marked as PFPE-dTG) compared to the droplet surface coated with PEG-PFPE₂. C. Long-term droplet incubation with fluorescein salt was stabilized with dendronized (PFPE-dTG) and PEG-PFPE₂.*

Leakage of fluorescein significantly decreases in the case of PFPE-dTG. D. Comparison of thermal stabilization of PFPE-dTG and PEG-PFPE₂. Droplets stabilized with PFPE-dTG remain monodispersed after PCR. Adapted from Chowdhury et al., Nature Communications, 10:4546, (2019).

Another modification demonstrated by Chowdhury et al. was replacing the PEG head with linear triglycerol. Droplets stabilized with the linear triglycerol PFPE diblock surfactant (PFPE-ITG) prevented inter-droplet transport of fluorescent dye even more efficiently than described previously PFPE-dTG. Nevertheless, the authors do not demonstrate its biocompatibility by cell cultivation in droplets (**Fig.13**)[111].

Fig. 13 *Stability of linear triglycerol fluorosurfactant. A. Chemical structure of the molecule of triglicerol- PFPE (marked as PFPE-ITG). B. Long-term incubation of droplets with fluorescein salt stabilized with PFPE-ITG and dendronized-PFPE (PFPE-dTG). C. Intensities os fluorescence from*

neighbouring (PBS) droplets co-incubated with droplets loaded with fluoresceine. PFPE-ITG minimize inter-droplet transfer more sufficiently than PFPE-dTG. Adapted from Chowdhury et al., Soft Matter, 17, 7260-7267 (2021).

Struggles in creating the perfect, biocompatible surfactants have led to many modifications of PFPE. New nonionic di- and tri-block fluorosurfactants increase the stability of the emulsion incubated in high temperatures and limit the inter-droplet transfer of reagents. Several new commercially available surfactants have entered the market. However, each of the recently existing emulsion stabilizers shows some imperfections and is not universally applicable to all microfluidic applications in biology. The fulfilment of some basic assumptions concerning droplet micro-bioreactors (such as emulsion stability in various, often extreme conditions and no leakage of reagents) is impossible with recently available surfactants. Hence, searching for new, biocompatible surfactants is the next milestone in droplet microfluidics.

1.6 Limitations of droplet-based microfluidics

The fundamental requirement of droplet microfluidics is that the droplets present a barrier to transporting chemical ingredients. Recent studies report molecular transport between droplets raising highly relevant questions about the compatibility of droplet-based systems in biological applications. Small molecules like fluorophores, but also DNA (up to 11 000 base pairs) or 100 nm poly(styrene) particles can be prone to leak from aqueous droplets [52,87,96,112-114]. First, like any metastable system, emulsions will strive to achieve equilibrium. Furthermore, emulsions are prone to destruction in some conditions. Ageing processes like coalescence, flocculation, gravitational separation or Ostwald ripening occur naturally in emulsions [115-117]. Moreover, most biological environments are characterized by higher salt concentrations, changing pH or increased temperatures leading to a decreased stabilization by fluorosurfactant molecules [95,109].
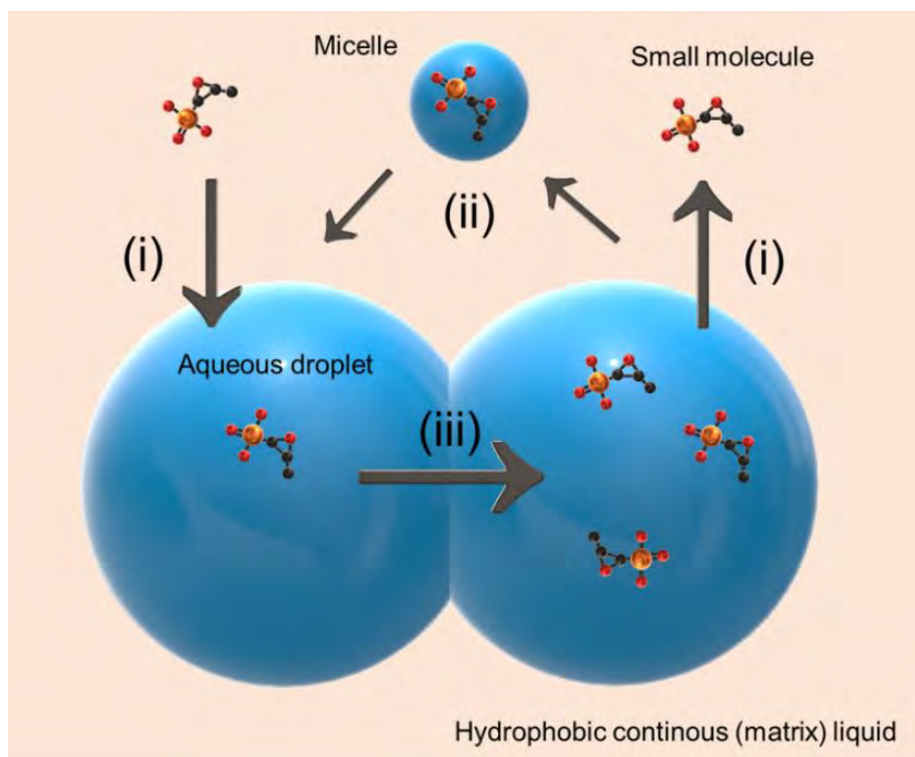

Fig.14 *Possible mechanisms of chemical transport between droplets: i) diffusion to the oil and transport from the oil to the droplet, ii) tiny micelles and or detached satellites, iii) transport between membranes of touching droplets. Published in: Ruszczak A, Jankowski P, Vasantham SK,*

Scheler O, Garstecki P: Physicochemical Properties Predict Retention of Antibiotics in Water-in-Oil Droplets. Analytical Chemistry 2023.

There are various physical ways by which chemicals might escape from droplets: i) diffusion to the oil phase, ii) production of micelles or tiny ripening droplets, and iii) transfer across a bilayer membrane between two droplets contacting each other (**Fig.14**) [52,95,96,116,118,119].

Fluorinated oils, the most commonly used in droplet microfluidics, are extremely nonpolar, so they are unsuitable solvents for most chemical compounds. However, small molecules with a hydrophobic nature will more likely escape from aqueous phases into the oil phase overcoming the surfactant barrier. It possibly explains problems with the retention molecules commonly used in life sciences, like fluorescein, coumarin or resorufin (**Fig.15**) [30,52,53,113,120].
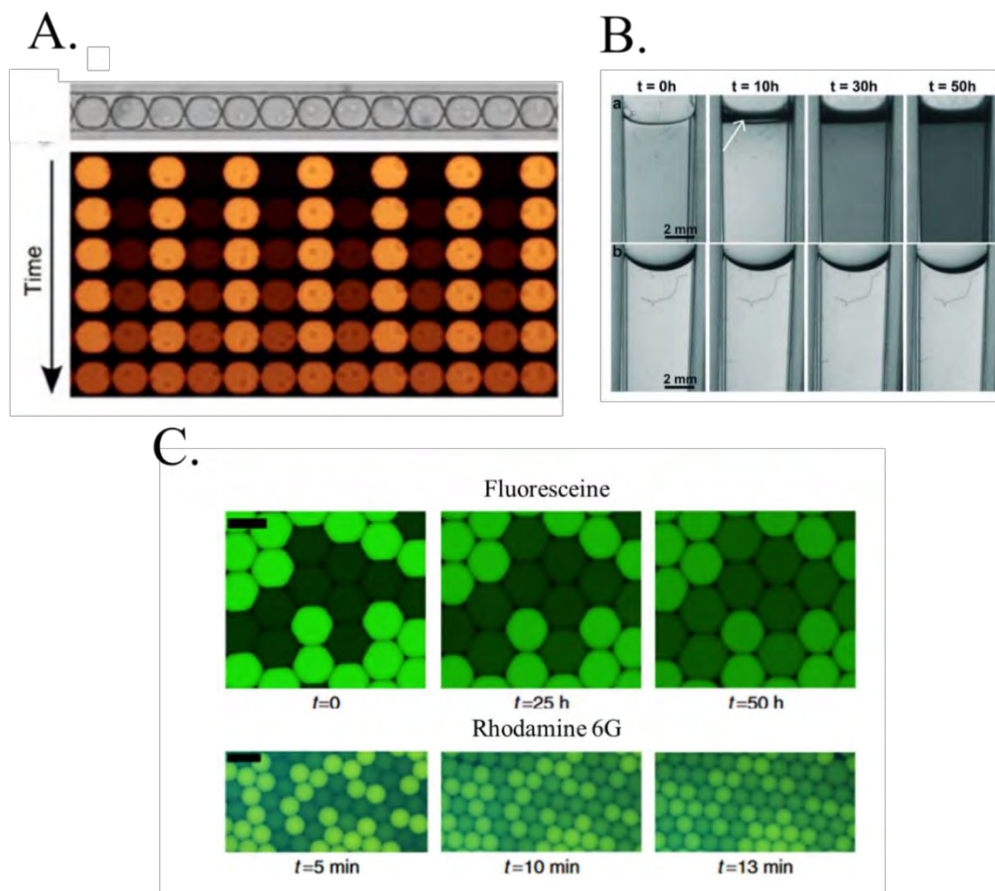
Fig.15 *Evidence of the leakage of fluorophores from droplets. A. Time-lapse photographs of the row of immobilized droplets. Orange signal of fluorescence coming from resorufin. Resorufin escapes from loaded droplets to empty neighbourdroplets after three h (the last row in rows of droplets (the last row represents three h of incubation), B. Spontaneous formation of micelles in HFE 7500 with surfactant FSH 2-Jeffamine900. The white arrow points to the layer of water–oil interface. Lower pictures of HFE 7500 without surfactant serve as a negative control. C. Leakage of fluorescein (upper photographs) and rhodamine 6G between droplets dispersed in HFE 7500 with PFPE–PEG–PFPE surfactant. Rhodamine 6G shows significantly faster transfer to surrounding droplets. Adapted from Gruner et al., Nat Comm, 7:10392 (2016), and Etienne et al., Lab Chip, 18, 3903 (2018).*

Furthermore, most droplet-based systems require relatively high surfactant concentrations (over critical micelle concentration CMC). Together with emulsion ageing, this can result in the spontaneous creation of reverse micelles (Fig. 15B). The literature shows that specific molecules

may be transported between droplets using micelles, capillaries, or even small spontaneously generated droplets. These spontaneously generated droplets can have sizes of up to 100 nm [95,119].

Finally, droplets in a dense emulsion- i.e. when they touch each other- display a tendency to form bilayers- areas of tightly conformal contact between the two surfactant monolayers that protect each of the two droplets in contact. Osmotic pressure and a thermodynamic force drive the diffusional flux of molecules through the membrane. This is yet another mechanism of transferring some chemical compounds between neighboring droplets [52,112,119].

Considering all of the observations made thus far, the magnitude of small molecule transport from droplets and between droplets may be heavily influenced by the properties of these molecules. While managing the retention of active chemicals is critical to the use of droplet systems in analytical studies, transport has so far been studied using model fluorophores [52,53,87,96,110,112,114]. Unfortunately, most antimicrobials are not fluorescent or very weakly fluorescent. However, differences in chemical structure between antibiotics and fluorophores exclude the possibility of comparing them.

1.6.1 Avoiding molecular transport between droplets

As the leakage affects mostly small hydrophobic molecules, chemical modification of the reagents seems to be one of the solutions for molecular leakage from droplets. For instance, changing the sulfonate groups on coumarin significantly reduced the transfer rate, increasing incubation time in droplets from hours to days[120]. Larger molecules will become less likely to overcome the surfactant barrier due to the higher required energy [121]. Moreover, additives like bovine serum albumin (BSA) or sugar derivatives increase droplet retention [51,122].

The choice of surfactant should also depend on the chemical composition of the droplets. It was demonstrated that the stability of droplets with different salt concentrations highly depends on the length of the PEG chain [95]. Furthermore, the surfactant's concentration can significantly influence the rate of micelle formation and thus accelerate the chemical leakage. Decreasing surfactant concentration can help reduce cross-contamination between droplets [30,112,122]. At the same time, studies show that increasing surfactant concentration decreases the gas

transport between droplets. Bacteria growing in droplets produces respiratory gases, which can lead to instabilities of emulsions with low concentrations of surfactant [90].

Numerous scientific studies show that the fundamental microfluidic assumption of treating the droplet as a separate, non-contacting laboratory tube might be incorrect. Everything mentioned above proves that microfluidics users must be cautious when planning experiments in the droplet format. Despite the dynamic development of droplet techniques, there is not enough research to optimize these techniques to increase their accuracy in microbiology. It seems necessary to investigate how the droplet environment influences the essential life functions of microorganisms and whether the cross-talk of droplets may influence the results of experiments.

1.7 The aims and objectives

Over the past 20 years, many microbial assays have been demonstrated in droplet-microfluidic format. While there is no consensus or established standard for such droplet-microfluidic assays, the majority of the reported studies share three typical features: i) with very few exceptions, all of these assays use fluorinated oils (either FC 40 or HFE 7500) as a continuous phase liquid and ii) one of the few commercially available fluorosurfactants are employed to stabilize the oil-water interface and prevent coalescence of the aqueous droplets. Finally, iii) determining the microorganism's viability is usually fluorescent-based, where metabolic marker molecules, especially resazurin, are added to the encapsulating aqueous medium.

The above-described typical microfluidic assay nevertheless has a few drawbacks. From a thermodynamical point of view, the water/fluorocarbon oil/fluorosurfactant ternary system is metastable. While surfactants hinder the coalescence of droplets by their steric repulsion at the oil-water interface, the emulsion may still be prone to age via Oswald ripening, where smaller droplets having higher Laplace pressure than the larger ones tend to dissolve in the larger droplets leading to an increase in of droplet size in time and coarsening the emulsion. This mechanism is possible only when the dispersed phase is even slightly soluble in the continuous phase.

Another possible issue is the molecular transport of the solute of the dispersed phase. This transport can occur in the continuous phase either directly by phase partitioning or via surfactant micelles of the continuous phase. Moreover, the solute of the disperse phase can be transported even between two aqueous droplets through surfactant bilayers which may form when two droplets come to close contact.

Both ageing and mass transport may significantly alter the outcome of the microfluidic droplet assay, leading to distorted or false results and questioning the reliability and applicability of such assays in clinical trials.

To date, these limitations of droplet microfluidic assays were demonstrated only using certain fluorescent molecules. Whether antibiotics are prone to "leak" (i.e. molecular transport from the aqueous phase to the oil phase) or to transport between droplets is yet to be uncovered.

Goal #1: Investigate if the modified version of metabolic marker molecule resorufin outperforms the conventionally used form and if such modified dye can be reliably used for microbial growth assays in droplets

Objective #1: Examine the time required for the detection of positive droplets (bacteria-loaded) incubated with resazurin and its derivative dodecylresazurin

Objective #2: Determine the duration of the time for differentiation of positive droplets incubated with resazurin and dodecylresazurin

Objective #3: Analyze and compare the performance of resorufin and C12R as markers of bacterial metabolism in micro-droplet assays by comparing selectivity, specificity, and signal-to-noise ratios for both assays

Goal #2: Determine the physicochemical parameters that can be used to predict antibiotic leakage between water-in-oil droplets and propose a predictive guideline for limiting inter-droplet transport of antibiotics

Objective #1: Finding leakage profiles of 15 antibiotics in microbial viability assay in droplets

Objective#2: Find a correlation between 36 parameters concerning the hydrophilic/hydrophobic nature of the molecules and the leakage of antibiotics

Objective #3: Build a model of the prediction of the molecular leakage of antimicrobials for over 100 antibiotics and to test the correctness of the model by experiments with three random antibiotics

Objective #4: Investigate whether other than physicochemical factors (concentration of the antimicrobial, mixing of the sample) influence the rate of the leakage

2. The leakage of resorufin-based metabolic markers from droplets

Chapter 2 is prepared based on the publication: Scheler O, Kaminski TS, Ruszczak A, Garstecki P: Dodecylresorufin (C12R) Outperforms Resorufin in Microdroplet Bacterial Assays. ACS Appl Mater Interfaces 2016, 8:11318-11325.

Author Contribution: A.R. and O.S executed the experiments. O.S. and T.S.K designed the experiments. O.S. analyzed the data. O.S., T.S.K and P.G. conceived the idea.

2.1 The aim of the study

Dodecylresorufin ($C_{24}H_{31}NO_4$ - C12R) is a resorufin derivative with comparable fluorescence characteristics. Previous research has revealed that C12R is kept stable for longer in aqueous droplets [123]. The performance of resorufin and C12R in bacterial tests in nanoliter monodisperse droplets was comprehensively assessed in this study. C12R is characterized by improved retention in droplets, which is surprising given that its molecule is more nonpolar than resorufin salts and is thus predicted to leak into the oil phase. The possible mechanism of better droplet retention can be related to better cell permeability and in-cell storage (**Fig.16**). In this chapter, resorufin and C12R were compared as markers of bacterial metabolism in droplet-based assays.
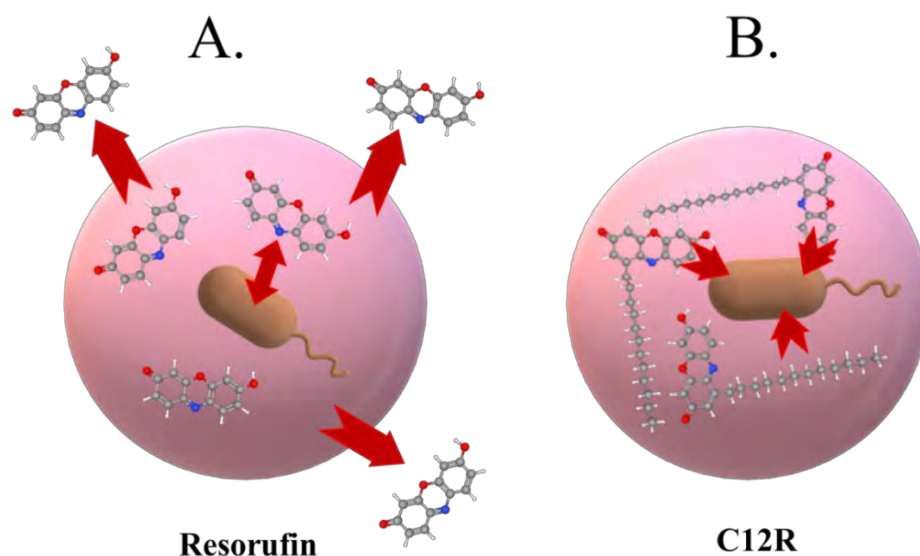
Fig.16 *Hypothetical explanation of the reason for better retention of C12R in droplets. A. After reduction by the metabolic activity of aerobic bacteria, resorufin escapes the cell to the aqueous solution of the droplet and can quickly leave the droplet. B. C12R is more lipophilic and is kept inside the cell longer. C12R can escape the droplet only when the bacterium dies.*

2.2 The method for the comparison of resorufin and C12R retention in droplet-based systems

The two marker dyes (resazurin and dodecylresazurin) were utilized to distinguish between positive (bacteria-containing) and negative (empty) droplets. The aerobic metabolism of bacteria transforms both dyes into intensely fluorescent compounds. Viability markers were used at 50 μM, comparable to the concentrations at which resazurin has been used in droplet microfluidic systems [26,32,124].

In the experiment, two different microorganisms were used: *Escherichia coli*, which expressed Enhanced Green Fluorescent Protein (EGFP) and *Enterobacter aerogenes*, a non-labelled strain. The fluorescent signals from GFP have served as an additional control for the influence of metabolic markers on the viability of bacteria incubated in droplets. Singel-cell bacteria have been encapsulated in 1 nl droplet with growth medium, and viability markers using the classical flow-focusing chip described previously by Kaminski et al. [125]. The inoculum of bacteria has been adjusted to receive around 20% of positive droplets in the final experiments (except for experiments on the influence of inoculum densities on the leakage – *Section 2.5*). In such conditions, approximately 18% of all positive droplets will contain a population that arose from a single cell. At the same time, around 2% will have more than one mother cell [46].

Fluorinated oil HFE 7500 enriched with 2% (w/w) $PFPE_2$-PEG surfactant served as a continuous phase. The surfactant concentration drastically increases the leakage of chemistry from the droplet reactor, as demonstrated in the literature [30,52,87,112]. Nevertheless, surfactant concentration remained at a high dose, as the experiments with lower concentrations failed due to problems with the stability of emulsions. Moreover, other droplet-based bacterial cultivation methods typically apply high concentrations of surfactants. Hence 2% of surfactant concentration serves as the universal representative condition for droplet-based platforms for bacterial cultivation.

The emulsion was generated in a flow-focusing device, collected in Eppendorf-type tubes and incubated at 37°C over different incubation times. After incubation, droplets were analyzed using a separate chip placed under the confocal microscope. The detection chip was designed to enable the separation of droplets by the flow of an additional portion of the oil from perpendicular

channels. As a result, droplets spaced by oil flowed to the detection area and were scanned by laser at the 561.7 nm excitation wavelengths (**Fig. 17**). The intensity of fluorescence emitted from droplets was measured at the different incubation times (from 3 to 24h, depending on the sample type).
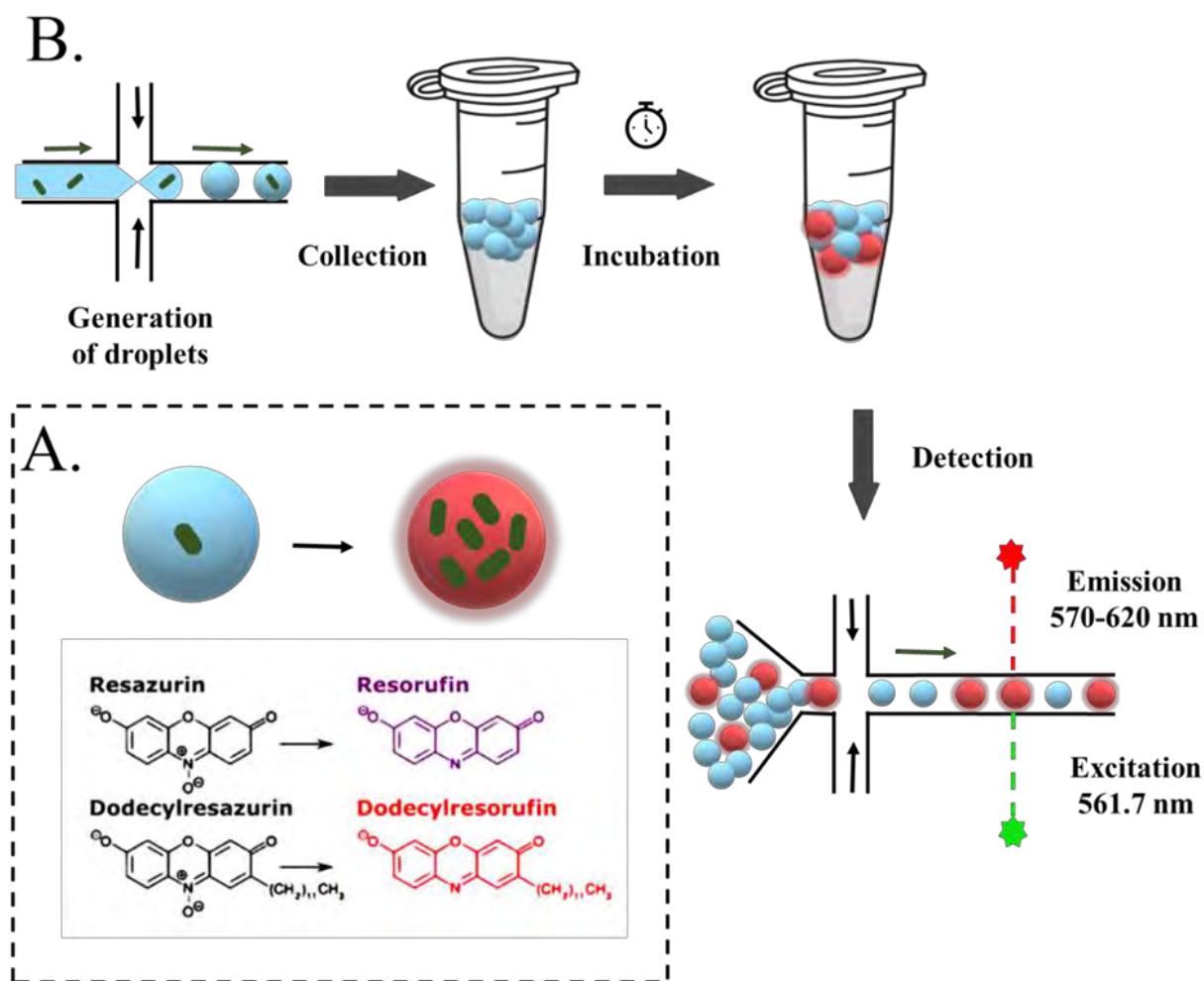
Fig. 17 *Viability detection and schematics of an experiment. A. Both resazurin and dodecylresazurin are reduced into fluorescent resorufin-based forms after reduction by bacterial activity in positive droplets. B. Bacterial cells were encapsulated with growth medium and viability markers (resazurin or dodecylresazurin) into one nanoliter droplets by the classical flow-focusing generator. Droplets suspended in HFE 7500 oil with 2% PFPE$_2$-PEG surfactant have been collected and incubated in the*

Eppendort-type tubes. The fluorescence detection was at different time points by scanning a single droplet flowing into the narrow channel of the detection chip. The detection chip separated droplets by the stream of oil through the additional junctions. A confocal microscope has performed the final readout by recording fluorescence signals of droplets flowing to the scanning area (excitation/emission wavelengths: 561.7 nm/570-20 nm).

## 2.3 The influence of resorufin and C12R on the viability of the cells

The fluorescence intensity in bacteria-loaded droplets differs in droplets with different type of viability markers. Positive signals from dodecyloresazurin samples arise considerably slower and have lower intensities. Droplets set with resazurin were positive after four h of incubation with *E. coli* and three h in the case of *E. aerogenes*. At the same time, C12R was allowed to distinguish positive droplets after five and four h of incubation with *E. coli* and *E. aerogenes*, respectively (**Tab.1**).

Tab. 1 *The time of incubation required to discriminate between positive signals and the background (negative droplets)*

	Resorufin	C12R
E. coli	4h	5h
E. aerogenes	3h	4h

The delay in incoming signals from C12R can be due to its molecular structure. The possible explanation is that the long hydrocarbon tail makes the compound highly lipophilic and can lead to lower reactivity with the reducing enzymes. Moreover, the chemical structure can lead to differences in the fluorescence properties. The fluorescence of resorufin is more robust, and it is thus easier to distinguish from the background. Moreover, dodecyloresazurin, with its strong nonpolar nature, can dissolve in a continuous phase, leading to its local decrease in the droplets. After escaping to the oil phase, dodecyloresazurin loses its fluorescent activity, so it can't be visualized [126].

Finally, it can be possible that both dyes can possess low toxicity to bacterial cells, leading to a decrease in the multiplication rates. The increase of fluorescent signals from GFP-producing bacteria encapsulated with resazurin and dodecylresazurin was compared to address this question. There were no significant differences in bacterial growth between the two tested molecules, as shown by a consistent rise in the GFP signal in droplets over time (**Fig.18**). Hence the negative impact of C12R on bacterial viability was ruled out.

GFP signal increase in droplets over time
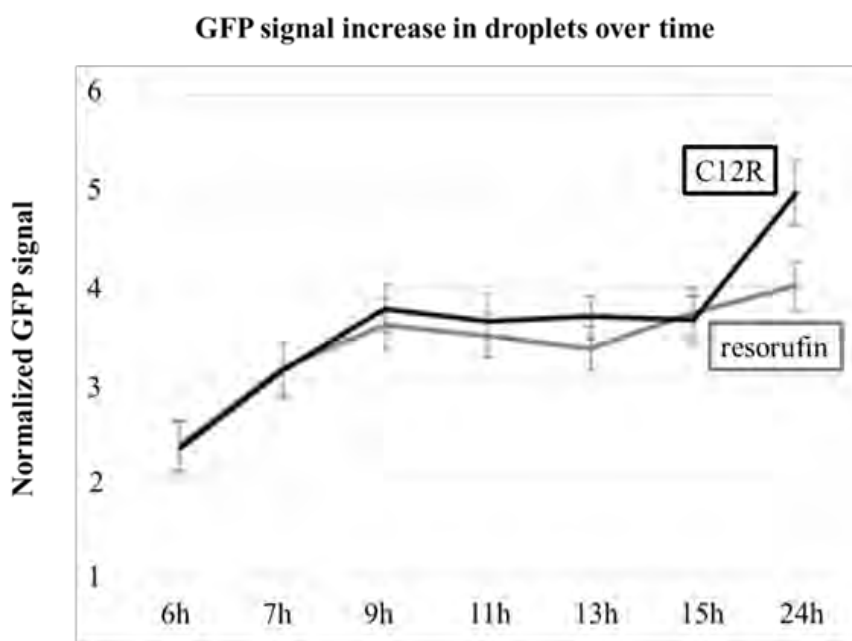
Fig.18 *Increase in GFP signals from droplets with different dyes (resorufin and dodecylresorufin). Both signals: GFP and resorufin-based signals arise at the same rate. The graph shows Median Absolute Deviation (MAD) values as error bars. Published in: Scheler O, Kaminski TS, Ruszczak A, Garstecki P: Dodecylresorufin (C12R) Outperforms Resorufin in Microdroplet Bacterial Assays. ACS Appl Mater Interfaces 2016, 8:11318-11325.*

2.4 Time-dependent leakage of C12R and resorufin to inner droplets

Long-term incubation of resazurin and dodecylresazurin was performed with two different species of bacteria: *E. coli* and *E.aerogenes,* to compare the minimal times required for the detection and times of the retention of the dyes in the droplet. Although the use of C12R requires a longer time for incubation to obtain the first positive signals, it enables significantly more prolonged incubation and reduced leakage (**Fig.19**). As demonstrated previously, resorufin has a strong tendency to escape from droplets. After prolonged incubation, the fluorescence of resorufin diminished due to the dye's leakage into empty droplets. After nine hours of incubation with *E. aerogenes*, resorufin could not distinguish between empty and bacterial-loaded droplets. The overall fluorescence signal from resorufin in the emulsion was averaged due to the leakage of the dye to inner droplets. At the same time, using C12R provides signals significantly more stable in time, which enables accurate differentiation between negative and positive droplets even in cultures incubated longer than 15h. This observation proves the expectations that the retention of C12R in droplets is better than the commonly used resorufin (**Fig.20**).
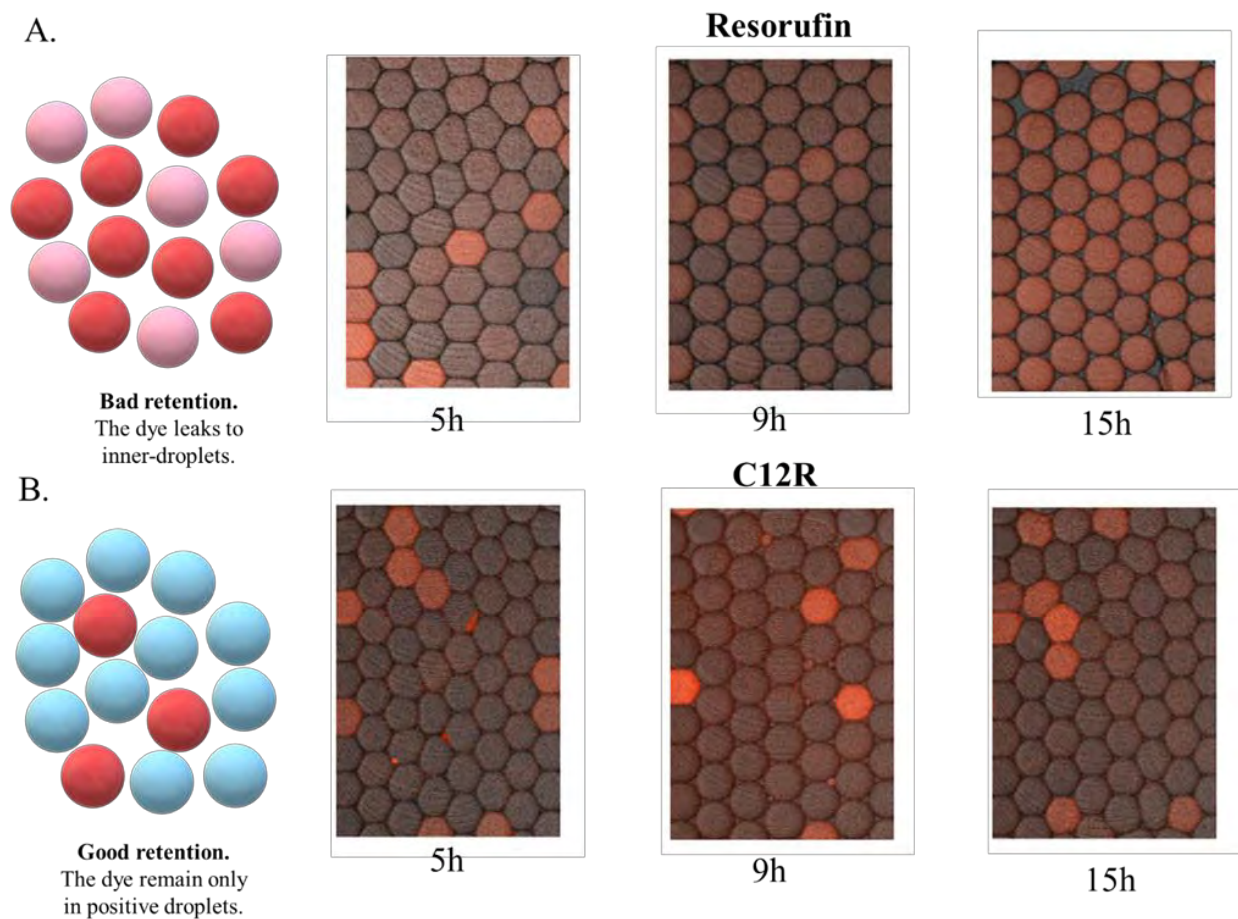
Fig.19 *The difference in the retention of resorufin and C12R in droplets with E. aerogenes. A. Resorufin represents the molecule with bad retention in droplets. After nine h of incubation, resorufin leaks from the positive into the negative droplets. Consequently, all droplets in the sample increase the fluorescence intensity. B. The transfer of C12R to the inner droplets is decreased. Only positive droplets remain fluorescent.*
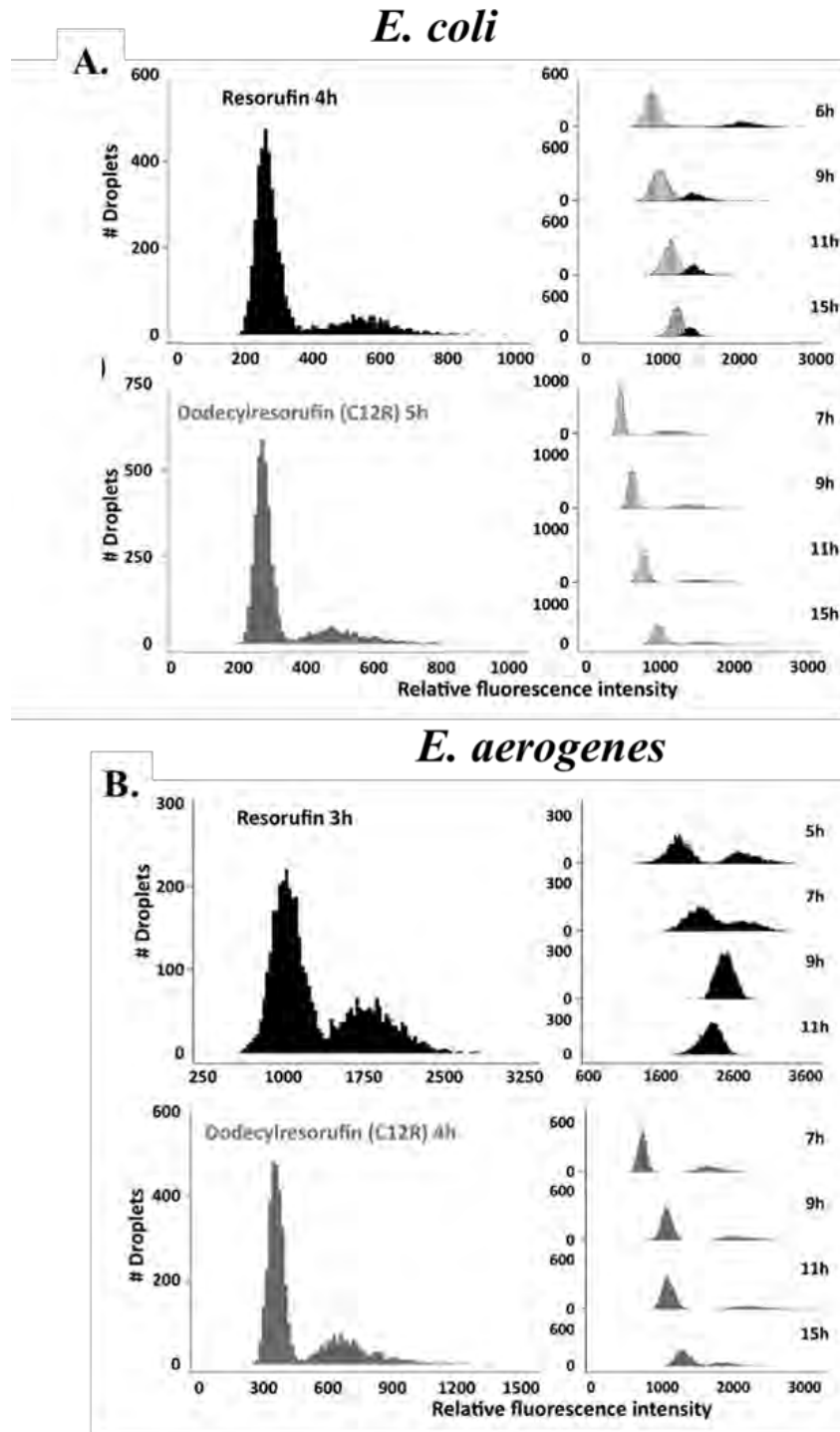
Fig.20 *Histograms with the distribution of the droplet fluorescence monitored at different incubation times. X-axes represent the relative fluorescence of the droplet, and Y-axes show the number of droplets with a particular fluorescence intensity. A. Histograms of intensities of droplets*
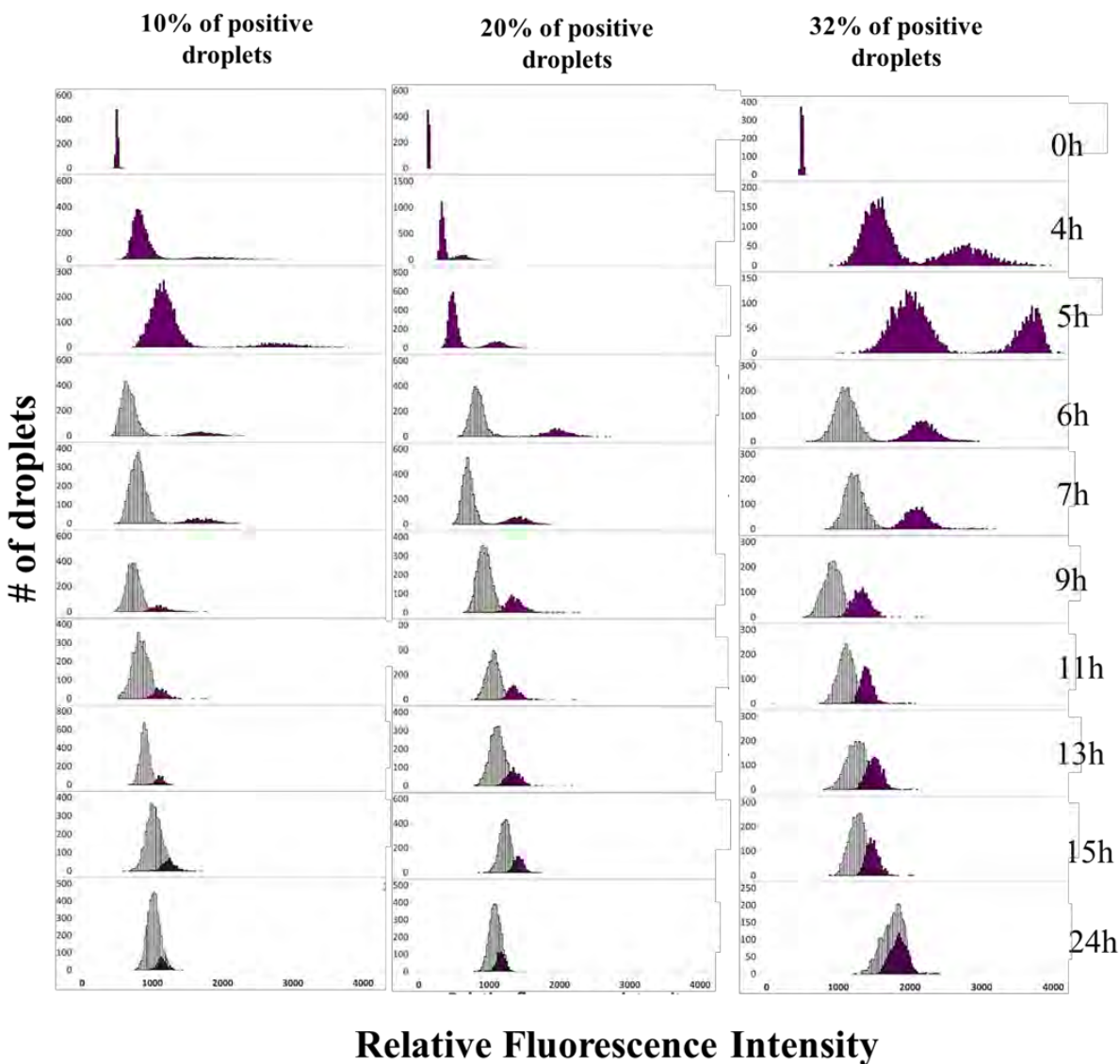
with E. coli, B. Intensities of droplets with E. aerogenes. The histograms show two separate peaks. The leftmost peak, in lower values, represents the empty population of droplets. The right, smaller peak corresponds to droplets with higher fluorescence values from viable bacteria (positive droplets). In the case of resorufin, prolonged incubation leads to increased fluorescence in negative droplets. Thus, the fluorescence peak in the negative droplet fraction moves toward the average intensities values. Published in: Scheler O, Kaminski TS, Ruszczak A, Garstecki P: Dodecylresorufin (C12R) Outperforms Resorufin in Microdroplet Bacterial Assays. ACS Appl Mater Interfaces 2016, 8:11318-11325.

2.5 Influence of the number of the positive fraction of droplets on the leakage rates

Various densities of *E. coli* were encapsulated to investigate if the number of positive droplets could influence the course and results of the experiment. Different fractions (10, 20 and 32%) of positive droplets were incubated with resazurin and dodecylresazurin, and intensity profiles of droplets at different time points were compared. After 24h incubation, the average signal from droplets moved toward higher intensities in emulsions with higher proportions of positive droplets (**Fig.21 and 22**). This experimental observation is in good agreement with the leaky droplet-based theoretical study that was described by Chen et al.. The authors of this work modelled the signal leakage between droplets in two-dimensional space. Their model showed that the leakage into negative droplets is related to the number of positive neighbors [113]. Bacteria-loaded droplets serve as reservoirs of resorufin. Hence, the more positive droplets in the sample, the faster and more efficient cross-contamination of droplets.
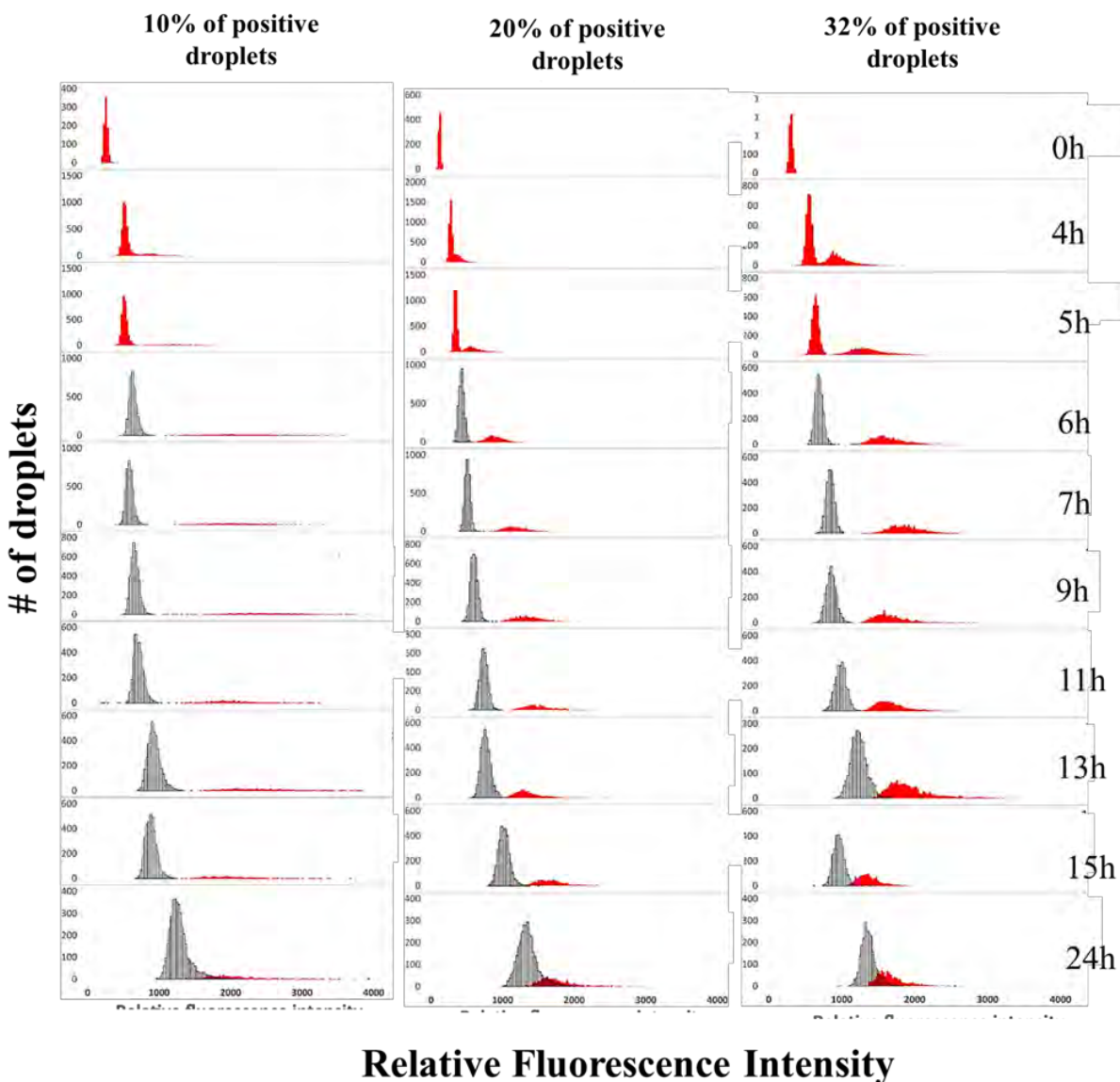
Fig.21 *Histograms represent the numbers of droplets with the different fluorescent intensities of C12R. Three samples differ in the fraction of droplets with encapsulated E.coli (from left: 10, 20, and 32%). Grey histograms represent signals from negative droplets, red histograms represent signals coming from droplets with bacteria and C12R. Time points from 0 -5 are marked with one color only, due to the fact that this time was too short to visualize bacteria by GFP detection. Published in: Scheler O, Kaminski TS, Ruszczak A, Garstecki P: Dodecylresorufin (C12R) Outperforms Resorufin in Microdroplet Bacterial Assays. ACS Appl Mater Interfaces 2016, 8:11318-11325.*

Fig.22 *Histograms represent the numbers of droplets with the different fluorescent intensities of resorufin. Three samples differ in the fraction of droplets with encapsulated E. coli (from left: 10, 20, and 32%). Grey histograms represent signals from negative droplets; violet histograms represent signals coming from droplets with bacteria and resorufin. Time points from 0 -5 are marked with one color only, due to the fact that this time was too short to visualize bacteria by GFP detection. Published in: Scheler O, Kaminski TS, Ruszczak A, Garstecki P: Dodecylresorufin (C12R) Outperforms Resorufin in Microdroplet Bacterial Assays. ACS Appl Mater Interfaces 2016, 8:11318-11325.*

2.6 Sensitivity and specificity of the assay

Test results generated by an analytical method are considered accurate if they are in good agreement with the actual value. The accuracy of a test may be quantified in terms of its sensitivity and specificity [113]. The "sensitivity" of the assay is defined as the rate of all true positive samples categorized correctly as positive. On the other hand, the term "specificity" refers to the fraction of all negative droplets correctly ranked as negative. For example, in the assay with 100 tested droplets, ten of the total population of droplets contain bacteria (positive droplets). At the endpoint of the experiment, 12 positive droplets were detected by the method (among which eight were discriminated correctly and four false positives). In such a scenario, two truly positive droplets were identified as negative (false negatives). The sensitivity of this assay is (10-2)/10=80%, and the specificity is (90-4)/90=~96%.

Since the marker dye diffuses from positive droplets to surrounding negative droplets over time, sensitivity and specificity decrease in leaky droplet tests. As a result, true positive droplets might be interpreted as false negative due to their reduced fluorescence, and *vice versa.* The fluorescently active molecules are transferred to negative droplets, which can generate an incorrect positive interpretation.

The accuracy of the two marker dyes in differentiating between the positive and negative droplets was estimated using Receiver Operating Characteristic (ROC) curves. The ROC curve is a standard method for illustrating a test's accuracy value. True Positive (sensitivity) and False Positive (1-specificity) rates are plotted to generate the curves. When the test is accurate, the ROC curve is closer to the top left corner and slopes downward toward the diagonal "Non-discrimination" line when the assay is erroneous [113,127,128]. The ROC curves of resorufin and C12R at various *E. coli* incubation times are compared in **Fig. 23**. Since the curves in C12R are constrained to the top left corner of the experiment, it is possible to achieve greater accuracy of the assay with time. A decrease in assay accuracy may be seen in the position of the resorufin curves, which are becoming closer to the diagonal "non-discrimination" line.
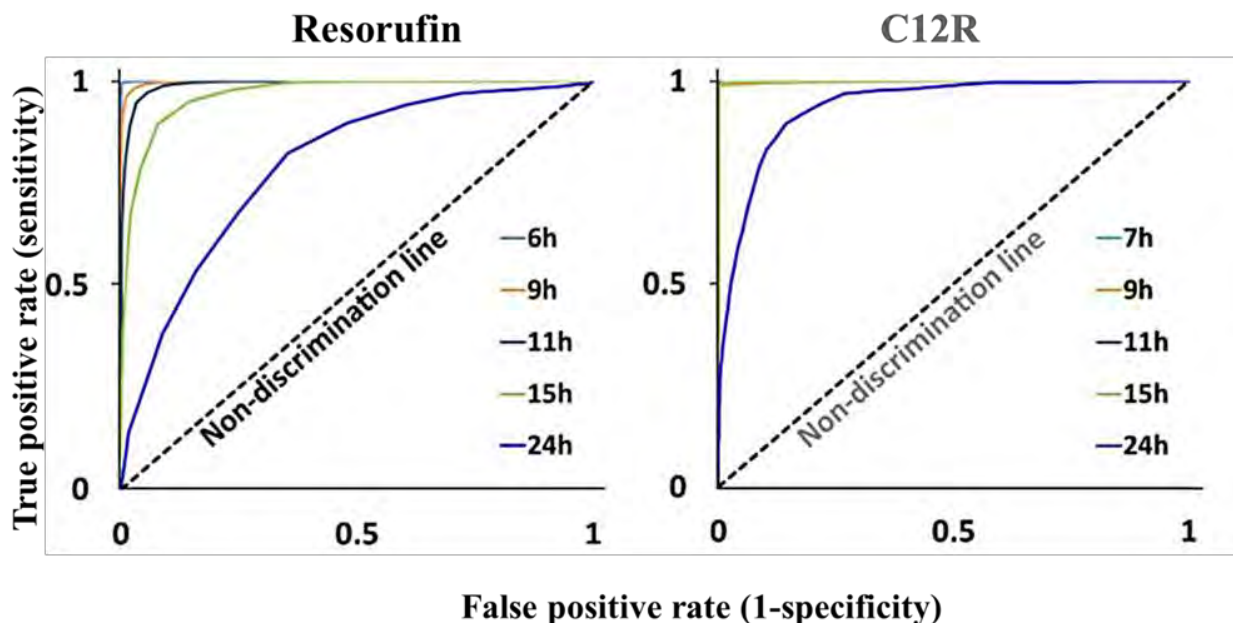
Fig.23 *Receiver Operating Characteristic (ROC) curves with resorufin and C12R after different incubation times ranging from 6 to 24h. The X-axis shows False positive and Y-axis true positive rates. Curves close to the upper left corner are accurate, while getting closer to the diagonal "No-discrimination line" shows inaccuracy. Published in: Scheler O, Kaminski TS, Ruszczak A, Garstecki P: Dodecylresorufin (C12R) Outperforms Resorufin in Microdroplet Bacterial Assays. ACS Appl Mater Interfaces 2016, 8:11318-11325.*
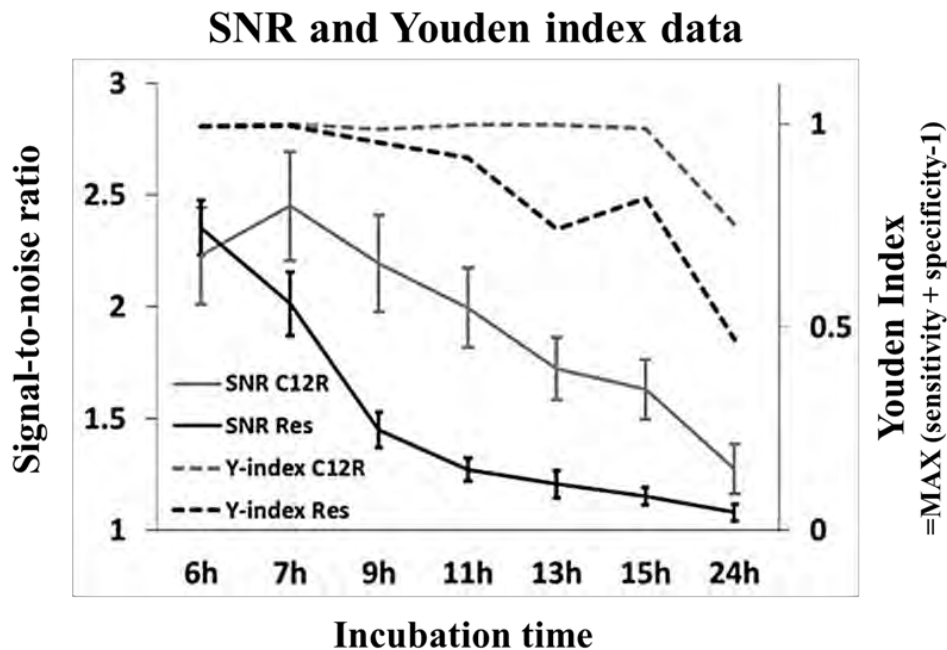
2.7 Youden Index Scores and Signal-to-Noise Ratio (SNR) for the comparison of the accuracy of the assays

To further the understanding of ROC curves, the Youden index (J) was determined using the formula: J = sensitivity + specificity - 1. The range of the dimensionless Youden index is 0–1. When the ROC curve is near the diagonal no-discrimination line, J=0, indicating that the test does not discriminate droplets (thus failing in the accuracy). The value J=1 means that the assay has excellent sensitivity and specificity. In most cases, high J values indicate reliable droplet-based assays [113,128-130].

The Youden index values for both marker dyes over many time intervals are shown in **Fig. 24**. C12R has better accuracy than resorufin because the J value remains close to 1

for most of the experiment and begins to drop significantly only at the 24 h checkpoint. In the case of resorufin, the slope of the curve might be seen as early as seven hours.

The signal-to-noise ratio (SNR) is another crucial factor used in this work to compare accuracy in droplet-based experiments. SNR indicates the dissimilarity between the fluorescence levels of droplets with and without microorganisms. Droplet fluorescence intensities were recorded for both positive and negative droplets, and their median values were used to produce the SNR values for the resorufin and C12R experiments. In **Fig. 24** black line represents the resorufin SNR values, and the grey line represents the C12R SNR values. These results show that the C12R had a better SNR than resorufin during most of the incubation duration, except for the first six hours of incubation, when the two were about equal within the margin of error.

Fig.24 *Youden index and signal-to-noise ratio (SNR) data for both marker dyes after different incubation times. Youden index shows the combined value of sensitivity and specificity (it is presented as dotted lines on the secondary axis). SNR values are shown on the primary axis as median fluorescence intensity ratios of positive droplets to empty droplets. Error bars indicate +/- 1 median absolute deviation (MAD). Published in: Scheler O, Kaminski TS, Ruszczak A, Garstecki P:*
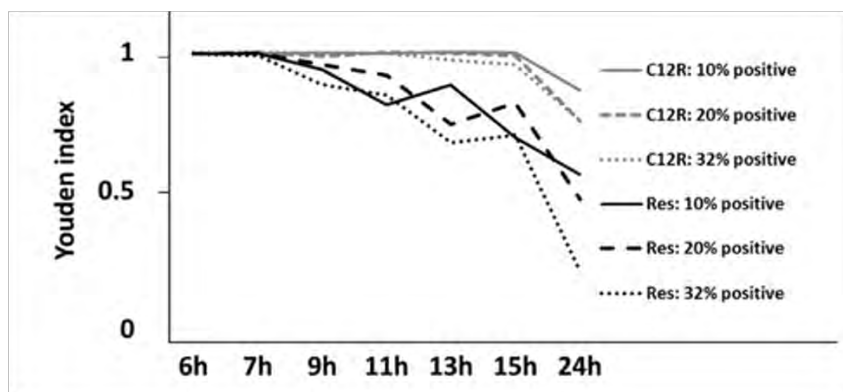
Dodecylresorufin (C12R) Outperforms Resorufin in Microdroplet Bacterial Assays. ACS Appl Mater Interfaces 2016, 8:11318-11325.

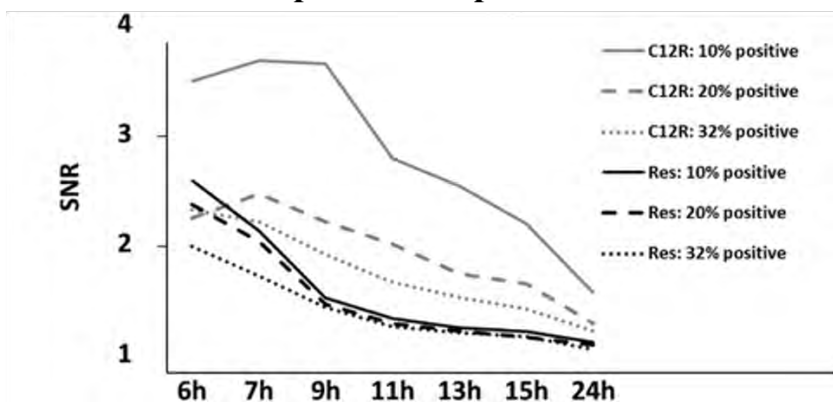## 2.8 Youden Index Scores and Signal-to-Noise Ratio (SNR) at various concentrations of bacteria

Next, the accuracy of both resorufin and C12R was tested for different fractions of bacteria-containing droplets. The outcomes of the previous experiment (within 20% of droplets containing *E. co*li) were compared to those obtained with droplet emulsions containing 10% and 32% positive droplets. The Youden index for both dyes at various bacterial concentrations is shown in **Fig. 25**. C12R results (grey lines) are more accurate than resorufin results (black lines) across the board for bacterial concentrations. C12R shows excellent accuracy, as its J values stay near one at all concentrations over 15 hours of the experiment. In contrast, for resorufin, the J value decreases after seven hours of incubation with all bacteria concentrations.

An in-depth examination of the Youden index data revealed that the loss of specificity with time is often more than the loss of sensitivity for both dyes. This shows once again how the leaking of dye from positive droplets (which is more pronounced with resorufin) boosts the fluorescence of empty droplets, raising the fraction of false positive results. Moreover, the SNR of both dyes at various bacterial concentrations were examined. SNR ratios for resorufin (black lines) and C12R (grey lines) at varied bacterial concentrations and incubation periods are shown in **Fig. 25**. C12R exhibits greater SNR values than resorufin for all three evaluated fractions of droplets with bacteria following various incubation durations. The SNR levels in a 20% positive droplet experiment were comparable only to a maximum of six h incubations. After that time, SNR for 10% of droplets with C12R significantly exceeds other values. These findings confirm that C12R consistently outperformed resorufin in our studies.

A. Youden index at different positive droplet fractions

## B. Signal-to-noise ratios (SNR) at different positive droplet fractions

Fig.25 Time-dependent plots of the Youden index and the signal-to-noise ratio (SNR). Both the black viability dye resorufin and the grey viability dye C12R were evaluated with varying concentrations of positive (bacteria-containing) droplets (10, 20%, and 32%). a) Graph displaying the Youden index of dyes at various incubation periods. SNR information b) after various incubation durations for both dyes. Published in: Scheler O, Kaminski TS, Ruszczak A, Garstecki P: Dodecylresorufin (C12R) Outperforms Resorufin in Microdroplet Bacterial Assays. ACS Appl Mater Interfaces 2016, 8:11318-11325.

## 2.9 Materials and Methods

2.9.1 Microfluidics

Two distinct microfluidic chips were employed in the study (**Fig.26**). One chip was used to create droplets, and another for analyzing them in detail. Both chips were manufactured from PDMS in few steps. In the first step, The polycarbonate (PC) molds were fabricated from 5 mm plates of polycarbonate (Macroclear, Bayer, Germany) using a CNC milling machine (MSG4025, Ergwind, Poland). The PC chip was then covered with PDMS (Sylgard 184, Dow Corning, USA), and the mold was polymerized at 95 °C for 45 minutes. For the following step, the PDMS mold was silanized using tridecafluoro-1,1,2,2,-tetrahydrooctyl-1-trichlorosilane (Alfa Aesar, Germany) vapours for 3 hours at 10 mbar pressure. Negative PDMS masters were cleaned and then bonded to a glass slide by exposing it and the PDMS to oxygen plasma for 30 seconds. The chip was soaked with Novec 1720 (3M, United States) to make the microfluidic channels hydrophobic for 10 min. The chips were baked at 135 °C for 1 hour after fluid evaporation at room temperature. In all microfluidic experiments, neMESYS(Cetoni, Germany) syringe pumps were used to regulate the flow of oil and water samples. Each experiment included the generation of droplets at a frequency of 300 Hz and their subsequent collection in 16 individual 200 mL containers for off-chip incubation.
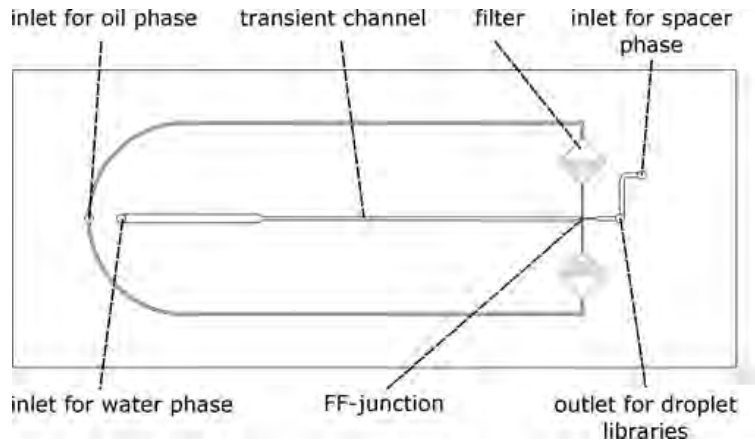
GENERATION CHIP

Channels dimensions (width x height):

• Main water phase channel: 800x800 µm

• Transient water phase channel: 300x300 µm

• Inlet for oil: 200x200 µm

• Flow-focusing junction: 100x90 µm
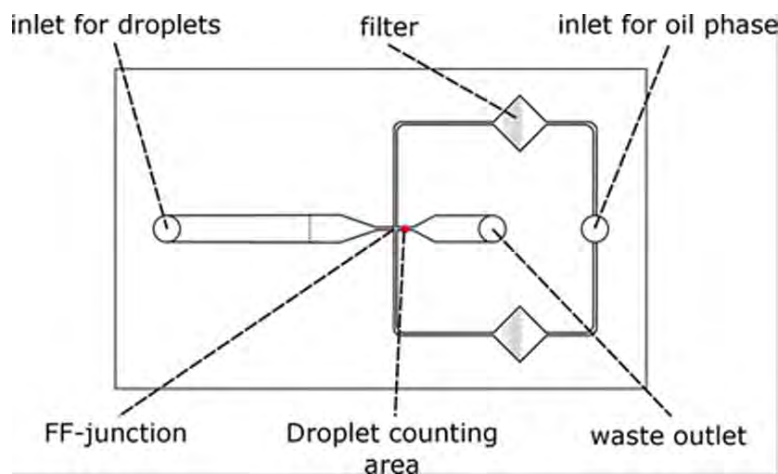
DETECTION CHIP

Channels dimensions (width x height):

• Droplet inlet channel: 1200x1200 µm at the inlet, 1200x100 at channel end (linear depth change until vertical dashed line)

• Flow-focusing junction: 24x100 µm

• Inlet for oil phase: 114x100 µm

Fig. 26 *Schematics and descriptions of chips used in the experiment. Top –droplet generation chip, bottom- detection chip.*

2.9.2 Bacteria

All experiments were performed on two different species of bacteria: i) *E. coli* DH5α genetically modified by a standard heat-shock transformation with plasmid placEGFP [131], ii) *E. aerogenes* PCM183 purchased from the Polish Collection of Microorganisms. Bacteria were incubated in LB-Lennox liquid media (Roth, Germany). Experiments with GFP detection were performed on the medium enriched with 100 µg/ml ampicillin and 1mM β-D-1-thiogalactopyranoside (both from Sigma Aldrich, Germany). Inoculum densities were estimated using a DEN-1 densitometer (Biosan SIA, Latvia).

2.9.3 Reagents

The continuous phase for droplet generation was Novec HFE 7500 (3M, USA), with 2% of PFPE$_2$-PEG surfactant synthesized in our lab according to the Holtze protocol [104]. The viability markers: resazurin sodium salt (Sigma Aldrich, Germany) or C12-resazurin (part of Vybrant® Cell Metabolic Assay Kit, Life Technologies, USA) were used as 50 μM solution in LB in all assays. The final media solution contained 1% dimethylsulfoxide (DMSO) (Life Technologies, USA) that was used for the solubilization of the dye. The concentration of 1% DMSO has proven to have low toxicity to *E. coli* cells [132]. Rhodamine 110 (Sigma Aldrich, Germany), at a low concentration (0.1 μM), was used as a tracer dye to label all droplets (background fluorescence enabled visualization of all scanning droplets).

2.9.4 Fluorescence Measurement and Data Analysis

The droplet-reading chip attached to the stage of an A1R confocal microscope (Nikon, Japan) was used to monitor droplet fluorescence at 488nm/500-550nm (for EGFP and Rhodamine 110) and 516.7nm/570-620nm (for resorufin/C12R) wavelengths. Fluorescent measurements of droplets were taken at 0, 6, 9, 11, 15, and 24 hours (for *E.aerogenes,* also for three h). Different sample aliquots from droplet collection were used at each time point. Around 4000 droplets were analyzed at each incubation time-point at a ~600 Hz frequency. The raw fluorescence data were analyzed using MS Office Excel (Microsoft, USA) with Real Statistics Resource Pack (http://www.real-statistics.com/). Droplet signals stand for peak relative fluorescence intensities allocated to each droplet.

**IChF**
Institute of Physical Chemistry PAS

3. Leakage of antimicrobials from droplets

Part 2 is prepared based on the publication: **Ruszczak A,** *Jankowski P, Vasantham SK, Scheler O, Garstecki P: Physicochemical Properties Predict Retention of Antibiotics in Water-in-Oil Droplets. Analytical Chemistry 2023.*

Author Contribution: A.R. designed, executed and analyzed all experiments, analyzed the data, P.J. prepared the software for the data analysis, S.K.V. with designing of incubation chamber, O.S. and P.G. conceived the idea.

3.1 The aim of the study

Controlling the retention of active compounds is the key to the use of droplet systems in analytical studies. Molecular transport between droplets has been so far tracked with the help of model fluorophores [52,95,96,112]. Unfortunately, antimicrobials are not fluorescent (or rather mildly fluorescent), making them difficult to track. Furthermore, variations in chemical structure between antibiotics and fluorophores preclude comparison without examining their properties. The physicochemical features of tiny molecules may significantly impact their leaking from droplets. This part of my work extends this strategy to create a method for characterizing a wide range of antibiotics, particularly those from various chemical groups, in order to produce a complete model of small molecule inter-droplet transport.
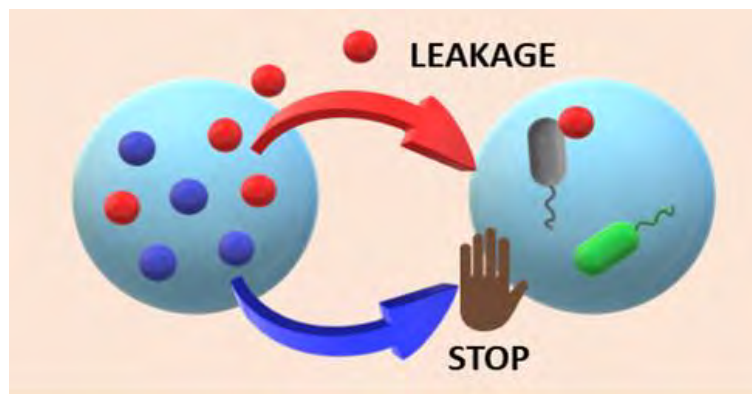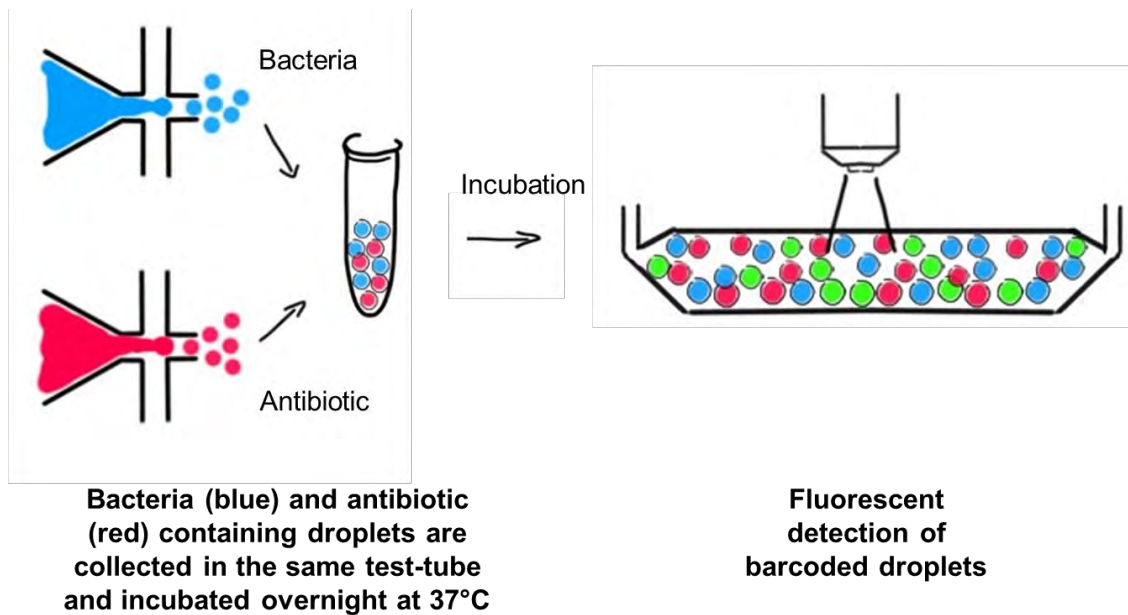
3.2 A color-coded method for the indirect analysis of antibiotic leakage in droplets

Since antimicrobials remain non-fluorescent, their transport between droplets was determined using an indirect method. The method was based on the co-incubation of two groups of droplets. The initial half of the emulsion was made up of droplets with an antibiotic concentration 100 times greater than the minimum inhibitory concentration (MIC). Antibiotics used in this study belong to different classes: i) aminoglycosides: kanamycin (KAN), amikacin (AMK), tobramycin (TOB), gentamycin (GEN), ii) beta-lactams: cefotaxime (CTX), ceftazidime (CAZ), iii) tetracyclines: tetracycline (TET), doxycycline (DOX), iv) fluoroquinolones: norfloxacin (NOR), ciprofloxacin (CIP), levofloxacin (LVX), trovafloxacin (TVA) v) other antibiotics: spectinomycin (SPT), chloramphenicol (CHL), fosfomycin (FOF). The red fluorescent dye Alexa Fluor was added to recognize the antibiotic-loaded group of droplets.

The second fraction of the emulsion was composed of droplets containing *Escherichia coli* that expressed green fluorescent protein (*E. coli* Top10 placEGFP). Reporter cells of GFP-producing *E. coli* were encapsulated with an initial inoculum of around ten cells per droplet. This portion of droplets was labelled with a blue fluorescent dye, Cascade Blue, to recognize them (**Fig.27**). The fluorescent markers used for barcoding have been previously applied in droplet experiments, and they do not leak from droplets[61].

Bacteria (blue) and antibiotic (red) containing droplets are collected in the same test-tube and incubated overnight at 37°C

Fluorescent detection of barcoded droplets

Fig.27 Scheme of the sample preparation. Two different fractions of droplets (either with bacteria or antibiotics) were generated. After overnight incubation, samples were injected into the observation chamber. Photographies of droplet monolayers were analyzed for the determination of green fluorescence signals.

Bacteria-loaded droplets have high fluorescence signals only after multiple replications of living cells. Antibiotic migration from neighbor droplets inhibits bacterial replication, and droplets remain only blue fluorescent. After the incubation, droplets were imaged at three different wavelengths: i) 405 nm for Cascade Blue, ii) 488 nm for GFP produced by actively growing bacteria, and iii) 635 nm for AlexaFluor (**Fig.28**). The intensities of green fluorescence of viable bacteria were extracted from a blue-coded population of droplets and compared to the control experiments (bacteria co-incubated with blank droplets without antibiotics). Bacteria can sense low concentrations of antibiotics (MIC values range from 0.004 to 3 µg/ml – depending on the type of the antimicrobial agent). If the transfer of antibiotics happens, bacterial cells stop proliferation, which can be easily detected as a decrease in the intensity of the GFP signal from droplets. The viability of bacteria in droplets was defined as the percentage of the positive droplets compared to the control sample (no antibiotics). Leakage of antibiotics was characterized as a decrease in bacterial viability after co-incubation with antibiotic-loaded droplets.
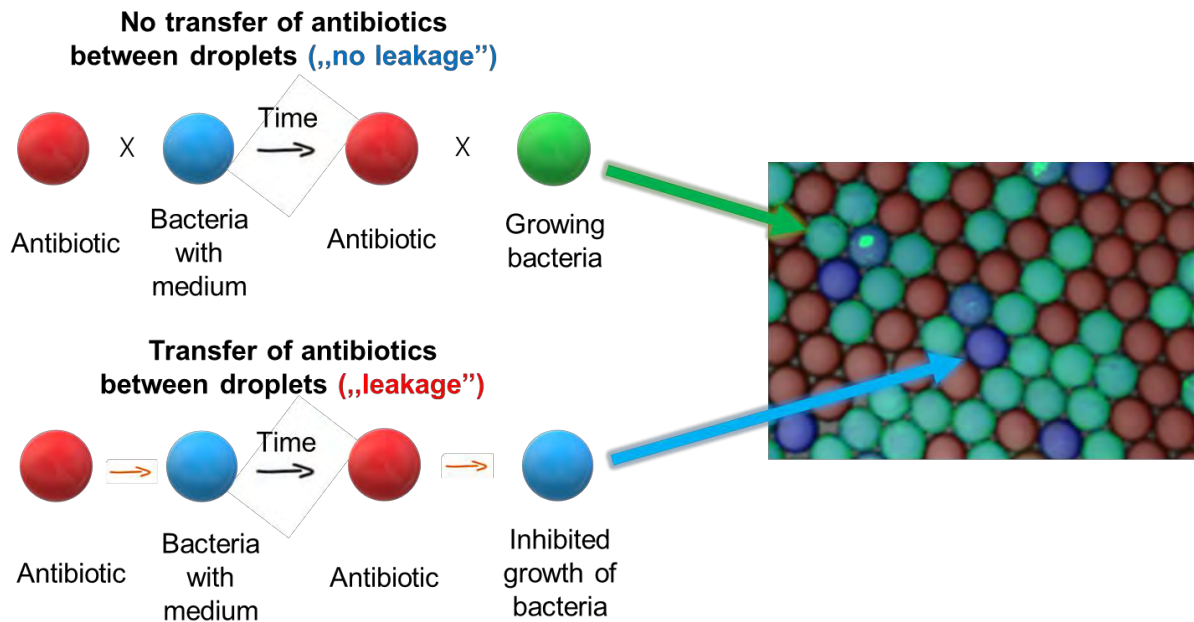
Fig.28 *A blue fluorescent dye (Cascade Blue) was used to mark droplets with bacteria. The red fluorescent dye (Alexa Fluor) was used to identify antibiotic-filled droplets. After overnight incubation (approximately 12-15 hours), droplet samples were injected into a custom-made microfluidic detection chamber. Images of 2D droplet monolayers were captured by confocal microscopy. The viability of bacteria is estimated by measuring the intensity of green fluorescence from actively growing bacteria. The leakage of antibiotics from droplets to neighboring bacteria-containing droplets inhibits bacteria growth and is verified by the emergence of fluorescent signals.*

Two different responses were seen when antibiotic-loaded droplets were co-incubated with droplets with bacteria. For certain antibiotics, there was a significant decrease in the fluorescence of bacteria in droplets (weak green signal), which can be associated with the transfer of antibiotics between droplets. The other antibiotics did not affect bacterial fluorescence in accompanying emulsions (intensive green signal). In this study, the term "leakage" is defined as the percentage of bacterial growth inhibition induced by the transfer of antibiotics. Antimicrobial agents that have no negative effect on the cultured bacterial population (leakage rates from 0-60) are AMK, TOB, KAN, CTX, GEN, SPT, FOF, CAZ. The highest leakage rates (above 60%) were observed in emulsions

consisting DOX, CHL, NOR, CIP, LVX and TVA. Only TET, with a leakage rate of 52%, exhibits average inhibition of bacterial viability. The findings of the significant transfer of antimicrobials between droplets in this complex emulsion motivated me to look further for a relationship between the chemical structure of these antibiotics and their leakage.

3.3 Physicochemical model

Screening the physicochemical characteristics of antimicrobial compounds was the initial step in looking for insights into how antibiotic structure affects leakage. This work focused only on parameters concerning the hydrophilic/hydrophobic nature of the molecules, i.e., partition coefficients and other descriptors describing the nature of the molecule's surface. The leakage of antimicrobials was modelled using 36 distinct factors, and their correlation with experimental data was assessed (**Tab.2**). Partition coefficient (XLogP) and fractional polar surface area (PSA) were shown to be the most predictive and discriminatory between leaky and non-leaky antibiotics after a thorough examination of all the characterizations (**Fig. 29**). The partition coefficient defines the ratio of the concentrations of two immiscible component systems in an equilibrium state. Small molecules with a high XlogP (hydrophobic nature) will more likely escape from aqueous phases into the hydrophobic phase. Fractional PSA is one of the parameters which describes the polarity of chemical compounds (including the molecular size of the compound).

Tab. 2 *Descriptions of chemical descriptors analyzed in work.*

	Description
Fractional PSA	Surface area descriptor. Calculates the topological polar surface area and expresses it as a ratio to molecule size
Topological PSA	Surface area descriptor. Calculation of topological polar surface area based on fragment contributions
PPSA3	Charged Partial Surface Area (CPSA) descriptor. Charge weighted partial positive surface area
WPSA3	Charged Partial Surface Area (CPSA) descriptor. PPSA.3 * total molecular surface area / 1000
RPSA	Charged Partial Surface Area (CPSA) descriptor. TPSA / total molecular surface area
DPSA2	Charged Partial Surface Area (CPSA) descriptor. Difference of FPSA.2 and PNSA.2
DPSA3	Charged Partial Surface Area (CPSA) descriptor. Difference of PPSA.3 and PNSA.3
TPSA	Charged Partial Surface Area (CPSA) descriptor. Sum of solvent accessible surface areas of atoms with absolute value of partial charges greater than or equal 0.2
FPSA3	Charged Partial Surface Area (CPSA) descriptor. PPSA.3 / total molecular surface area
WPSA2	Charged Partial Surface Area (CPSA) descriptor. PPSA.2 * total molecular surface area /1000
PPSA2	Charged Partial Surface Area (CPSA) descriptor. Partial positive surface area * total positive charge on the molecule
WNSA1	Charged Partial Surface Area (CPSA) descriptor. PNSA.1 * total molecular surface area /1000
PNSA1	Charged Partial Surface Area (CPSA) descriptor. Partial negative surface area - sum of surface area on negative parts of molecule.
FPSA2	Charged Partial Surface Area (CPSA) descriptor. PPSA.2 / total molecular surface area
FNSA1	Charged Partial Surface Area (CPSA) descriptor. PNSA.1 / total molecular surface area
WPSA1	Charged Partial Surface Area (CPSA) descriptor. PPSA.1 * total molecular surface area / 1000
Molar refractivity	a measure of the total polarizability of a mole of a substance and is dependent on the temperature, the index of refraction, and the pressure.

RPCS	Charged Partial Surface Area (CPSA) descriptor. Relative positive charge surface area - most positive surface area * RPCG
PPSA1	Charged Partial Surface Area (CPSA) descriptor. Partial positive surface area - sum of surface area on positive parts of molecule
RNCG	Charged Partial Surface Area (CPSA) descriptor. Relative negative charge - most negative charge / total negative charge
RPCG	Charged Partial Surface Area (CPSA) descriptor. Relative positive charge -most positive charge / total positive charge
THSA	Charged Partial Surface Area (CPSA) descriptor. Sum of solvent accessible surface areas of atoms with absolute value of partial charges less than 0.2
RNCS	Charged Partial Surface Area (CPSA) descriptor. Relative negative charge surface area - most negative surface area * RNCG
DPSA1	Charged Partial Surface Area (CPSA) descriptor. Difference of PPSA.1 and PNSA.1
FPSA1	Charged Partial Surface Area (CPSA) descriptor. PPSA.1 / total molecular surface area
PNSA3	Charged Partial Surface Area (CPSA) descriptor. Charge weighted partial negative surface area
WNSA3	Charged Partial Surface Area (CPSA) descriptor. PNSA.3 * total molecular surface area / 1000
FNSA3	Charged Partial Surface Area (CPSA) descriptor. PNSA.3 / total molecular surface are
FNSA2	Charged Partial Surface Area (CPSA) descriptor. PNSA.2 / total molecular surface area
PNSA2	Charged Partial Surface Area (CPSA) descriptor. Partial negative surface area * total negative charge on the molecule
WNSA2	Charged Partial Surface Area (CPSA) descriptor. PNSA.2 * total molecular surface area / 1000
MannholdlogP	Partition coefficient descriptor . Prediction of logP based on the number of carbon and hetero atoms
RHSA	Charged Partial Surface Area (CPSA) descriptor. THSA / total molecular surface area
AlogP	Partition coefficient descriptor . This class calculates ALOGP (Ghose-Crippen LogKow)

| JlogP	Partition coefficient descriptor. Model donated by Lhasa Limited. It is based on an atom contribution model.
XlogP	Partition coefficient descriptor. Prediction of logP based on the atom-type method.
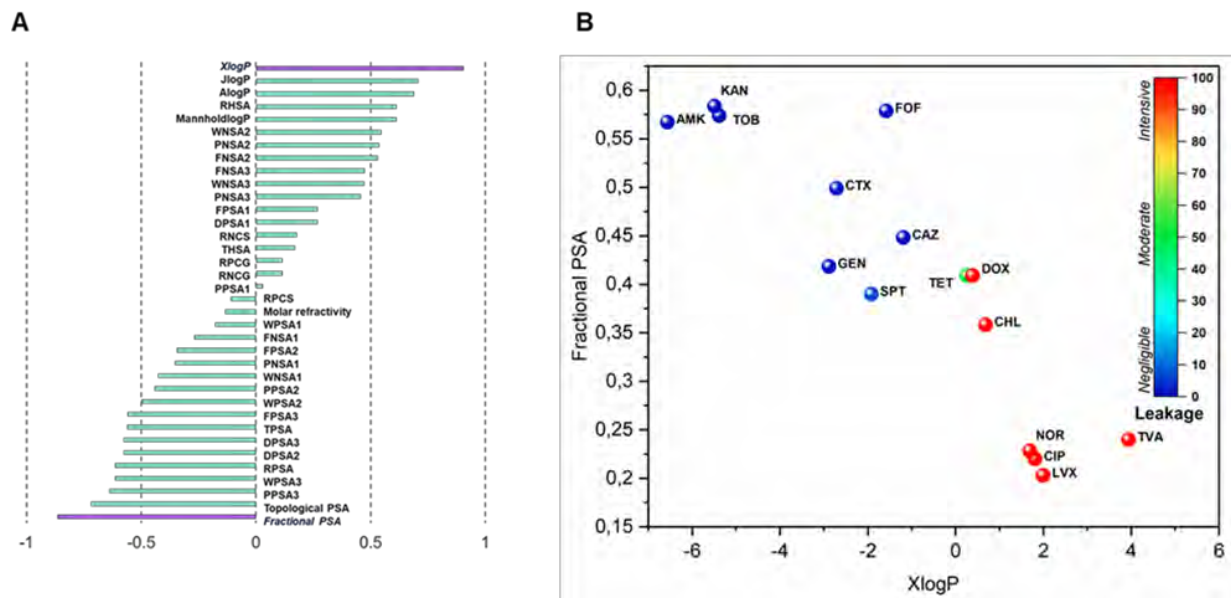
Fig.29. *The leakage of antibiotics as assessed empirically correlates best with XlogP and fractional PSA .A. Pearson correlation analysis of 36 chemical parameters and leakage values. The best descriptors for sorting antibiotics into leaky and non-leaky categories are those with a correlation close to 1/-1. B. Dependence of XlogP and fractional PSA values on the ability to leak for 15 tested antibiotics: kanamycin (KAN), amikacin (AMK), tobramycin (TOB), gentamycin (GEN), cefotaxime (CTX), ceftazidime (CAZ), tetracycline (TET), doxycycline (DOX), norfloxacin (NOR), ciprofloxacin (CIP), levofloxacin (LVX), trovafloxacin (TVA), spectinomycin (SPT), chloramphenicol (CHL), fosfomycin (FOF). Published in: Ruszczak A, Jankowski P, Vasantham SK, Scheler O, Garstecki P: Physicochemical Properties Predict Retention of Antibiotics in Water-in-Oil Droplets. Analytical Chemistry 2023.*

The next step was to estimate if using these two descriptors enables the determination of whether the antibiotic will leak out the droplets with a higher or lower probability. The predictive model

was built by determining the XlogP and fractional PSA values of 95 different antibiotics. The K-means algorithm was used to recognize two groups of antimicrobial escape. This algorithm determines clusters within an unlabeled multidimensional dataset (**Fig.30**).

Experiments were conducted with three antibiotics chosen at random to confirm the prediction model: i) 75 µg/ml imipenem (IPM), ii) 10 µg/ml meropenem (MEM) and iii) 300 µg/ml nitrofurantoin (NIT). Only NIT lead to a decrease in bacterial viability, indicating a substantial cross-talk between droplets. The bacterial population co-incubated with IPM, and MEM stayed unaffected. As expected, these experimental results are consistent with the prediction model. (**Fig.30D**).
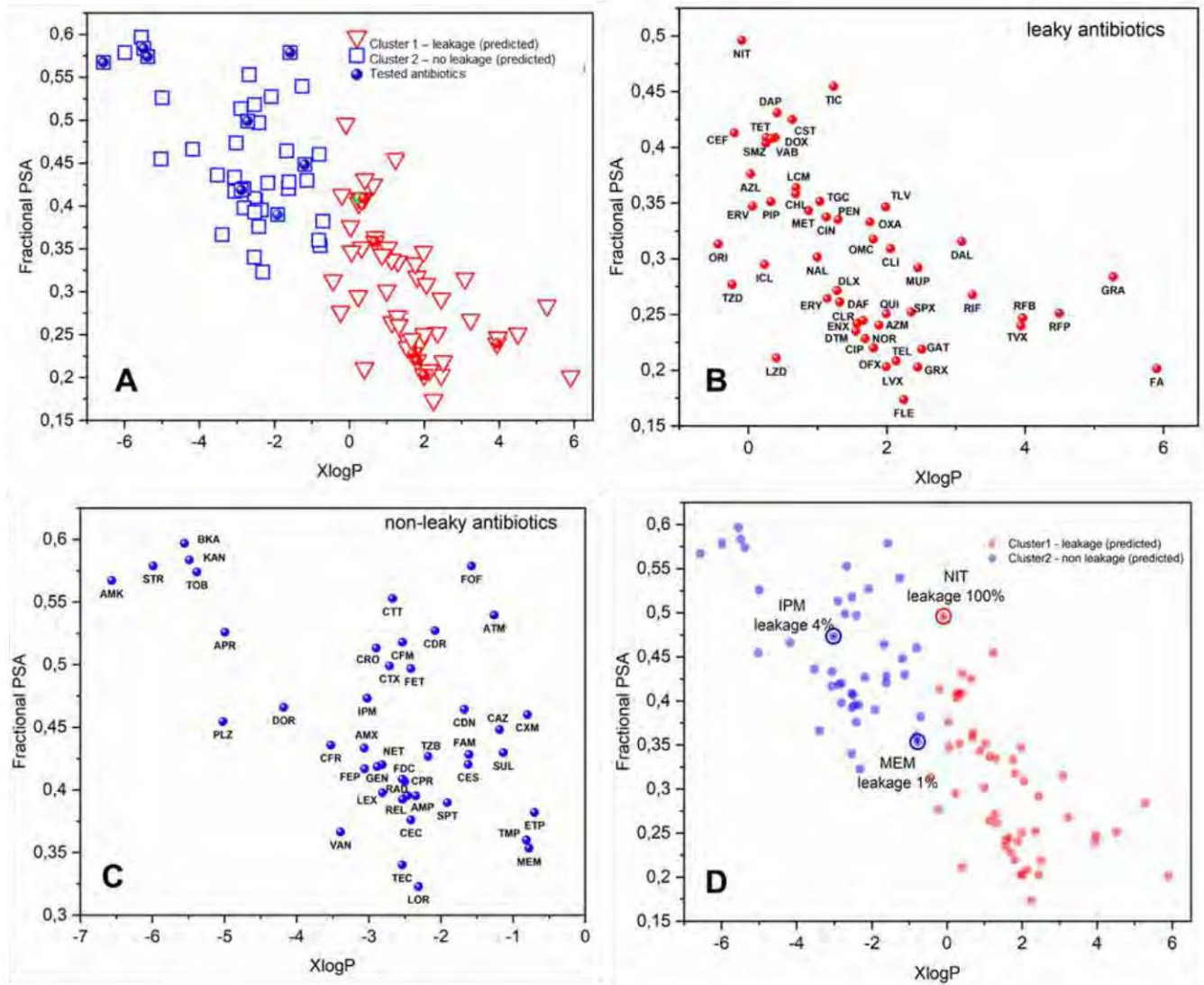
AMK- Amikacin, AMP- Ampicillin, AMX- Amoxicillin, APR- Apramycin, ATM- Aztreonam, AZL- Azlocillin, AZM- Azithromycin, BKA- Bekanamycin, CAZ- Ceftazidime, CDN- Cefditoren, CDR- Cefdinir, CEC- Cefaclor, CEF- Cephalothin, CES- Cefsulodin, CFM- Cefixime, CFR- Cefadroxil, CHL- Chloramphenicol, CIN- Cinoxacin, CIP- Ciprofloxacin, CLI- Clindamycin, CLR- Clarithromycin, CPR- Cefprozil, CRO- Ceftriaxone, CST- Colistin, CTT- Cefotetan, CTX- Cefotaxime, CXM- Cefuroxime, DAF- Dalfopristin, DAL- Dalbavancin, DAP- Daptomycin, DLX- Delafloxacin, DOR- Doripenem, DOX- Doxycycline, DTM- Dirithromycin, ENX-Enoxacin, ERV- Eravacycline, ERY- Erythromycin, ETP- Ertapenem, FA- Fusidic Acid, FAM- Cefamandole, FDC- Cefiderocol, FEP- Cefepime, FET- Cefetamet, FLE- Fleroxacin, FOF- Fosfomycin, GAT- Gatifloxacin, GEN- Gentamycin, GRA- Gramicidine, GRX- Grepafloxacin, ICL- Iclaprim, IPM- Imipenem, KAN- Kanamycin, LCM- Lincomycin, LEX- Cephalexin, LOR- Loracarbef, LVX- Levofloxacin, LZD- Linezolid, MEM- Meropenem, MET- Methicillin, MUP- Mupirocin, NAL- Nalidixic acid, NET- Netilmicin, NIT- Nitrofurantoin, NOR- Norfloxacin, OFX- Ofloxacin, OMC- Omadacycline, ORI- Oritavancin, OXA- Oxacillin, PEN- Benzopenicillin, PIP- Piperacillin, PLZ- Plazomicin, QUI- Quinupristin, RAD- Cephradiney, REL- Relebactam, RFB- Rifabutin, RFP- Rifapentine, RIF- Rifampicin, SMZ- Sulfamethoxazole, SPT- Spectinomycin, SPX- Sparfloxacin, STR- Streptomycin, SUL- Sulbactam, TEC- Teicoplanin, TEL- Telithromycin, TET- Tetracycline, TGC- Tigecycline, TIC- Ticarcillin, TLV- Telavancin, TMP- Trimethoprim, TOB- Tobramycin, TVX- Trovafloxacin, TZB- Tazobactam, TZD- Tedizolid, VAB- Vaborbactam , VAN- Vancomycin.

Fig.30 *Values of XlogP and fractional PSA are related to antimicrobial leakage. A. Theoretically predicted model of the antibiotics leakage from droplets. The model is based on experimental data*

for 15 antibiotics. The leakage values are defined as a percentage decrease in the viability of bacteria incubated with the companion of antibiotics. XlogP and fractional PSA descriptors correlate with the leakage rates of tested antibiotics. K-means plot enables the segregation of leaky and non-leaky groups of antibiotics. B. Predicted group of leaking antibiotics, C. Predicted group of non-leaky antibiotics, D. Confirmation of the correct operation of the prediction. In the case of the three antibiotics chosen to study (NIT, IPM, and MEM), the experimental results agree with the prediction. Published in: Ruszczak A, Jankowski P, Vasantham SK, Scheler O, Garstecki P: Physicochemical Properties Predict Retention of Antibiotics in Water-in-Oil Droplets. Analytical Chemistry 2023.

The next question that needed to be addressed was whether or not antibiotic leakage in water-in-oil systems could be predicted based on the similarity in properties of different classes of antibiotics (**Fig.31**). This was identified through the use of a graph depicting XlogP values vs fractional PSA for each group of antibiotics. It was possible to pinpoint the source of the leak using only an understanding of the antibiotic class. The figure showed that aminoglycosides were located in the non-leaky region, but (fluoro)quinolones, tetracyclines, and macrolides were all positioned in the leaky parts. Both leaky and non-leaky antibiotics were found in beta-lactams and glycopeptides. Beta lactams had the most representatives in the current study. Hence their retention behavior was analyzed by their sub-classes. Most cephems and carbapenems were found to be leak-proof, but most penicillins showed potentially leaky parameters.
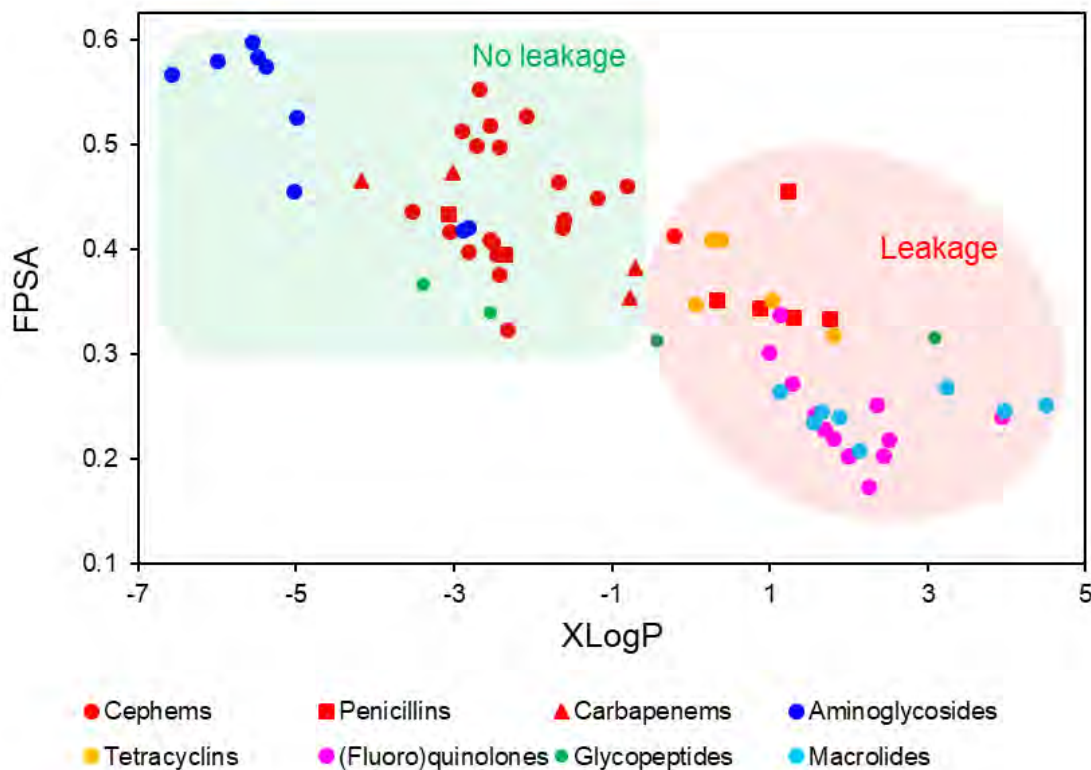
Fig.31 *Antibiotic class or sub-class predict the retention characteristics of the antibiotics in most cases. The X-axis represents XlogP values, while the y-axis represents the fractional PSA. A green background indicates antibiotics that are likely to be kept in water-in-oil droplets, whereas a red background indicates antimicrobials that may leak. Aminoglycosides (blue dots) and beta-lactam sub-classes carbapenems, and most of the cephems (red triangles and dots) remain in droplets. Beta-lactam penicillins (red squares), tetracyclines (yellow dots), (fluoro)quinolones (purple dots) and macrolides (light blue dots) are most likely all leaky types. There are both leaky and non-leaky antibiotics among glycopeptides (green dots) and penicillins (red squares). Published in: Ruszczak A, Jankowski P, Vasantham SK, Scheler O, Garstecki P: Physicochemical Properties Predict Retention of Antibiotics in Water-in-Oil Droplets. Analytical Chemistry 2023.*

3.4 Distance and mixing-related transfer of antibiotics

As was demonstrated previously based on fluorescent dyes, droplets loaded with reagents serve as a source of the local chemical leakage to neighbor empty droplets [112]. Since the way of packing droplets in the complex emulsion can significantly influence the leakage rate from droplets. The cross-contamination should be higher if an antibiotic-loaded droplet meets a neighbor droplet with bacteria. Hence, it is interesting to understand if the emulsion preparation can decrease the inner-droplet contact and limit molecular transport.

Bacteria-containing droplets and droplets containing the antibiotics NOR and LVX, both of which have been shown to leak, were co-incubated to test the hypothesis that the droplet's close proximity speeds up antibiotic transmission. The first emulsion was prepared according to the standard protocol described in **paragraph 3.2** — droplets with 100x MIC of antibiotics and droplets with bacteria in equal ratio. After generation, droplets were mixed thoroughly right before incubation. The second sample was not mixed, resulting in two ordered layers of droplets with different content (encapsulated layer of antibiotics and the layer with bacteria). Usually, when introducing the second type of droplets, the tip of the teflon tube is immersed in the oil phase (well below the first droplet layer). The buoyant droplets settle on the bottom of the first layer, giving rise to a second layer. Given the small diameter of the Eppendorf tube, droplets in those two layers have minimal freedom to move or inter-mix. Hence, contact of droplets with the different compositions is generally limited to the interface of the two layers. This might potentially alter the results of the experiments. A 15 µl layer of empty droplets labelled with a low concentration of AlexaFluor was used to separate the two samples with droplets. After overnight incubation, the green fluorescence of droplets was measured, and the cross-talk-related decrease in the viability of bacteria was compared. After incubation, antibiotic transfer was significantly reduced in both unmixed and separated emulsions compared to mixed samples (**Fig.32**). According to these results, preventing the transmission of antimicrobials between droplets of varying chemical compositions can be achieved by separating the various portions of emulsions.
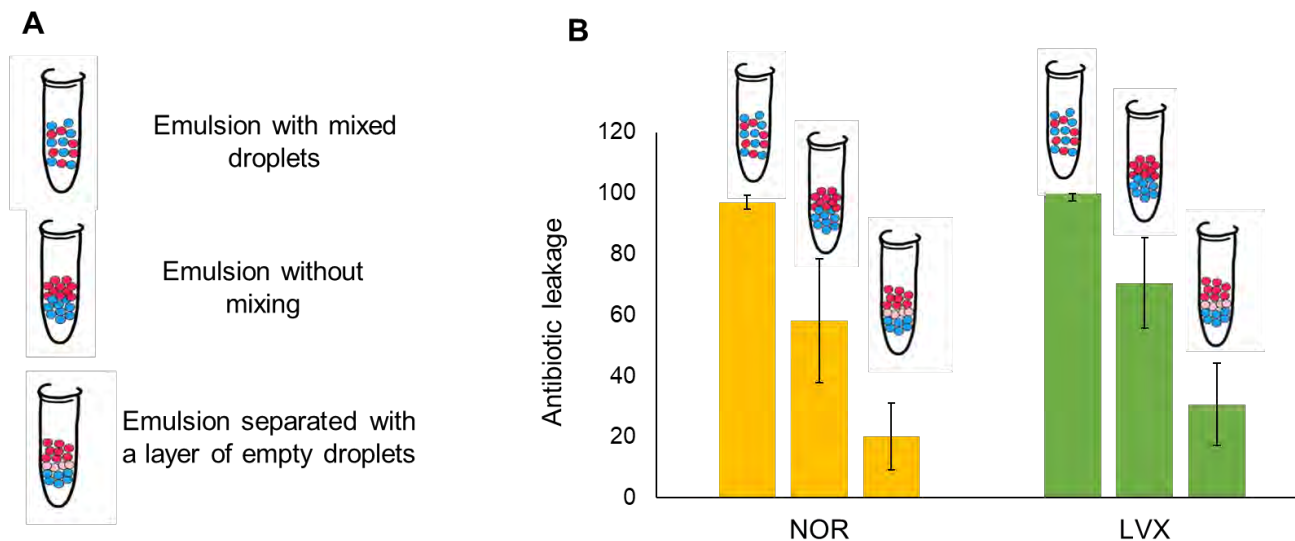
Fig.32 *Antimicrobials leakage is enhanced by concentration and direct contact with neighboring droplets. A. Different ways of incubation of droplets with antibiotics and bacteria. Two different emulsions could be mixed, no mixed or no mixed, with the separation layer of blank droplets, B. The cross-talk between droplets is fast along the concentration gradient with properly mixed droplets. The most significant reduction of bacteria viability in droplets was shown when emulsions of antibiotics and bacteria were adequately mixed and were in close proximity. Unmixed or separated emulsions demonstrated higher viability of bacteria than well-mixed emulsions. Published in: Ruszczak A, Jankowski P, Vasantham SK, Scheler O, Garstecki P: Physicochemical Properties Predict Retention of Antibiotics in Water-in-Oil Droplets. Analytical Chemistry 2023.*

3.5 Concentration-dependent transfer of antibiotics.

The next step was to characterize the leakage rate of the antibiotic in relationship to concentration. Cross-talk between droplets is strongly influenced by the concentration gradient between them. Samples with three different concentrations of antibiotics (100, 10 and 1x MIC) were prepared to determine the concentration-dependent transfer of antimicrobials. In this part of the study, four representatives from different antibiotic classes with the tendency to leak were selected for the experiment. The following antimicrobial agent concentrations were used: i) 100, 10 and 1 µg/ml TET; ii) 50, 5 and 0.5 µg/ml DOX; iii) 100, 10 and 1 µg/ml CHL; iv) 2, 0.2 and 0.02

µg/ml NOR. As in previously described experiments, a detection chamber was used to measure the fluorescence intensity of droplets with bacteria. The most important observation was that antimicrobials are transported efficiently even at 10x MIC doses. Emulsions containing the smallest concentration of antibiotics (1x MIC) showed no change in bacterial viability. However, diluting a small amount of the antibiotic may compensate for its harmful effect on bacteria but does not exclude its transport, even at a minimal rate (**Fig.33**).
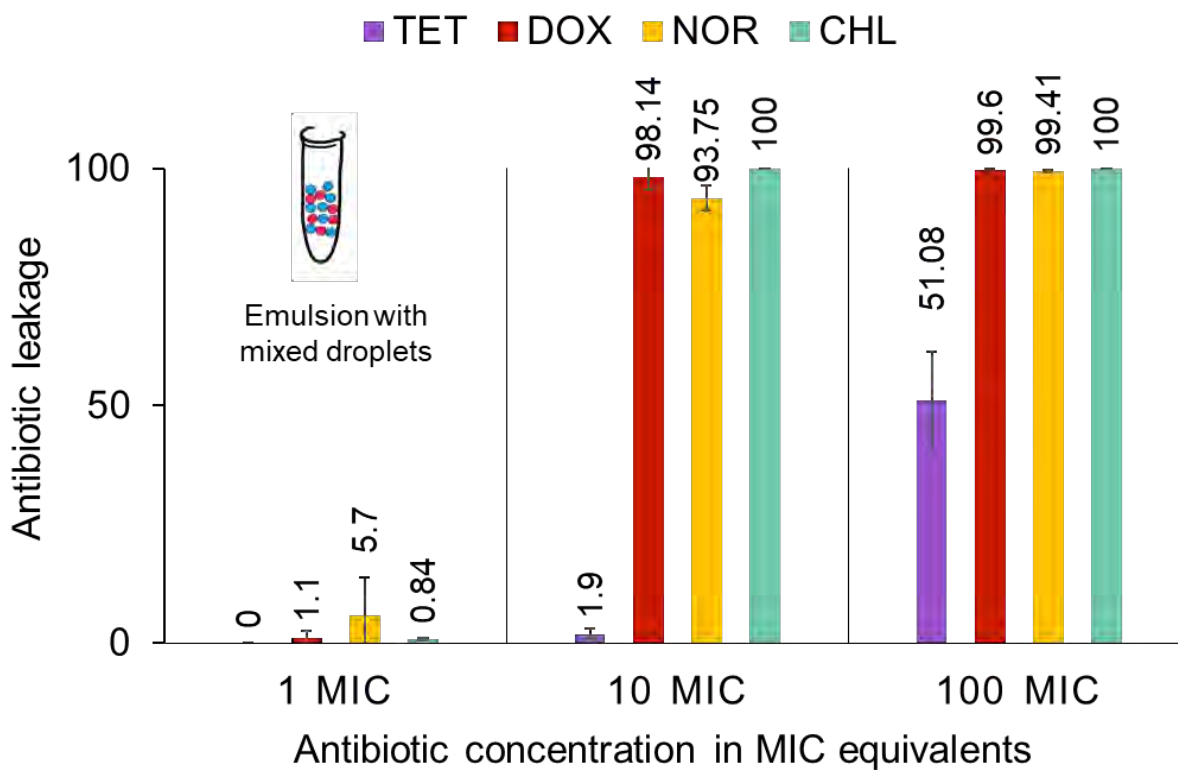

Fig.33 *Antibiotic leakage between droplets is concentration-dependent. Incubation with higher concentrations of antimicrobials results in lower rates of bacterial viability. Samples with antibiotic concentrations around 1x MIC do not show a significant decrease in the viability of bacteria. Published in: Ruszczak A, Jankowski P, Vasantham SK, Scheler O, Garstecki P: Physicochemical Properties Predict Retention of Antibiotics in Water-in-Oil Droplets. Analytical Chemistry 2023.*

3.6 Materials and Methods

3.6.1 Microfluidic

Two different microfluidic chips were used in the study: i) module for the generation of droplets and ii) chip for the detection (**Fig.34**). Both devices were made of poly(dimethylsiloxane) (PDMS) (SylgardTM Silicone Elastomer Kit, Dow Corning, USA). Both chips were made using the same method. In the first step, molds were fabricated from polycarbonate (PC) (Macroclear, Bayer, Germany) using CNC milling machine (MSG4025, Ergwind, Poland). Next, PDMS negative masters were prepared by pouring PDMS on PC chip. PDMS polymerized during incubation at 95°C for 45 min. After polymerization PC chip was removed. Further, PDMS mold was silanized using tridecafluoro-1,1,2,2-tetrahydrooctyl-1-trichlorosilane (United Chemical Technologies, USA) for three h under 10 mbar pressure with vapors. Finally, PDMS replicas were prepared, by pouring PDMS on silanized negative masters and incubation at 95°C for 45 min. After that time, chips were bounded with glass slides by exposing them to oxygen plasma. Before the use, channels in chips were modified by filling the chip with Novec 1720 (3M, USA) to make channels hydrophobic.
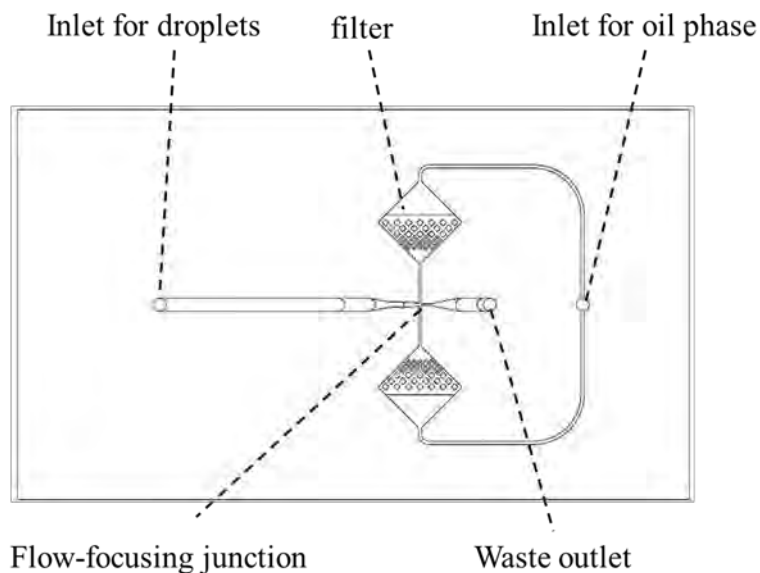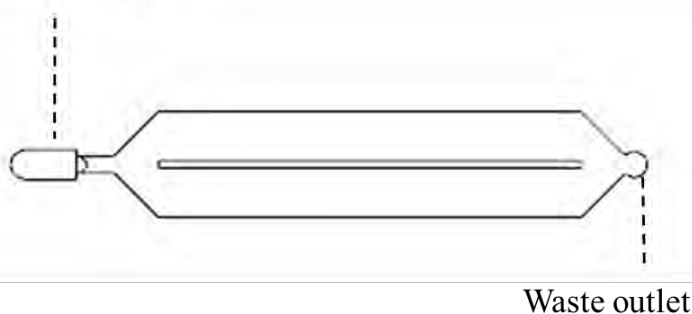
GENERATION CHIP

Channels dimensions (width x height):

- Droplet inlet channel: 800x800 µm at the inlet
- Flow-focusing junction: 12x120 µm
- Secondary oil delivering channel: 800x800 µm

DETECTION CHIP

Channels dimensions (width x height):

- Droplet inlet channel: 500x200 µm at the inlet
- Chamber: 3200x200 µm

Fig.34 *Schematics and descriptions of chips used in the experiment. Top –droplet generation chip, bottom- detection chip.*

3.6.2 Bacteria

The fluorescent strain of *Escherichia coli* Top10 placEGFP was obtained from prof. Weibel's group Department of Biochemistry, University of Wisconsin-Madison, USA. Bacteria were incubated on Luria-Miller Agar (Roth, Germany) plates with the addition of 100 µg/ml ampicillin sodium salt (Sigma Aldrich, Germany). After incubation, a colony of bacteria were inoculated in liquid Muller Hinton medium (Roth, Germany) and 100 µg ampicillin and incubated overnight. Before the experiment, the inoculum of bacteria was prepared by dilution with the fresh medium

to reach the optical density of 0.1, representing around 10^8 CFU/ml. The prepared bacterial culture was encapsulated with the use of the droplet-generating chip. Droplets in the experiment procedure included roughly ten bacterial cells enclosed (control samples always contained more than 85% positive droplets).

3.6.3 Antibiotics

Stock solutions of kanamycin sulfate (Fisher Chemical, UK), cefotaxime sodium salt (Roth, Germany), gentamycin sulfate (Toku-E, USA), spectinomycin dihydrochloride pentahydrate (Roth, Germany), tetracycline hydrochloride (Roth, Germany), doxycycline hyclate (Roth, Germany), ceftazidime pentahydrate (Acros Organics, Belgium), amikacin sulfate (Toku-E, USA), tobramycin sulfate (Toku-E, USA), fosfomycin sulfate (Toku-E, USA), imipenem (Toku-E, USA), meropenem (Toku-E, USA) were dissolved in distilled water. Chloramphenicol (Toku-E, USA), levofloxacin (Toku-E, USA) in 50% ethanol. Norfloxacin (Toku-E, USA) in 5% acetic acid (Poch, Poland). Ciprofloxacin (Toku-E, USA) in 0.1 M NaOH (Poch, Poland). Trovafloxacin mesylate (Sigma, Germany) and nitrofurantoin (Toku-E, USA) in DMSO (Roth, Germany). The conventional broth dilution procedure was used to obtain the MIC values of the tested antibiotics. The MIC values were: 1.5 µg/ml kanamycin; 0.64 µg/ml cefotaxime; 0.75 µg/ml gentamycin; 3 µg/ml spectinomycin; 1.5 µg/ml tetracycline; 0.5 µg/ml doxycycline; 1 µg/ml chloramphenicol; 0.02 µg/ml norfloxacin; 0.006 µg/ml ciprofloxacin; 0.004 µg/ml levofloxacin; 4 µg/ml amikacin; 4 µg/ml fosfomycin; 0.004 µg/ml trovafloxacin; 1 µg/ml ceftazidime; 1.5 µg/ml tobramycin; 0.75 µg/ml imipenem; 0.1 µg/ml meropenem; 3 µg/ml nitrofurantoin.

3.6.4 Droplet generation and incubation.

Two emulsions were prepared by encapsulation of i) suspension of 10^6 CFU/ml of GFP-producing *E. coli* and ii) antimicrobials (at concentrations of 100, 10 or 1x MIC). Both populations of droplets were encapsulated using the flow-focusing device at a flow rate of 1.8 µl/s and a sample flow rate of 1.7 µl/s. The fluorocarbon oil Novec 7500 (3M, USA) as a continuous phase was enriched with 2% surfactant (PFPE)$_2$PEG (self-produced in the Institute of Physical Chemistry, Poland15) or 2% FluoSurf (Emulseo, France). FluoSurf N is a mixture of diblock and triblock polymer (PFPE-b-PPO-PEO-PPO-b-PFPE) with a molecular weight ranging from 7kD to 13kD. There were no

significant differences between the results for those two surfactants; therefore, both experiments were treated as duplicates.

Before emulsification, both the cell suspension and the antibiotic solution were barcoded with fluorescent dies. 6 mg/L Alexa Fluor was added to the antibiotic solution and 2 mg/L Cascade Blue to the bacteria suspension, respectively. In the experiment with the determination of the contact-less incubation of droplets, the layer with empty droplets was labelled with AlexaFluo with a lower concentration (1mg/mL). Those dyes were previously tested as no leaking compounds [61].

The emulsion composed of two types of droplet samples was adequately mixed in a 0.5 ml Eppendorf-type tube at the ratio of 1:1 (and the excess amount of the continuous liquid) and incubated at 37°C overnight (12-15h). After incubation, droplets were carefully drawn into a Teflon tube with a glass syringe and re-injected into a dedicated droplet detection chamber. Images of around 30-50 µl of emulsions were taken at three excitation wavelengths: i) 405 nm corresponding to Cascade Blue labelling (droplets loaded with bacteria), ii) 488 nm for GFP detection (live bacteria), and iii) 635 nm for AlexaFluor (antibiotics). Irregular droplets with no matched coding and size were excluded from the data analysis. The identical incubation and detection process with droplets containing bacteria mixed with droplets containing only a growth medium (instead of antibiotics) was performed as a control.

3.6.5 Detection software

Images of the droplets were captured using an inverted fluorescence microscope in the epi-configuration in three channels: red, green, and blue (RGB). The software was created by one of the co-authors of the work (dr. Paweł Jankowski). The software was customized to automate the reading of the intensity for many experiments and facilitate the analysis of the obtained results and was supported with the ImageJ particle analysis module. Fluorescence intensity was first calculated by evaluating the blue channel image (signal from Cascade Blue) and, subsequently, the green channel image to estimate the area occupied by droplets containing bacteria. Because all marked red droplets carried just antibiotics and lacked reporter cells, the red channel was removed from the analysis (**Fig. 35**).
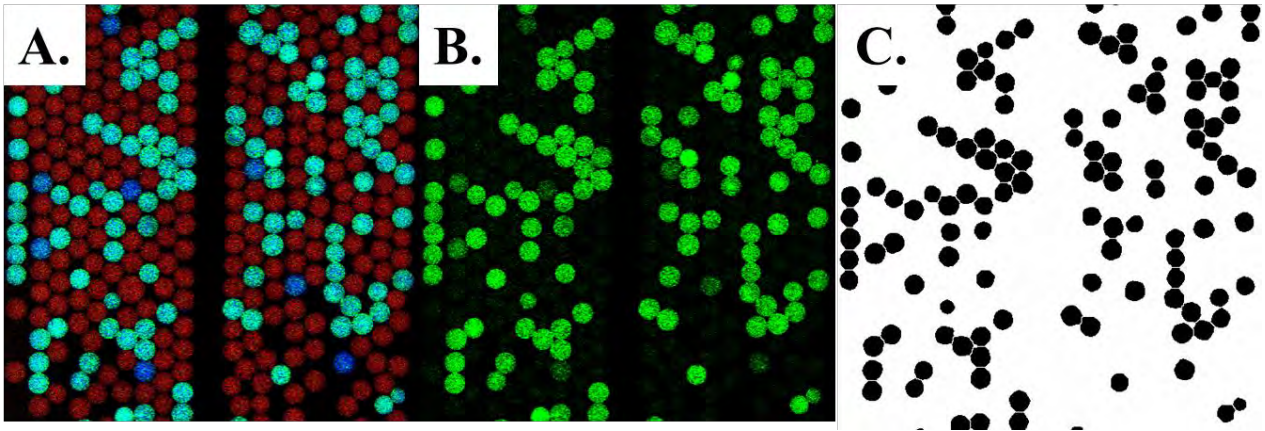
Fig. 35 Detection of the fluorescence intensity from monolayers of droplets. A. Monolayer of droplets acquired in 3 channels (RGB), B. Microscopic photography of the droplet monolayer in green channel responding to droplets with GFP-producing bacteria, C. Detection of areas occupied by the bacteria-loaded droplets by analyzing the image from the blue and green channels

Histograms with droplet intensities were plotted to calculate the number of positive drops in the emulsion (**Fig.36**). The fraction over the cut-off value was recognized as positive droplets. Survival rates of bacteria were determined by comparing them to the control (no-treated) samples. The percentage of positive droplets and the sample quantities for each experiment are presented in **Tab. 2**.
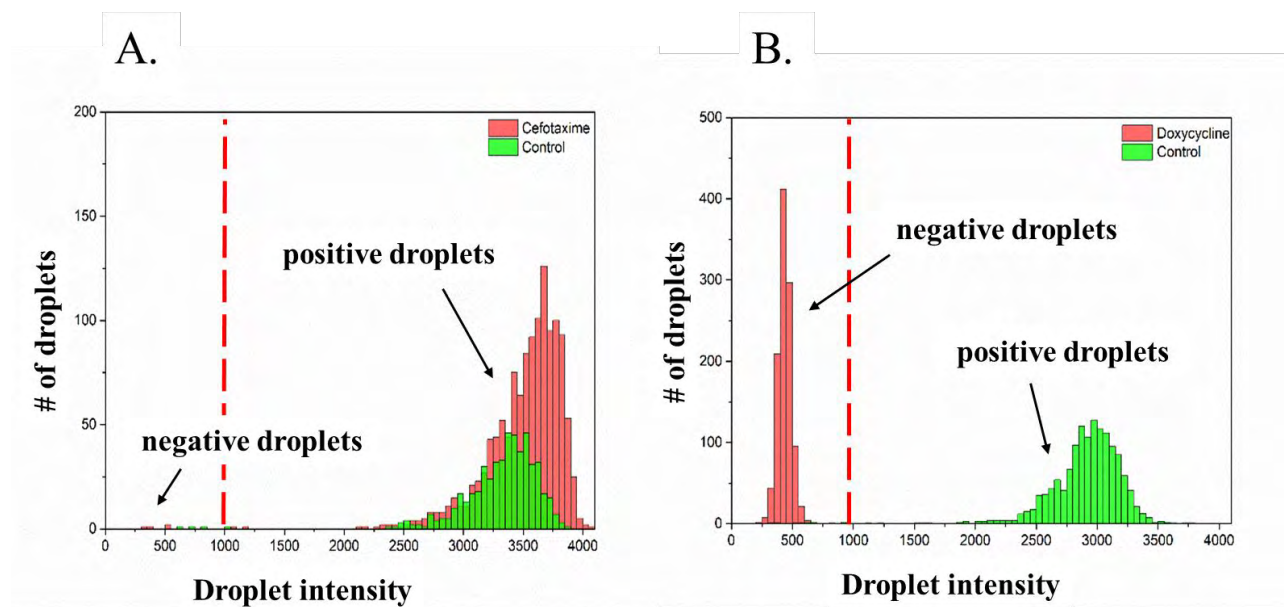
Fig.36 *Histograms presenting the number of droplets with different green fluorescence intensities. The red line represents the cut-off value for separating positive and negative droplets.*

Tab. 2 Number of positive droplets scanned in each experiment. Each experiment was performed in emulsion enriched with 2% of PEG(PFPE)$_2$ or FluoroSurf. The percentage of positive droplets is defined as a ratio of droplets with bacteria to the entire population of positive droplets.

	PEG(PFPE)$_2$		FluoroSurf	
	Number of droplets (Cascade blue labelled)	Positive droplets [%]	Number of droplets (Cascade blue labelled)	Positive droplets [%]
Cefotaxime (CTX)	988	90.99	1273	99.7
Chloramphenicol (CHL)	1272	0	582	0
Ciprofloxacin (CIP)	1808	0.83	1656	0.3
Gentamycin (GEN)	773	90.03	1658	98.19
Spectinomycin (SPT)	1189	75.2	11663	97.11
Levofloxacin (LVX)	741	0.13	868	0
Doxycycline (DOX)	1336	0.22	1097	0.46
Kanamycin (KAN)	1956	95.55	1125	99.73
Norfloxacin (NOR)	1414	1.06	1109	0.27
Tetracycline (TET)	1924	39.76	1105	54
Amikacin (AMK)	1990	92.96	1134	99.82
Ceftazidime (CAZ)	1012	95.36	1113	99.82
Fosfomycin (FOF)	1549	97.74	1013	99.8
Tobramycin (TOB)	1741	95.46	1013	99.3
Trovafloxacin (TVA)	1652	0.6	1041	0.96
Imipenem (IPM)	1252	99.92	1264	92.64
Meropenem (MEM)	1181	99.58	1553	98.65
Nitrofurantoin (NIT)	890	0.45	1463	0

3.6.6 Data analysis.

Values for all tested descriptors were determined using the software (programmed in Microsoft Visual Studio Community 2022) designed by the co-author of the work- dr.Paweł Jankowski. The software was created using .NET Chemistry Development Kit libraries (NCDK). The NCDK is a commonly used open-source library for chemo- and bio-informatics [133]. The program was developed (using C# programming language) for the NCDK library maintenance to improve the computing of chemical descriptors. NCDK calculates XlogP (partition coefficient) and PSA (polar surface area) according to algorithms described in the literature [134-136]. The table below collects values of two most significant descriptors – XlogP and fPSA (**Tab. 3**).

Tab.3 *XlogP and fractional PSA values for all antibiotics described in this study*

	Name	Abbreviation	XlogP	Fractional PSA
1	Tobramycin	TOB	-5.381	0.573921372
2	Amikacin	AMK	-6.562	0.567141789
3	Ceftazidime	CAZ	-1.186	0.448197008
4	Kanamycin	KAN	-5.486	0.583617903
5	Fosfomycin	FOF	-1.578	0.578733747
6	Cefotaxime	CTX	-2.712	0.498948549
7	Gentamycin	GEN	-2.88	0.418443748
8	Spectinomycin	SPT	-1.913	0.389904392
9	Tetracycline	TET	0.259	0.4089129
10	Ciprofloxacin	CIP	1.809	0.220092687
11	Trovafloxacin	TVX	3.942	0.239744514
12	Norfloxacin	NOR	1.689	0.228368579
13	Doxycycline	DOX	0.387	0.4089129
14	Levofloxacin	LVX	1.995	0.203021631
15	Chloramphenicol	CHL	0.685	0.358309264
16	Enoxacin	ENX	1.573	0.242011558
17	Azlocillin	AZL	0.032	0.376135586
18	Trimethoprim	TMP	-0.813	0.360001239
19	Amoxicillin	AMX	-3.064	0.43346489
20	Ampicillin	AMP	-2.35	0.395377237
21	Apramycin	APR	-4.994	0.525960289
22	Bekanamycin	BKA	-5.553	0.596787558
23	Cefaclor	CEC	-2.414	0.376063216
24	Cefadroxil	CFR	-3.524	0.435871225
25	Cefamandole	FAM	-1.612	0.428196096
26	Cefdinir	CDR	-2.081	0.527243339
27	Cefditoren	CDN	-1.674	0.464262351

28	Cefepime	FEP	-3.056	0.41678733
29	Cefetamet	FET	-2.415	0.496862547
30	Cefiderocol	FDC	-2.533	0.408666869
31	Cefixime	CFM	-2.533	0.517789449
32	Quinupristin	QUI	1.993	0.250589061
33	Cefotetan	CTT	-2.671	0.552780547
34	Cefprozil	CPR	-2.5	0.40672874
35	Cefsulodin	CES	-1.621	0.420412825
36	Oritavancin	ORI	-0.434	0.313297914
37	Ceftriaxone	CRO	-2.896	0.51322448
38	Cefuroxime	CXM	-0.803	0.460184671
39	Cephalexin	LEX	-2.81	0.397673279
40	Cephalothin	CEF	-0.203	0.413109644
41	Cephradine	RAD	9.061	0.12365815
42	Methicillin	MET	0.872	0.343247976
43	Cinoxacin	CIN	1.128	0.337443132
44	Loracarbef	LOR	-2.311	0.322931857
45	Clarithromycin	CLR	1.66	0.244703217
46	Clindamycin	CLI	2.056	0.308949125
47	Colistin	CST	0.634	0.42490585
48	Dalbavancin	DAL	3.086	0.315500551
49	Dalfopristin	DAF	1.323	0.261266407
50	Rifampicin	RIF	3.238	0.267690453
51	Daptomycin	DAP	0.415	0.431101766
52	Delafloxacin	DLX	1.283	0.271469202
53	Dirithromycin	DTM	1.555	0.235253855
54	Eravacycline	ERV	0.06	0.347054156
55	Oxacillin	OXA	1.759	0.333080247
56	Erythromycin	ERY	1.141	0.264376615
57	Fleroxacin	FLE	2.249	0.173624456
58	Vancomycin	VAN	-3.391	0.36650472
59	Fusidic Acid	FA	5.904	0.201531886
60	Gatifloxacin	GAT	2.509	0.218866947
61	Vaborbactam	VAB	0.33	0.407830474
62	Grepafloxacin	GRX	2.45	0.202915366
63	Iclaprim	ICL	0.236	0.294915545
64	Imipenem	IPM	-3.02	0.47316232
65	Plazomicin	PLZ	-5.023	0.454618207
66	Piperacillin	PIP	0.328	0.351397834
67	Linezolid	LZD	0.405	0.210918911
68	Omadacycline	OMC	1.808	0.317568346
69	Meropenem	MEM	-0.779	0.353593821
70	Tigecycline	TGC	1.033	0.351558311

71	Nalidixic acid	NAL	0.997	0.30148464
72	Netilmicin base	NET	-2.815	0.42021828
73	Nitrofurantoin	NIT	-0.093	0.495937932
74	Telithromycin	TEL	2.137	0.208386441
75	Ofloxacin	OFX	1.995	0.203021631
76	Streptomycin	STR	-5.988	0.578788697
77	Tedizolid	TZD	-0.232	0.276802891
78	Telavancin	TLV	1.983	0.346650904
79	Rifapentine	RFP	4.497	0.251183158
80	Rifabutin	RFB	3.967	0.246963314
81	Teicoplanin aglycone	TEC	-2.538	0.340138039
82	Relebactam	REL	-2.529	0.392576658
83	Sulfamethoxazole	SMZ	0.255	0.403711311
84	Sulbactam (sodium salt)	SUL	-1.132	0.429676482
85	Sparfloxacin	SPX	2.353	0.252189126
86	Tazobactam	TZB	-2.177	0.426891476
87	Azithromycin	AZM	1.888	0.240585102
88	Lincomycin	LCM	0.69	0.363823226
89	Mupirocin	MUP	2.451	0.291925701
90	Benzopenicillin	PEN	1.296	0.335260181
91	Ticarcillin	TIC	1.232	0.454660287
92	Aztreonam	ATM	-1.261	0.539544878
93	Ertapenem	ETP	-0.703	0.382138938
94	Doripenem	DOR	-4.179	0.465921458
95	Gramicidine	GRA	5.273	0.283854321

The Pearson correlation coefficient was used to determine the correlation between the descriptors and the empirically measured leakage **(Tab. 4).** The k-means algorithm was applied to assign antibiotics to the appropriate cluster (leaky or non-leaky cluster). Both Pearson correlation and K-means were calculated by the use of software - Origin 2020b.

Tab.4 *Pearson Correlation values*

Descriptor	Pearson correlation	Descriptor	Pearson Correlation
Fractional PSA	-0.86553	PPSA1	0.03127
Topological PSA	-0.71818	RNCG	0.11564
PPSA3	-0.6396	RPCG	0.11672
WPSA3	-0.61497	THSA	0.17183
RPSA	-0.61399	RNCS	0.17797
DPSA2	-0.57702	DPSA1	0.26974
DPSA3	-0.57619	FPSA1	0.27
TPSA	-0.56239	PNSA3	0.45836
FPSA3	-0.55965	WNSA3	0.47352
WPSA2	-0.49904	FNSA3	0.47549
PPSA2	-0.4418	FNSA2	0.53166
WNSA1	-0.42602	PNSA2	0.53805
PNSA1	-0.35331	WNSA2	0.54751
FPSA2	-0.34582	MannholdlogP	0.61309
FNSA1	-0.27	RHSA	0.61399
WPSA1	-0.1784	AlogP	0.68878
Molar refractivity	-0.13412	JlogP	0.70904
RPCS	-0.10921	XlogP	0.90559

IChF
Institute of Physical Chemistry PAS

4. Conclusions

The central assumption of droplet micro-bioreactors is their airtightness, leading to stability in the chemical composition. There is considerably much data addressing the problem of the chemical escape of some molecules from droplets [52,96,112]. However, many scientific works neglect the immensely crucial observations of droplet chemical leakage. Thus, optimizing microfluidic systems is vital as it directly impacts the quality of the results. The results obtained by the microfluidic method must correlate with studies conducted on a macro scale and be aligned with the universal clinical guidelines (i.e. European Committee on Antimicrobial Susceptibility Testing EUCAST recommendations). Every microbioreactor must maintain its chemical stability and not be prone to leakage and the influx of other reactants. In this work, I aimed to understand the phenomena of molecular leakage from droplets. In the first section of my PhD thesis, I discussed the leakage of fluorescent reagents from droplet bioreactors (Goal 1). The second part of this work concerns the leakage of antimicrobial agents (Goal 2).

Goal #1: Investigate if the modified version of metabolic marker molecule resorufin outperforms the conventionally used form and if such modified dye can be reliably used for microbial growth assays in droplets

Dodecylresorufin (C12R) remain longer inside the droplet

One of the most popular methods for detecting the bacterial presence in droplets is based on using metabolic markers. Resorufin is a fluorescent dye increasingly employed in droplet microfluidic tests. In droplet-based systems, resorufin escapes into the oil phase and surrounding droplets. As a result of signal averaging across bacterial-containing and empty droplets, leakage reduces test performance. One of the ways to reduce the leakage of chemicals from the droplets is the chemical modification or synthesis of new, non-leaky reagents. The main reason for using C12R instead of resorufin is its better cell permeability, allowing longer retention inside the bacterial cell and, thus, in the droplet. I compared the efficiency of resorufin and C12R in microdroplet assays. The main finding of this work confirms that C12R is characterized by higher accuracy in the long-term incubation of bacteria in droplets. There is a big chance that findings of the increased retention of C12R demonstrated in my work will pave the way for new possibilities in applying droplet-based research in microbiology.

C12R outperforms resorufin in droplet-based assays for microbiology

The potential applications of the C12R dye in droplet assays include digital droplet quantification of aerobic bacteria and antibiotic susceptibility testing. Since resorufin leaks from droplets, the only way to prevent cross-contamination was to separate droplet bioreactions in the long channel physically. Replacing resorufin with C12 enables the incubation of thousands of droplets in densely packed emulsions, reducing the need for incubation in channels and significantly improving the high throughput of the method.

Unfortunately, all resorufin derivatives have the same imperfection in the lack of fluorescence in anaerobic metabolism, which makes it challenging to detect anaerobes. This is a significant drawback of using resorufin derivatives in droplet microfluidics, highlighting the need to develop alternative detection methods, particularly those based on the direct detection of unlabeled cells.

Goal #2: Determine the physicochemical parameters that can be used to predict antibiotic leakage between water-in-oil droplets and propose a predictive guideline for limiting inter-droplet transport of antibiotics

Partition coefficient and fractional polar surface area are the main parameters enabling the prediction of the leakage of non-fluorescent molecules from droplets

The second part of this work concerns the problem of the leakage of antibiotics from droplet bioreactors. The direct determination of the leakage of antimicrobial agents is hard to perform, primarily due to its weak fluorescence. I set out to find the chemical factors that accelerate the escape from droplets. The strategy outlined in this study is built on indirect leakage detection using reporter cells. The cross-talk of antibiotics between droplets can significantly interfere with the course of the experiment. Surprisingly, nobody before has attempted to understand the impact of the chemical nature of antimicrobials in this unfavorable phenomenon. I found that certain classes of antibiotics possess a high tendency to cross-talk between droplets. The analysis of chemical descriptors concerning the hydrophilic/hydrophobic nature of the molecules has shown that two of them, partition coefficient and fractional polar surface area, remain in good correlation with experimental data. The results of this work enabled me to create a leakage prediction model of antibiotics encapsulated within water-in-oil emulsions. The model's effectiveness in predicting antimicrobial leakage tendency was confirmed experimentally. I hope

the study I presented in this work will soon help other microfluidics users plan experiments with antimicrobials more carefully. Hopefully, this work will open an earnest discussion on the validity of experiments performed using two-phase microfluidic systems.

The spatial separation of droplets with different chemical content significantly decreases cross-contamination

Moreover, there is a reasonable observation that methods of sample incubation significantly influence the correctness of the antimicrobial susceptibility experiments carried out in droplets. Droplets remaining in direct contact are more prone to cross-contamination [17]. The experiments I carried out in this study confirmed that the way the samples are incubated impacts the experiment results performed in a droplet format. Incubation of complex emulsions consisting of droplets with various antimicrobials should limit direct droplet contact. One of the ways to do it is by separating each sample with different chemical content with a layer of blank droplets. It is worth noting that high concentrations of antimicrobials greatly influence the leakage and contamination of neighboring micro-bioreactors. This crucial observation should be taken into account when planning droplet experiments. One strategy to reduce the risk of droplet leakage and boost test accuracy is to avoid using antibiotics at very high concentrations.

The method presented in this work can be used for future research on new surfactants

There were no significant differences in results between two commonly used surfactants: i) (PFPE)$_2$PEG and ii) FluoSurf N. Nevertheless, the antimicrobial escape in other surfactants or oils should be preceded by the determination with the methodology presented in this work. As shown in the literature, developing new surfactants raises the greatest hopes for overcoming the leakage of droplets. Leakage from droplets of non-fluorescent substances is generally difficult to trace. Therefore, most of the research is based on fluorophore studies. The very non-polar structure of several of these chemicals can cause inaccurate interpretations of the results. My work maps out a strategy for researching new surfactants that can improve emulsion stability and reduce the leakage of various non-fluorescent antimicrobial agents. The ability of bacteria to rapidly react to even minimal amounts of antibiotics (range below a few µg/ml) makes this assay of utmost sensitivity.

References

1. Whitesides GM: **The origins and the future of microfluidics**. *Nature* 2006, **442**:368-373.

2. Abram TJ, Cherukury H, Ou CY, Vu T, Toledano M, Li Y, Grunwald JT, Toosky MN, Tifrea DF, Slepenkin A, et al.: **Rapid bacterial detection and antibiotic susceptibility testing in whole blood using one-step, high throughput blood digital PCR**. *Lab Chip* 2020, **20**:477-489.

3. Gowda HN, Kido H, Wu X, Shoval O, Lee A, Lorenzana A, Madou M, Hoffmann M, Jiang SC: **Development of a proof-of-concept microfluidic portable pathogen analysis system for water quality monitoring**. *Sci Total Environ* 2022, **813**:152556.

4. Manz A, Graber N, Widmer HM: **Miniaturized Total Chemical-Analysis Systems - a Novel Concept for Chemical Sensing**. *Sensors and Actuators B-Chemical* 1990, **1**:244-248.

5. Qin D, Xia Y, Whitesides GM: **Soft lithography for micro- and nanoscale patterning**. *Nature Protocols* 2010, **5**:491-502.

6. Lee JN, Park C, Whitesides GM: **Solvent compatibility of poly(dimethylsiloxane)-based microfluidic devices**. *Anal Chem* 2003, **75**:6544-6554.

7. Thorsen T, Roberts R, Arnold F, Quake S: **Dynamic Pattern Formation in Vesicle-Generating Microfluidic Device**. *Physical review letters* 2001, **86**:4163-4166.

8. Kaminski TS, Garstecki P: **Controlled droplet microfluidic systems for multistep chemical and biological assays**. *Chemical Society Reviews* 2017, **46**:6210-6226.

9. Postek W, Garstecki P: **Droplet Microfluidics for High-Throughput Analysis of Antibiotic Susceptibility in Bacterial Cells and Populations**. *Acc Chem Res* 2022, **55**:605-615.

10. Ruszczak A, Bartkova S, Zapotoczna M, Scheler O, Garstecki P: **Droplet-based methods for tackling antimicrobial resistance**. *Current Opinion in Biotechnology* 2022, **76**:102755.

11. Anna SL, Bontoux N, Stone HA: **Formation of dispersions using "flow focusing" in microchannels**. *Applied Physics Letters* 2003, **82**:364-366.

12. Garstecki P, Gitlin I, DiLuzio W, Whitesides GM, Kumacheva E, Stone HA: **Formation of monodisperse bubbles in a microfluidic flow-focusing device**. *Applied Physics Letters* 2004, **85**:2649-2651.

13. Huang D, Wang K, Wang Y, Sun H, Liang X, Meng T: **Precise control for the size of droplet in T-junction microfluidic based on iterative learning method**. *Journal of the Franklin Institute* 2020, **357**:5302-5316.

14. Cramer C, Fischer P, Windhab EJ: **Drop formation in a co-flowing ambient fluid**. *Chemical Engineering Science* 2004, **59**:3045-3058.

15. Liu L, Xiang N, Ni Z, Huang X, Zheng J, Wang Y, Zhang X: **Step emulsification: high-throughput production of monodisperse droplets**. *BioTechniques* 2020, **68**:114-116.

16. Amstad E, Chemama M, Eggersdorfer M, Arriaga LR, Brenner MP, Weitz DA: **Robust scalable high throughput production of monodisperse drops**. *Lab on a Chip* 2016, **16**:4163-4172.

17. Conchouso D, Castro D, Khan SA, Foulds IG: **Three-dimensional parallelization of microfluidic droplet generators for a litre per hour volume production of single emulsions**. *Lab on a Chip* 2014, **14**:3011-3020.

18. Yadavali S, Jeong H-H, Lee D, Issadore D: **Silicon and glass very large scale microfluidic droplet integration for terascale generation of polymer microparticles**. *Nature Communications* 2018, **9**:1222.

19. Azimi-Boulali J, Madadelahi M, Madou MJ, Martinez-Chapa SO: **Droplet and Particle Generation on Centrifugal Microfluidic Platforms: A Review**. *Micromachines (Basel)* 2020, **11**.

20. Kao Y-T, Kaminski TS, Postek W, Guzowski J, Makuch K, Ruszczak A, von Stetten F, Zengerle R, Garstecki P: **Gravity-driven microfluidic assay for digital enumeration of bacteria and for antibiotic susceptibility testing**. *Lab on a Chip* 2020, **20**:54-63.

21. Byrnes SA, Phillips EA, Huynh T, Weigl BH, Nichols KP: **Polydisperse emulsion digital assay to enhance time to detection and extend dynamic range in bacterial cultures enabled by a statistical framework**. *Analyst* 2018, **143**:2828-2836.

22. Byrnes SA, Chang TC, Huynh T, Astashkina A, Weigl BH, Nichols KP: **Simple Polydisperse Droplet Emulsion Polymerase Chain Reaction with Statistical Volumetric Correction Compared with Microfluidic Droplet Digital Polymerase Chain Reaction**. *Analytical Chemistry* 2018, **90**:9374-9380.

23. Hatori MN, Kim SC, Abate AR: **Particle-Templated Emulsification for Microfluidics-Free Digital Biology**. *Anal Chem* 2018, **90**:9813-9820.

24. Boedicker JQ, Li L, Kline TR, Ismagilov RF: **Detecting bacteria and determining their susceptibility to antibiotics by stochastic confinement in nanoliter droplets using plug-based microfluidics**. *Lab on a Chip* 2008, **8**:1265-1272.

25. Abbyad P, Tharaux P-L, Martin J-L, Baroud CN, Alexandrou A: **Sickling of red blood cells through rapid oxygen exchange in microfluidic drops**. *Lab on a Chip* 2010, **10**:2505-2512.

26. Boitard L, Cottinet D, Bremond N, Baudry J, Bibette J: **Growing microbes in millifluidic droplets**. *Engineering in Life Sciences* 2015, **15**.

27. Watterson WJ, Tanyeri M, Watson AR, Cham CM, Shan Y, Chang EB, Eren AM, Tay S: **Droplet-based high-throughput cultivation for accurate screening of antibiotic resistant gut microbes**. *Elife* 2020, **9**.

28. Yin J, Chen X, Li X, Kang G, Wang P, Song Y, Ijaz U, Yin H, Huang H: **A droplet-based microfluidic approach to isolating functional bacteria from gut microbiota**. *Frontiers in Cellular and Infection Microbiology* 2022, **12**.

29. Kehe J, Kulesa A, Ortiz A, Ackerman CM, Thakku SG, Sellers D, Kuehn S, Gore J, Friedman J, Blainey PC: **Massively parallel screening of synthetic microbial communities**. *Proc Natl Acad Sci U S A* 2019, **116**:12804-12809.

30. Kulesa A, Kehe J, Hurtado JE, Tawde P, Blainey PC: **Combinatorial drug discovery in nanoliter droplets**. *Proc Natl Acad Sci U S A* 2018, **115**:6685-6690.

31. Li H, Zhang P, Hsieh K, Wang TH: **Combinatorial nanodroplet platform for screening antibiotic combinations**. *Lab Chip* 2022, **22**:621-631.

32. Churski K, Kaminski TS, Jakiela S, Kamysz W, Baranska-Rybak W, Weibel DB, Garstecki P: **Rapid screening of antibiotic toxicity in an automated microdroplet system**. *Lab Chip* 2012, **12**:1629-1637.

33. Churski K, Ruszczak A, Jakiela S, Garstecki P: **Droplet Microfluidic Technique for the Study of Fermentation**. *Micromachines* 2015, **6**:1514-1525.

34. Wang J, Wang J, Feng L, Lin T: **Fluid mixing in droplet-based microfluidics with a serpentine microchannel**. *RSC Advances* 2015, **5**:104138-104144.

35. Pacocha N, Boguslawski J, Horka M, Makuch K, Lizewski K, Wojtkowski M, Garstecki P: **High-Throughput Monitoring of Bacterial Cell Density in Nanoliter Droplets: Label-Free Detection of Unmodified Gram-Positive and Gram-Negative Bacteria**. *Anal Chem* 2021, **93**:843-850.

36. Wang BL, Ghaderi A, Zhou H, Agresti J, Weitz DA, Fink GR, Stephanopoulos G: **Microfluidic high-throughput culturing of single cells for selection based on extracellular metabolite production or consumption**. *Nat Biotechnol* 2014, **32**:473-478.

37. Abalde-Cela S, Gould A, Liu X, Kazamia E, Smith AG, Abell C: **High-throughput detection of ethanol-producing cyanobacteria in a microdroplet platform**. *Journal of The Royal Society Interface* 2015, **12**:20150216.

38. de Cena JA, Zhang J, Deng D, Damé-Teixeira N, Do T: **Low-Abundant Microorganisms: The Human Microbiome's Dark Matter, a Scoping Review**. *Front Cell Infect Microbiol* 2021, **11**:689197.

39. Wouters Y, Dalloyaux D, Christenhusz A, Roelofs HMJ, Wertheim HF, Bleeker-Rovers CP, Te Morsche RH, Wanten GJA: **Droplet digital polymerase chain reaction for rapid broad-spectrum detection of bloodstream infections**. *Microb Biotechnol* 2020, **13**:657-668.

40. Zhang PF, Kaushik AM, Hsieh K, Li SX, Lewis S, Mach KE, Liao JC, Carroll KC, Wang TH: **A Cascaded Droplet Microfluidic Platform Enables High-Throughput Single Cell Antibiotic Susceptibility Testing at Scale**. *Small Methods* 2022, **6**.

41. Guerin TF, Mondido M, McClenn B, Peasley B: **Application of resazurin for estimating abundance of contaminant-degrading micro-organisms**. *Lett Appl Microbiol* 2001, **32**:340-345.

42. Karakashev D, Galabova D, Simeonov I: **A simple and rapid test for differentiation of aerobic from anaerobic bacteria**. *World Journal of Microbiology and Biotechnology* 2003, **19**:233-238.

43. Mariscal A, Lopez-Gigosos RM, Carnero-Varo M, Fernandez-Crehuet J: **Fluorescent assay based on resazurin for detection of activity of disinfectants against bacterial biofilm**. *Appl Microbiol Biotechnol* 2009, **82**:773-783.

44. Sarker SD, Nahar L, Kumarasamy Y: **Microtitre plate-based antibacterial assay incorporating resazurin as an indicator of cell growth, and its application in the in vitro antibacterial screening of phytochemicals**. *Methods* 2007, **42**:321-324.

45. O'Brien J, Wilson I, Orton T, Pognan F: **Investigation of the Alamar Blue (resazurin) fluorescent dye for the assessment of mammalian cell cytotoxicity**. *Eur J Biochem* 2000, **267**:5421-5426.

46. Najah M, Griffiths AD, Ryckelynck M: **Teaching Single-Cell Digital Analysis Using Droplet-Based Microfluidics**. *Analytical Chemistry* 2012, **84**:1202-1209.

47. Liu Y, Jung S-Y, Collier CP: **Shear-driven redistribution of surfactant affects enzyme activity in well-mixed femtoliter droplets**. *Analytical chemistry* 2009, **81**:4922-4928.

48. Bui M-PN, Li CA, Han KN, Choo J, Lee EK, Seong GH: **Enzyme Kinetic Measurements Using a Droplet-Based Microfluidic System with a Concentration Gradient**. *Analytical Chemistry* 2011, **83**:1603-1608.

49. Hess D, Rane A, deMello AJ, Stavrakis S: **High-Throughput, Quantitative Enzyme Kinetic Analysis in Microdroplets Using Stroboscopic Epifluorescence Imaging**. *Analytical Chemistry* 2015, **87**:4965-4972.

50. Mazutis L, Baret J-C, Treacy P, Skhiri Y, Araghi AF, Ryckelynck M, Taly V, Griffiths AD: **Multi-step microfluidic droplet processing: kinetic analysis of an in vitro translated enzyme**. *Lab on a Chip* 2009, **9**:2902-2908.

51. Sandoz PA, Chung AJ, Weaver WM, Di Carlo D: **Sugar Additives Improve Signal Fidelity for Implementing Two-Phase Resorufin-Based Enzyme Immunoassays**. *Langmuir* 2014, **30**:6637-6643.

52. Gruner P, Riechers B, Semin B, Lim J, Johnston A, Short K, Baret JC: **Controlling molecular transport in minimal emulsions**. *Nat Commun* 2016, **7**:10392.

53. Scheler O, Kaminski TS, Ruszczak A, Garstecki P: **Dodecylresorufin (C12R) Outperforms Resorufin in Microdroplet Bacterial Assays**. *ACS Appl Mater Interfaces* 2016, **8**:11318-11325.

54. Kaminski TS, Scheler O, Garstecki P: **Droplet microfluidics for microbiology: techniques, applications and challenges**. *Lab Chip* 2016, **16**:2168-2187.

55. Horka M, Sun S, Ruszczak A, Garstecki P, Mayr T: **Lifetime of Phosphorescence from Nanoparticles Yields Accurate Measurement of Concentration of Oxygen in Microdroplets, Allowing One To Monitor the Metabolism of Bacteria**. *Anal Chem* 2016, **88**:12006-12012.

56. Tovar M, Mahler L, Buchheim S, Roth M, Rosenbaum MA: **Monitoring and external control of pH in microfluidic droplets during microbial culturing**. *Microbial Cell Factories* 2020, **19**:16.

57. Zirath H, Spitz S, Roth D, Schellhorn T, Rothbauer M, Muller B, Walch M, Kaur J, Worle A, Kohl Y, et al.: **Bridging the academic-industrial gap: application of an oxygen and pH sensor-integrated lab-on-a-chip in nanotoxicology**. *Lab Chip* 2021, **21**:4237-4248.

58. Marcoux PR, Dupoy M, Mathey R, Novelli-Rousseau A, Heran V, Morales S, Rivera F, Joly PL, Moy J-P, Mallard F: **Micro-confinement of bacteria into w/o emulsion droplets for rapid detection and enumeration**. *Colloids and Surfaces A: Physicochemical and Engineering Aspects* 2011, **377**:54-62.

59. Baret JC, Miller OJ, Taly V, Ryckelynck M, El-Harrak A, Frenz L, Rick C, Samuels ML, Hutchison JB, Agresti JJ, et al.: **Fluorescence-activated droplet sorting (FADS): efficient microfluidic cell sorting based on enzymatic activity**. *Lab Chip* 2009, **9**:1850-1858.

60. Huebner A, Srisa-Art M, Holt D, Abell C, Hollfelder F, deMello AJ, Edel JB: **Quantitative detection of protein expression in single cells using droplet microfluidics**. *Chemical Communications* 2007:1218-1220.

61. Scheler O, Makuch K, Debski PR, Horka M, Ruszczak A, Pacocha N, Sozanski K, Smolander OP, Postek W, Garstecki P: **Droplet-based digital antibiotic susceptibility screen reveals single-cell clonal heteroresistance in an isogenic bacterial population**. *Sci Rep* 2020, **10**:3282.

62. Terekhov SS, Smirnov IV, Stepanova AV, Bobik TV, Mokrushina YA, Ponomarenko NA, Belogurov AA, Rubtsova MP, Kartseva OV, Gomzikova MO, et al.: **Microfluidic droplet platform for ultrahigh-throughput single-cell screening of biodiversity**. *Proceedings of the National Academy of Sciences* 2017, **114**:2550-2555.

63. Hsu RH, Clark RL, Tan JW, Ahn JC, Gupta S, Romero PA, Venturelli OS: **Microbial Interaction Network Inference in Microfluidic Droplets**. *Cell Syst* 2019, **9**:229-242 e224.

64. **Global burden of bacterial antimicrobial resistance in 2019: a systematic analysis**. *Lancet* 2022, **399**:629-655.

65. Aslam B, Khurshid M, Arshad MI, Muzammil S, Rasool M, Yasmeen N, Shah T, Chaudhry TH, Rasool MH, Shahid A, et al.: **Antibiotic Resistance: One Health One World Outlook**. *Front Cell Infect Microbiol* 2021, **11**:771510.

66. Schoepp NG, Schlappi TS, Curtis MS, Butkovich SS, Miller S, Humphries RM, Ismagilov RF: **Rapid pathogen-specific phenotypic antibiotic susceptibility testing using digital LAMP quantification in clinical samples**. *Sci Transl Med* 2017, **9**.

67. Kang D-K, Ali MM, Zhang K, Huang SS, Peterson E, Digman MA, Gratton E, Zhao W: **Rapid detection of single bacteria in unprocessed blood using Integrated Comprehensive Droplet Digital Detection**. *Nature Communications* 2014, **5**:5427.

68. Antonello M, Scutari R, Lauricella C, Renica S, Motta V, Torri S, Russo C, Gentile L, Cento V, Colagrossi L, et al.: **Rapid Detection and Quantification of Mycobacterium tuberculosis DNA in Paraffinized Samples by Droplet Digital PCR: A Preliminary Study**. *Frontiers in Microbiology* 2021, **12**.

69. Kaushik AM, Hsieh K, Mach KE, Lewis S, Puleo CM, Carroll KC, Liao JC, Wang T-H: **Droplet-Based Single-Cell Measurements of 16S rRNA Enable Integrated Bacteria Identification and Pheno-Molecular Antimicrobial Susceptibility Testing from Clinical Samples in 30 min**. *Advanced Science* 2021, **8**:2003419.

70. Ulep TH, Day AS, Sosnowski K, Shumaker A, Yoon JY: **Interfacial Effect-Based Quantification of Droplet Isothermal Nucleic Acid Amplification for Bacterial Infection**. *Sci Rep* 2019, **9**:9629.

71. Collins DJ, Neild A, deMello A, Liu A-Q, Ai Y: **The Poisson distribution and beyond: methods for microfluidic droplet production and single cell encapsulation**. *Lab on a Chip* 2015, **15**:3439-3459.

72. Ostafe R, Prodanovic R, Lloyd Ung W, Weitz DA, Fischer R: **A high-throughput cellulase screening system based on droplet microfluidics**. *Biomicrofluidics* 2014, **8**:041102.

73. Sjostrom SL, Bai Y, Huang M, Liu Z, Nielsen J, Joensson HN, Andersson Svahn H: **High-throughput screening for industrial enzyme production hosts by droplet microfluidics**. *Lab on a Chip* 2014, **14**:806-813.

74. Lyu F, Pan M, Patil S, Wang J-H, Matin AC, Andrews JR, Tang SKY: **Phenotyping antibiotic resistance with single-cell resolution for the detection of heteroresistance**. *Sensors and Actuators B: Chemical* 2018, **270**:396-404.

75. Band VI, Crispell EK, Napier BA, Herrera CM, Tharp GK, Vavikolanu K, Pohl J, Read TD, Bosinger SE, Trent MS, et al.: **Antibiotic failure mediated by a resistant subpopulation in Enterobacter cloacae**. *Nat Microbiol* 2016, **1**:16053.

76. Alexander HK, MacLean RC: **Stochastic bacterial population dynamics restrict the establishment of antibiotic resistance from single cells**. *Proc Natl Acad Sci U S A* 2020, **117**:19455-19464.

77. Li J, Rayner CR, Nation RL, Owen RJ, Spelman D, Tan KE, Liolios L: **Heteroresistance to Colistin in Multidrug-Resistant <i>Acinetobacter baumannii</i>**. *Antimicrobial Agents and Chemotherapy* 2006, **50**:2946-2950.

78. Pryszlak A, Wenzel T, Seitz KW, Hildebrand F, Kartal E, Cosenza MR, Benes V, Bork P, Merten CA: **Enrichment of gut microbiome strains for cultivation-free genome sequencing using droplet microfluidics**. *Cell Rep Methods* 2022, **2**:None.

79. Tauzin AS, Pereira MR, Van Vliet LD, Colin P-Y, Laville E, Esque J, Laguerre S, Henrissat B, Terrapon N, Lombard V, et al.: **Investigating host-microbiome interactions by droplet based microfluidics**. *Microbiome* 2020, **8**:141.

80. Tan HY, Toh YC: **What can microfluidics do for human microbiome research?** *Biomicrofluidics* 2020, **14**:051303.

81. Arnold JW, Roach J, Azcarate-Peril MA: **Emerging Technologies for Gut Microbiome Research**. *Trends Microbiol* 2016, **24**:887-901.

82. Nicoloff H, Andersson DI: **Indirect resistance to several classes of antibiotics in cocultures with resistant bacteria expressing antibiotic-modifying or -degrading enzymes**. *Journal of Antimicrobial Chemotherapy* 2015, **71**:100-110.

83. Sorg RA, Lin L, van Doorn GS, Sorg M, Olson J, Nizet V, Veening JW: **Collective Resistance in Microbial Communities by Intracellular Antibiotic Deactivation**. *PLoS Biol* 2016, **14**:e2000631.

84. Bottery MJ, Matthews JL, Wood AJ, Johansen HK, Pitchford JW, Friman V-P: **Inter-species interactions alter antibiotic efficacy in bacterial communities**. *The ISME Journal* 2022, **16**:812-821.

85. Kehe J, Ortiz A, Kulesa A, Gore J, Blainey PC, Friedman J: **Positive interactions are common among culturable bacteria**. *Sci Adv* 2021, **7**:eabi7159.

86. Tan JY, Wang S, Dick GJ, Young VB, Sherman DH, Burns MA, Lin XN: **Co-cultivation of microbial sub-communities in microfluidic droplets facilitates high-resolution genomic dissection of microbial 'dark matter'**. *Integr Biol (Camb)* 2020, **12**:263-274.

87. Baret J-C: **Surfactants in droplet-based microfluidics**. *Lab on a Chip* 2012, **12**:422-433.

88. Haupt A: **11 Fluoroorganic compounds – unusual properties and versatile applications**. In *Organic and Inorganic Fluorine Chemistry: Methods and Applications*. Edited by: De Gruyter; 2021:283-300.

89. Abbyad P, Dangla R, Alexandrou A, Baroud CN: **Rails and anchors: guiding and trapping droplet microreactors in two dimensions**. *Lab on a Chip* 2011, **11**:813-821.

90. Ki S, Kang D-K: **Gas Crosstalk between PFPE–PEG–PFPE Triblock Copolymer Surfactant-Based Microdroplets and Monitoring Bacterial Gas Metabolism with Droplet-Based Microfluidics**. *Biosensors* 2020, **10**:172.

91. Song H, Chen DL, Ismagilov RF: **Reactions in Droplets in Microfluidic Channels**. *Angewandte Chemie International Edition* 2006, **45**:7336-7356.

92. Zakhidov A, Lee J-K, Fong HH, Defranco J, Chatzichristidi M, Taylor P, Ober C, Malliaras G: **Hydrofluoroethers as Orthogonal Solvents for the Chemical Processing of Organic Electronic Materials**. *Advanced Materials* 2008, **20**:3481-3484.

93. Liao P, Huang Y: **Digital PCR: Endless Frontier of 'Divide and Conquer'**. *Micromachines* 2017, **8**:231.

94. Perinelli DR, Cespi M, Lorusso N, Palmieri GF, Bonacucina G, Blasi P: **Surfactant Self-Assembling and Critical Micelle Concentration: One Approach Fits All?** *Langmuir* 2020, **36**:5745-5753.

95. Etienne G, Kessler M, Amstad E: **Influence of Fluorinated Surfactant Composition on the Stability of Emulsion Drops**. *Macromolecular Chemistry and Physics* 2017, **218**:1600365.

96. Etienne G, Vian A, Biočanin M, Deplancke B, Amstad E: **Cross-talk between emulsion drops: how are hydrophilic reagents transported across oil phases?** *Lab on a Chip* 2018, **18**:3903-3912.

97. Clausell-Tormos J, Lieber D, Baret J-C, El-Harrak A, Miller OJ, Frenz L, Blouwolff J, Humphry KJ, Köster S, Duan H, et al.: **Droplet-Based Microfluidic Platforms for the Encapsulation and Screening of Mammalian Cells and Multicellular Organisms**. *Chemistry & Biology* 2008, **15**:427-437.

98. Seo S, Disney-McKeethen S, Prabhakar RG, Song X, Mehta HH, Shamoo Y: **Identification of Evolutionary Trajectories Associated with Antimicrobial Resistance Using Microfluidics**. *ACS Infect Dis* 2022, **8**:242-254.

99. Cserháti T, Forgács E, Oros G: **Biological activity and environmental impact of anionic surfactants**. *Environment International* 2002, **28**:337-348.

100. Falk NA: **Surfactants as Antimicrobials: A Brief Overview of Microbial Interfacial Chemistry and Surfactant Antimicrobial Activity**. *J Surfactants Deterg* 2019, **22**:1119-1127.

101. Roach LS, Song H, Ismagilov RF: **Controlling nonspecific protein adsorption in a plug-based microfluidic system by controlling interfacial chemistry using fluorous-phase surfactants**. *Anal Chem* 2005, **77**:785-796.

102. Miers J, Zhou W: **Droplet Formation at Megahertz Frequency**. *AIChE Journal* 2016, **63**.

103. Tsai CS, Mao RW, Lin SK, Tsai SC, Boss G, Brenner M, Smaldone G, Mahon S, Shahverdi K, Zhu Y: **Ultrasound-driven Megahertz Faraday Waves for Generation of Monodisperse Micro Droplets and Applications**. *Physics Procedia* 2015, **70**:872-875.

104. Holtze C, Rowat AC, Agresti JJ, Hutchison JB, Angilè FE, Schmitz CHJ, Köster S, Duan H, Humphry KJ, Scanga RA, et al.: **Biocompatible surfactants for water-in-fluorocarbon emulsions**. *Lab on a Chip* 2008, **8**:1632-1639.

105. Riess JG: **Fluorous micro- and nanophases with a biomedical perspective**. *Tetrahedron* 2002, **58**:4113-4131.

106. Sadtler VM, Krafft MP, Riess JG: **Achieving Stable, Reverse Water-in-Fluorocarbon Emulsions**. *Angewandte Chemie International Edition in English* 1996, **35**:1976-1978.

107. Johnston KP, Randolph T, Bright F, Howdle S: **Toxicology of a PFPE surfactant**. *Science* 1996, **272**:1726.

108. Hey MJ, Ilett SM, Davidson G: **Effect of temperature on poly(ethylene oxide) chains in aqueous solution. A viscometric, 1H NMR and Raman spectroscopic study**. *Journal of the Chemical Society, Faraday Transactions* 1995, **91**:3897-3900.

109. Malisova B, Tosatti S, Textor M, Gademann K, Zürcher S: **Poly(ethylene glycol) Adlayers Immobilized to Metal Oxide Substrates Through Catechol Derivatives: Influence of Assembly Conditions on Formation and Stability**. *Langmuir* 2010, **26**:4018-4026.

110. Chowdhury MS, Zheng W, Kumari S, Heyman J, Zhang X, Dey P, Weitz DA, Haag R: **Dendronized fluorosurfactant for highly stable water-in-fluorinated oil emulsions with minimal inter-droplet transfer of small molecules**. *Nat Commun* 2019, **10**:4546.

111. Chowdhury MS, Zheng W, Singh AK, Ong ILH, Hou Y, Heyman JA, Faghani A, Amstad E, Weitz DA, Haag R: **Linear triglycerol-based fluorosurfactants show high potential for droplet-microfluidics-based biochemical assays**. *Soft Matter* 2021, **17**:7260-7267.

112. Skhiri Y, Gruner P, Semin B, Brosseau Q, Pekin D, Mazutis L, Goust V, Kleinschmidt F, El Harrak A, Hutchison JB, et al.: **Dynamics of molecular transport by surfactants in emulsions**. *Soft Matter* 2012, **8**:10618-10627.

113. Chen Y, Wijaya Gani A, Tang SKY: **Characterization of sensitivity and specificity in leaky droplet-based assays**. *Lab on a Chip* 2012, **12**:5093-5103.

114. Janiesch J-W, Weiss M, Kannenberg G, Hannabuss J, Surrey T, Platzman I, Spatz JP: **Key Factors for Stable Retention of Fluorophores and Labeled Biomolecules in Droplet-Based Microfluidics**. *Analytical Chemistry* 2015, **87**:2063-2067.

115. Ariyaprakai S, Dungan SR: **Influence of surfactant structure on the contribution of micelles to Ostwald ripening in oil-in-water emulsions**. *Journal of Colloid and Interface Science* 2010, **343**:102-108.

116. Weiss J, Canceliere C, McClements DJ: **Mass Transport Phenomena in Oil-in-Water Emulsions Containing Surfactant Micelles: Ostwald Ripening**. *Langmuir* 2000, **16**:6833-6838.

117. Gupta A, Eral HB, Hatton TA, Doyle PS: **Nanoemulsions: formation, properties and applications**. *Soft Matter* 2016, **12**:2826-2841.

118. Debon AP, Wootton RC, Elvira KS: **Droplet confinement and leakage: Causes, underlying effects, and amelioration strategies**. *Biomicrofluidics* 2015, **9**:024119.

119. Thiam AR, Bremond N, Bibette J: **From Stability to Permeability of Adhesive Emulsion Bilayers**. *Langmuir* 2012, **28**:6291-6298.

120. Woronoff G, El Harrak A, Mayot E, Schicke O, Miller OJ, Soumillion P, Griffiths AD, Ryckelynck M: **New generation of amino coumarin methyl sulfonate-based fluorogenic substrates for amidase assays in droplet-based microfluidic applications**. *Anal Chem* 2011, **83**:2852-2857.

121. Fletcher PDI, Howe AM, Robinson BH: **The kinetics of solubilisate exchange between water droplets of a water-in-oil microemulsion**. *Journal of the Chemical Society, Faraday Transactions 1: Physical Chemistry in Condensed Phases* 1987, **83**:985-1006.

122. Courtois F, Olguin LF, Whyte G, Theberge AB, Huck WTS, Hollfelder F, Abell C: **Controlling the Retention of Small Molecules in Emulsion Microdroplets for Use in Cell-Based Assays**. *Analytical Chemistry* 2009, **81**:3008-3016.

123. Stapleton JA, Swartz JR: **Development of an in vitro compartmentalization screen for high-throughput directed evolution of [FeFe] hydrogenases**. *PLoS One* 2010, **5**:e15275.

124. Pan M, Lyu F, Tang SKY: **Fluorinated Pickering Emulsions with Nonadsorbing Interfaces for Droplet-based Enzymatic Assays**. *Analytical Chemistry* 2015, **87**:7938-7943.

125. Kaminski TS, Jakiela S, Czekalska MA, Postek W, Garstecki P: **Automated generation of libraries of nL droplets**. *Lab on a Chip* 2012, **12**:3995-4002.

126. Bueno C, Villegas ML, Bertolotti SG, Previtali CM, Neumann MG, Encinas MV: **The Excited-State Interaction of Resazurin and Resorufin with Aminesin Aqueous Solutions. Photophysics and Photochemical Reaction¶**. *Photochemistry and Photobiology* 2002, **76**:385-390.

127. Akobeng AK: **Understanding diagnostic tests 3: Receiver operating characteristic curves**. *Acta Paediatr* 2007, **96**:644-647.

128. Fawcett T: **An introduction to ROC analysis**. *Pattern Recognition Letters* 2006, **27**:861-874.

129. Linnet K: **A review on the methodology for assessing diagnostic tests**. *Clin Chem* 1988, **34**:1379-1386.

130. Youden WJ: **Index for rating diagnostic tests**. *Cancer* 1950, **3**:32-35.

131. Froger A, Hall JE: **Transformation of plasmid DNA into E. coli using the heat shock method**. *J Vis Exp* 2007:253.

132. Ansel HC, Norred WP, Roth IL: **Antimicrobial activity of dimethyl sulfoxide against Escherichia coli, Pseudomonas aeruginosa, and Bacillus megaterium**. *Journal of Pharmaceutical Sciences* 1969, **58**:836-839.

133. Steinbeck C, Han Y, Kuhn S, Horlacher O, Luttmann E, Willighagen E: **The Chemistry Development Kit (CDK): an open-source Java library for Chemo- and Bioinformatics**. *J Chem Inf Comput Sci* 2003, **43**:493-500.

134. Willighagen EL, Mayfield JW, Alvarsson J, Berg A, Carlsson L, Jeliazkova N, Kuhn S, Pluskal T, Rojas-Chertó M, Spjuth O, et al.: **The Chemistry Development Kit (CDK) v2.0: atom typing, depiction, molecular formulas, and substructure searching**. *J Cheminform* 2017, 9:33.

135. Wang R, Gao Y, Lai L: **Calculating partition coefficient by atom-additive method**. *Perspectives in Drug Discovery and Design* 2000, 19:47-66.

136. Ertl P, Rohde B, Selzer P: **Fast Calculation of Molecular Polar Surface Area as a Sum of Fragment-Based Contributions and Its Application to the Prediction of Drug Transport Properties**. *Journal of Medicinal Chemistry* 2000, 43:3714-3717.

Acknowledgement